Aus dem Max-Delbrück-Centrum für Molekulare Medizin und

der Medizinischen Fakultät Charité – Universitätsmedizin Berlin

DISSERTATION

Subset-specific transduction of $CD4^+$ and $CD8^+$ T cells *in vivo*

Subgruppen-spezifische *in vivo* Transduktion von $CD4^+$ und $CD8^+$ T-Zellen

zur Erlangung des akademischen Grades

Doctor medicinae (Dr. med.)

vorgelegt der Medizinischen Fakultät

Charité – Universitätsmedizin Berlin

von

Christoph Philipp Kemna

aus Bremen, Deutschland

Datum der Promotion: 30.11.2023

1. Table of Contents

1. Table of Contents ..... ***ii***

2. List of Tables ..... ***v***

3. List of Figures ..... ***vi***

4. Abbreviations ..... ***vii***

5. Zusammenfassung ***1***

6. Summary ***3***

7. Introduction ***5***

7.1. T cells and the immune system **5**

7.1.1. Innate and adaptive immunity 5

7.1.2. T and B cells 5

7.1.3. The T cell receptor 6

7.1.4. T cell maturation in the thymus 7

7.1.5. The generation of T cell receptors by somatic recombination 8

7.1.6. T cell activation 8

7.1.7. T cell subsets 9

7.2. Cancer immunotherapies **10**

7.2.1. Checkpoint-inhibitor therapy 11

7.3. Adoptive T cell therapy **12**

7.3.1. Unmodified T cells 12

7.3.2. Tumour-infiltrating lymphocytes 13

7.3.3. Receptor-modified T cells 13

7.3.4. CAR T cells 15

7.3.5. TCR-engineered T cells 16

7.4. Limitations of *ex vivo* cultured T cells **17**

7.5. Viral vectors **18**

7.5.1. Gammaretroviral vectors 19

7.5.2. Pseudotyping 19

7.5.3. Pseudotyping of lentiviral vectors using *Measles* virus envelope 20

7.5.4. Pseudotyping of gammaretroviral vectors using *Measles* virus envelope 20

8. Aims of the thesis 22

9. Materials and Methods 23

9.1. TCR chain subtype and CDR3 identification 23

9.2. Techniques of molecular biology 24

9.3. Construction of MP71- and 506-SB-plasmids 25

9.4. Cell culture 26

9.4.1. Generation of AB1 HA and 4T1 HA 27

9.5. Large scale virus production 27

9.5.1. Titration of MVm8- and MVm4-vectors 29

9.6. Antibodies 29

9.6.1. Anti-SFE TCR antibody production 29

9.6.2. Antibody staining and flow cytometry 30

9.7. Co-culture and ELISA assays 31

9.8. BALB/c-derived splenocytes 32

9.8.1. Isolation of splenocytes 32

9.8.2. Magnetic-activated cell sorting (MACS) 33

9.8.3. BALB/c-derived splenocyte culture 33

9.9. Transduction 33

9.9.1. *In vitro* transduction 33

9.9.2. *In vivo* transduction 33

9.9.3. *In vivo* imaging 34

9.10. Data analysis 34

10. Results 35

10.1. Detection of TCR chain subtypes and CDR3 regions 35

10.2. Generation of cell lines expressing HA 37

10.2.1. Electroporation of AB1 and 4T1 38

10.2.2. AB1 HA and 4T1 HA 39

10.2.3. Growth of cancer cell lines and derivatives in BALB/c mice 40

10.3. Transduction of 58m4 and 58m8 and titration of viral supernatants 41

10.4. Production of the 6.5 antibody for TCR-specific staining 42

10.5. Transduction of primary BALB/c-derived T cells *in vitro* 44

10.5.1. Transduction of BALB/c-derived $CD8^+$ T cells by MVm8 *in vitro* 44

10.5.2. Transduction of BALB/c-derived $CD4^+$ T cells by MVm4 *in vitro* 45

10.5.3. Co-culture assays using MVm8/Clone 1- and Clone 4-transduced T cells..... 46

10.5.4. Co-culture assays using MVm4/SFE-transduced T cells 48

10.6. Transduction of BALB/c lymphocytes *in vivo* 50

***11. Discussion*.....56**

11.1. Limitations of *ex vivo* manufacturing of T cell-based immunotherapies 56

11.2. The synergy of $CD4^+$ and $CD8^+$ T cells and their clinical application..... 57

11.3. Cell lines and immune escape 59

11.4. TCR avidity and co-culture 60

11.5. TCR-engineering by subset-specific *in vivo* transduction of $CD4^+$ and $CD8^+$ T cells 61

11.6. Titre and variety of pseudotyped retroviral vectors..... 62

11.7. Conclusion and outlook..... 63

***12. References*.....65**

***13. Curriculum Vitae*.....83**

***14. Publications*.....84**

***15. Acknowledgements*.....85**

***16. Statistics certificate*.....86**

2. List of Tables

Table 1 Mouse strains harbouring TCR transgenes 23
Table 2 List of primers used for TCR chain subtype and CDR3 identification..... 23
Table 3 List of generated Plasmids 25
Table 4 Plasmids used in large scale virus production..... 28
Table 5 Antibodies and tetramer used in flow cytometry..... 30
Table 6 Peptides used in co-culture assays..... 32
Table 7 TCR chain segments reported in the literature..... 36
Table 8 TCR chain segments and CDR3 regions determined by sequencing..... 37

3. List of Figures

Figure 1 AB1 and 4T1 express GFP after electroporation with 506-SB-HAiGFP. 39
Figure 2 AB1 and 4T1 single cell clones AB1 HA and 4T1 HA show expression of HA and GFP. 40
Figure 3 AB1 HA and 4T1 HA grow similarly to their respective parental cell lines AB1 and 4T1 in BALB/c mice. 41
Figure 4 MVm8/Clone 1 and MVm8/Clone 4 transduce 58m8 and MVm4/SFE transduces 58m4. 42
Figure 5 Staining using clonotypic 6.5 mAb on 58m4 transduced with MVm4/SFE. 43
Figure 6 MVm8/Clone 1 and MVm8/Clone 4 transduce BALB/c-derived $CD8^+$ splenocytes efficiently and exclusively. 44
Figure 7 MVm4-pseudotyped gRV/SFE transduces BALB/c-derived $CD4^+$ splenocytes effectively and exclusively. 46
Figure 8 MVm8/Clone 1- and MVm8/Clone 4-transduced BALB/c-derived $CD8^+$ T cells recognize their epitope presented on unsorted splenocytes. 47
Figure 9 MVm8/Clone 1- and MVm8/Clone 4-transduced BALB/c-derived $CD8^+$ T cells recognize the antigen expressing cell lines AB1 HA and 4 T1 HA. 48
Figure 10 MVm4/SFE-transduced BALB/c-derived $CD4^+$ T cells recognize peptide presented on DCs. 49
Figure 11 MVm4/SFE-transduced BALB/c-derived $CD4^+$ T cells recognize their epitope presented on DCs after processing of antigen derived from cell lysate. 50
Figure 12 *In vivo* transduction of BALB/c mice, synopsis. 53
Figure 13 *In vivo* transduction of BALB/c mice, detailed. 55

4. Abbreviations

ACK	ammonium-chloride-potassium Lysing Buffer
Allo-SCT	allogeneic haematopoietic stem cell transplantation
APC	professional antigen presenting cells
ACT	adoptive cell therapy
B6	C57BL/6 mice
BCG	bacillus Calmette-Guerin
BCMA	B cell maturation antigen
BCR	B cell receptor
C	constant region
CAR	chimeric antigen receptor
CD	cluster of differentiation
CDR3	Complementary-determining region 3
CEA	carcinoembryonic antigen
Cish	cytokine-inducible SH2-containing protein
CML	chronic myeloid leukaemia
CR	complete response
CTLA4	cytotoxic T lymphocyte antigen 4
D	Diversity
DC	dendritic cells
DLI	donor lymphocyte infusions
DMEM	Dulbecco´s modified Eagle´s medium
ELISA	enzyme-linked immunosorbent assay
F	membrane fusion protein
FACT	Foundation for the Accreditation of Cellular Therapy
FCS	fetal calf serum
FDA	U.S. Food and Drug Administration
FLuc	Firefly luciferase
GM-CSF	granulocyte-macrophage colony-stimulating factor
GFP	green fluorescent protein
gRV	gammaretroviral/gammaretrovirus
GVHD	graft-versus-host disease
GVL	graft-versus-leukaemia effect
H	hemagglutinin
ICAM	intercellular adhesion molecule 1; CD54
IFN	interferon
IL	Interleukin
IVIS	In Vivo Imaging System
HA	*Influenza* A/PR/8/34 H1N1 hemagglutinin
IRES	internal ribosomal entry site
ITAM	immunoreceptor tyrosine-based activation motifs

IYSTVASSL-Tetramer	Clone 1 TCR and Clone 4 TCR specific H-2K^d *Influenza* A/PR/8/34 H1N1 HA tetramer-IYSTVASSL-PE
J	joining
JACIE	Joint Accreditation Committee ISCT-Europe & EBMT
LFA-1	lymphocyte function-associated antigen 1 (LFA-1)
LMO2	LIM domain only 2
LV	Lentiviral/*Lenti* virus
NV	*Nipah* virus
mAbs	monoclonal antibodies
MAGE	melanoma antigen
MART-1	melanoma-associated antigen recognized by T cells
mCD4	murine CD4
mCD8	murine CD8
MDC	Max-Delbrück-Centrum, Berlin, Deutschland
MHC	major histocompatibility complex
MiHA	minor histocompatibility antigens
MP71	Myeloproliferative sarcoma virus-derived promoter variant
MV	*Measles* virus
MVm4	MV-envelope-based pseudotyped gammaretroviral vector targeting murine CD4
MVm8	MV-envelope-based pseudotyped gammaretroviral vector targeting murine CD8
NKT cells	natural killer T cells
NSCLC	non-small cell lung cancer
NY-ESO-1	New York oesophageal squamous cell carcinoma 1
OVA	ovalbumin
P/S	Penicillin/Streptomycin
PAMPs	pathogen-associated molecular patterns
PMA	phorbol 12-myristate 13-acetate
PRR	pattern-recognition receptors
PCR	polymerase chain reaction
PD1	programmed cell death 1
PDL1	programmed cell death ligand 1
PEI	polyethylenimine
PBS	Phosphate-buffered saline
PKC	protein kinase C
PMA	phorbol-12-myristate-13-acetate
pMHC	peptide presented on MHC molecules
PR	partial response
PTK	Src-family protein tyrosine kinases
RAG	recombination activating genes
RLuc	Renilla luciferase
ROI	region of interest
RPMI	Roswell Park Memorial Institute medium
RV	retroviral vectors

SB	*Sleeping Beauty* transposon system
SEM	standard error of the mean
scFv	single-chain variable fragment
SCID	severe combined immunodeficiency
SCLC	small-cell lung cancer
SIRS	systemic inflammatory response syndrome
SMAC	supramolecular activation cluster
SMN1	survival motor neuron 1
SPF	specific pathogen-free
ss	single-stranded
TAA	tumour associated antigen
TME	tumour microenvironment
TCR	T cell receptor
TRA	TCR α-chain
TRB	TCR β-chain
Tfh	follicular B helper T cells
TIL	tumour-infiltrating lymphocytes
TNF	tumour necrosis factor
Treg	regulatory T cells
TRUCKs	T cells redirected for antigen-unrestricted cytokine-initiated killing
TU/ml	transducing units per ml
V	Variable
ZAP-70	Syk-family kinase ζ-associated protein of 70 kDa

5. Zusammenfassung

T-Zell-basierte Immuntherapie ist ein vielversprechender Fortschritt in der Behandlung von hämatologischen und soliden malignen Erkrankungen. Der T-Zell-Rezeptor (TCR) bestimmt die Spezifität von T-Zellen. Mittels TCR erkennen T-Zellen Epitope innerhalb von Peptiden, die durch Haupthistokompatibilitätskomplex-Moleküle (MHC) präsentiert werden. Derzeitige Immuntherapien fokussieren sich auf $CD8^+$ T-Zellen und vernachlässigen die Rolle von $CD4^+$ T-Zellen. Der Einschluss von $CD4^+$ T-Zellen würde eine umfassendere T-Zell-Antwort induzieren. Aktuelle Herstellungsprotokolle verwenden langwierige und kostspielige *ex vivo* Transduktion, ein Prozess, der nicht für die Herstellung gemischter T-Zell-Produkte geeignet ist. Das Ziel dieser Dissertation war der T-Zell-Subgruppen-spezifische *in vitro* und *in vivo* Gentransfer mittels Masernvirus (MV)-Hüllprotein-pseudotypisierter gammaretroviraler Vektoren (gRV). Diese Methode vereinfacht den Herstellungsprozess T-Zell-basierter Immuntherapien und umgeht die *ex vivo* T-Zell-Kultur. Im Rahmen dieser Dissertation wurden TCRs ausgewählt, die ein Modellantigen, *Influenza* A/PR/8/1934 H1N1 Hämagglutinin (HA), erkennen. Diese wurden sequenziert, optimiert und in MV-Hüllprotein-pseudotypisierte gRV, spezifisch entweder für CD4 (MVm4) oder CD8 (MVm8), integriert. Die verwendeten TCRs waren die zwei MHC Klasse I H-$2K^d$ restringierten TCR Clone 1 und Clone 4, sowie der MHC Klasse II H2-IE^d restringierte SFE TCR. Es wurden zwei Krebszelllinien für *in vitro* und *in vivo* Versuche ausgewählt, die eine Tumorerkrankung in immunkompetenten BALB/c Mäusen etablieren und Antigen-exprimierende Derivate dieser Zelllinien generiert. Mit den MV-Hüllprotein-pseudotypisierten gRV MVm4 und MVm8 wurden unsortierte Splenozyten *in vitro* transduziert und ein Transgen, kodierend für den passenden TCR für die jeweilige Subgruppe, übertragen. Transduzierte $CD8^+$ T-Zellen, die entweder Clone 1 oder Clone 4 TCR exprimierten, zeigten eine dosisabhängige IFNγ-Sekretion in Ko-Kultur-Experimenten nach Antigenstimulus, sowohl durch Peptid-beladene Splenozyten als auch durch Antigen-exprimierende Zelllinien. Demgemäß sekretierten SFE TCR-transduzierte $CD4^+$ T-Zellen dosisabhängig IL-2 in Ko-Kultur-Experimenten mit Peptid- oder Krebszelllysat-beladenen dendritischen Zellen. MVm4 and MVm8 wurden in einem *in vivo* Modell erprobt, indem sie systemisch BALB/c Mäusen appliziert wurden, um deren T-Zellantwort gegen HA-exprimierende Krebszelllinien zu richten. Homing, Expansion und Kontraktion der T-Zellen wurde über einen Zeitraum von 73 Tagen im Live-Imaging mittels,

neben dem TCR koexprimierter, Luziferase dargestellt. Zusammenfassend lässt sich sagen, dass das MV-Hüllprotein pseudotypisierte gRV-System die spezifische *in vivo* Transduktion von $CD8^+$ T-Zellen in BALB/c Mäusen zeigen konnte, weiterführend wurden erstmalig die zielgerichtete *in vivo*-Transduktion von $CD4^+$ T-Zellen und die resultierende MHC Klasse II-restringierte T-Zellantwort gezeigt.

6. Summary

T cell-based immunotherapy is a promising approach in treating haematological and solid malignancies. The specificity of a T cell is determined by its T cell receptor (TCR). The TCR recognizes epitopes within peptides that are bound to major histocompatibility complex (MHC) molecules. Current T cell-based therapies focus on $CD8^+$ T cells, disregarding the $CD4^+$ T cell population. The inclusion of $CD4^+$ T cells could lead to a more complete T cell response. Current manufacturing protocols utilise *ex vivo* transduction, a protracted and costly process unsuited for generating mixed T cell products. The aim of this thesis was to show subset-specific gene transfer targeting T cell subsets *in vitro* and *in vivo* with a gammaretroviral (gRV) vector system pseudotyped with a *Measles* virus (MV) envelope. This approach simplifies the manufacturing process of mixed therapeutic T cell products while bypassing *ex vivo* culture. In the scope of this thesis, TCRs targeting a model antigen, *Influenza* A/PR/8/34 H1N1 hemagglutinin (HA), were selected, sequenced, optimised, and integrated into MV-pseudotyped gRV specific for either CD4 (MVm4) or CD8 (MVm8). The TCRs used were two MHC class I H-$2K^d$-restricted TCRs called Clone 1 and Clone 4 as well as the MHC class II H2-IE^d-restricted SFE TCR. Two cancer cell lines capable of tumorigenesis in immunocompetent BALB/c mice were chosen for *in vitro* and *in vivo* evaluation, and derivate cell lines expressing the target antigen were generated. The MV-pseudotyped gRV vectors MVm4 and MVm8 were used to transduce unsorted splenocytes *in vitro*, delivering a transgene encoding for the model TCRs to their corresponding subsets. $CD8^+$ T cells transduced with either Clone 1 or Clone 4 TCR exhibited secretion of IFNγ relative to the dose of antigenic stimulus upon co-culture with peptide-loaded splenocytes and antigen-expressing cancer cell lines. Correspondingly, $CD4^+$ T cells transduced with the SFE TCR showed antigen-dependent secretion of IL-2 in co-culture experiments with dendritic cells loaded with peptide or cancer cell lysate. MVm4 and MVm8 were tested in an *in vivo* model - they were applied systemically to BALB/c mice to redirect their T cell response against the antigenic stimulus of HA-expressing cancer cells. Homing, expansion, and contraction of T cells was monitored via live imaging for a timeframe of 73 days by luciferases co-expressed with the TCR. In conclusion, the MV-pseudotyped gRV system was successfully adopted to BALB/c mice, confirming targeted *in vivo* transduction of $CD8^+$ T cells and providing the first

evidence of targeted *in vivo* transduction of $CD4^+$ T cells leading to a functional MHC class II-restricted T cell response.

7. Introduction

7.1. T cells and the immune system

7.1.1. Innate and adaptive immunity

The immune system is an organism's defence against infection and aberrant cells. In mammals, it can be divided into the innate and adaptive immune system, both of which need to able to differentiate self from non-self. The innate immune system employs pattern-recognition receptors (PRR), which recognize pathogen-associated molecular patterns (PAMPs), such as certain glycoproteins, nucleic acids, or foreign membrane structures, providing a fast-acting initial defence (1, 2). PAMPs are predefined and therefore limited in the number and diversity of targets. In contrast to the adaptive immune system, innate immunity can only recognize a fixed set of non-self structures. The innate immune system plays a vital role in the immediate immune response and is closely intertwined with the adaptive immune system (3-5).

Adaptive immunity is an intricate and highly developed system mediated by a diverse set of antigen receptors expressed on T cells and B cells, which are the main effector cells of the adaptive immune system. Both T and B cells are equipped with unique antigen receptors generated by somatic recombination, enabling them to elicit a specific immune response against virtually every pathogen. These receptors form a unique repertoire in every individual and can provide a long-lasting immunological memory to protect against recurring pathogens.

7.1.2. T and B cells

T and B cells are the central agonists of the adaptive immune response, and both are derivative of a common lymphoid progenitor arising from hematopoietic stem cells in the bone marrow. T and B cells can be distinguished by their antigen receptor. B cells produce antibody molecules, which in naïve and memory B cells are presented as part of the B cell receptor (BCR), and after activation they differentiate into plasma cells. Plasma cells secrete antibodies which are released into blood, tissue fluid and secretions, where they can encounter their specific antigen (6-8).

The functions of T cells are highly heterogenous, and they can be grouped into a variety of subsets. Two major subsets are called $CD8^+$ cytotoxic T cells and $CD4^+$ helper T cells. T cells have the capability to directly induce cell death, they can kill virus-infected cells and cancer cells, and they are able to secrete cytokines to recruit other immune cells. $CD4^+$ T cells aid the immune response indirectly; they orchestrate if and how other parts of the immune system respond to immunogenic insults. T cells recognize epitopes bound to major histocompatibility complex (MHC) molecules via an antigen receptor, called the T cell receptor (TCR), expressed on the cell surface (9-12). MHC molecules come in two varieties, MHC class I and II. MHC class I is typically found on the cell surface of every nucleated cell and is loaded with peptides - preferentially of a length of 8-9 amino acids - obtained by proteasomal degradation of proteins (13, 14). MHC class II is expressed by professional antigen presenting cells (APC). Dendritic cells (DC) are the most prominent representative of this group, but macrophages and B cells are also capable of antigen presentation on MHC class II. APC can process phagocyted cells, pathogens, and debris into peptides - preferentially of a length of 12-20 amino acids - and load them onto MHC class II molecules in a specialized compartment called a phagolysosome (15-17). $CD8^+$ T cells recognize epitopes presented on MHC class I, while $CD4^+$ T cells are restricted to MHC class II (11, 12).

7.1.3. The T cell receptor

A functional TCR is a heterodimer consisting of an α- and a β-chain. Both chains are made up of a constant (C) and a variable region (V). The variable region is, in the case of the TCR α-chain (TRA), made up of a variable (V) and a joining (J) segment, while the β-chain (TRB) has an additional diversity (D) segment, thus being made up by a VDJ-sequence (18-20). The constant regions of the TCR's α- and β-chains are interlinked via a disulphide bridge and anchored to the T cell membrane (21). The TCR α- and β-chains are flanked by transmembrane proteins called CD3, a complex made up of four chains: γ- δ- and two ε-chains. Together with two more polypeptides, called ζ-chains, they make up the TCR complex. The CD3 and ζ-chains provide the coupling of the TCR's signal to intracellular transduction pathways via immunoreceptor tyrosine-based activation motifs (ITAM) (22). Engagement of the TCR triggers phosphorylation of ITAM by Src-family protein tyrosine kinases (PTK), such as Lck and Fyn. Downstream signalling involves the phosphorylation of Syk-family kinase ζ-associated protein of

70 kDa (ZAP-70), which associates with the activated TCR complex. Adapter PTK are recruited, and a signalling complex is formed (23-26).

7.1.4. T cell maturation in the thymus

The lymphoid progenitors of T cells migrate to the thymus and enter without expression of their characteristic antigen receptor, the TCR. The main task of the thymus is the maturation of the residing T cell progenitors, called thymocytes, to generate T cells capable of differentiating self from non-self. This process involves positive and negative selection; positive selection to ensure that T cells recognize peptide bound to MHC, and negative selection to prevent autoimmunity. 'Double negative' thymocytes rearrange their TCRs in a process called somatic recombination, which is described below. After successfully rearranging their TCR they express CD4 and CD8, thus becoming 'double positive' $CD4^+CD8^+$ thymocytes. $CD4^+CD8^+$ T cells are selected for TCR affinity to self-peptide presented on MHC (27). In the thymic cortex, epithelial cells present self-peptides on MHC class I and MHC class II. Maturing T cells undergo positive selection to select for T cells with sufficient interaction and restriction to an individual's repertoire of MHC. Thymocytes weakly interacting with MHC receive survival signals, while those unable to interact sufficiently undergo neglect-induced apoptosis (28). This process restricts thymocytes to one type of MHC allele (29). Negative selection occurs when a thymocyte undergoes apoptosis due to too high affinity to self-pMHC as well as interaction with medullary thymic epithelial and dendritic cells (30, 31). This process deletes most TCRs with too high affinity for the presented self-peptides from the repertoire, preventing them from causing auto-reactivity resulting in autoimmune disease (32-34). A subset of high affinity $CD4^+$ T cells does not undergo apoptosis and differentiates into regulatory T cells inhibiting immune responses and counteracting autoimmunity (35, 36). Thymocytes' recognition of peptides presented on MHC class I or class II decides which T cell subset they are committed to. Thymocytes recognizing self-peptide bound to MHC class I become single-positive $CD4^-CD8^+$ T cells, also called cytotoxic T cells. Avidity to self-peptide presented on MHC class II leads to a differentiation resulting in single-positive $CD4^+CD8^-$ T helper cells (37). Thymocytes, having undergone positive and negative selection, leave the thymus as naïve T cells restricted to a singular, not yet encountered foreign peptide on a specific MHC allele.

7.1.5. The generation of T cell receptors by somatic recombination

The immense diversity of TCRs is enabled by a genetic rearrangement process called somatic recombination. T cell progenitors undergo this process during development in the thymus to rearrange a functional TCR. It is initiated by recombination activating genes (RAG) 1 and 2 in interaction with other factors; together they form the VDJ-recombinase complex (38-40). Mice deficient for either RAG-1 or -2 show an early arrest in T cell development (41, 42). Somatic recombination starts with the first β-DJC cluster of the β-chain by joining a β-D to a β-J segment, then a β-V is added. The resulting β-VDJ sequence is joined to β-C. If the resulting recombined β-chain is productive, it pairs with a germline-encoded α-chain and is expressed on the cell surface (43). A short period of proliferation follows, the rearrangement of the α-chain is initiated, and α-V and α-J are joined and fused to α-C (44). These cells make up the α:β T cell lineage, accounting for the vast majority of T cells. If the somatic recombination of the β-DJC fails on both chromosomes, thymocytes may rearrange the δ locus and enter a lineage called γ:δ T cells (45, 46).

The process of somatic recombination includes double-stranded DNA breaks, where one strand is cut imprecisely, then exonucleases and transferases add or subtract nucleotides (47). These hypervariable regions between segments - in the case of the β-chain, the V-D-J junction, and in the case of α-chain, V-J - are called complementary determining regions 3 (CDR3). The CDR3 is a TCR's most diverse region and provides the principal peptide binding residues. It is the main determinant of antigen specificity; its vital role in antigen recognition and exceptional diversity even allows for profiling the clonotypes of T cells (48-50).

7.1.6. T cell activation

When a naïve T cell encounters its specific pMHC it gets activated in a process referred to as priming. If the pMHC is presented by a DC, the T cell receives a first activating signal by the binding of the TCR complex and its co-receptor CD4 or CD8. The second signal is received by the binding of CD28 to the DCs costimulatory CD80 and CD86 which mediates an antiapoptotic response. The third signal consists of costimulatory cytokines and interleukins aiding proliferation and differentiation (51, 52). The initial encounter with its specific antigen induces the T cell to express Interleukin (IL)-2 and an IL-2 receptor (IL-2R) α-chain (CD25) which together with a β- (CD122) and γ-chain (CD132), making up the moderate affinity IL-2 receptor

of a naïve T cell, form a high affinity IL-2 receptor. IL-2, especially in conjunction with the co-stimulation of CD28, is a main driver for proliferation and differentiation of effector T cells (53, 54). The activated T cells cease to migrate and undergo clonal expansion and differentiation in the lymph node. These cells differentiate into effector and memory T cells in the case of $CD8^+$ T cells and in the case of $CD4^+$ T cells, dependent on co-stimulatory interleukins and cytokines, an array of effector cell types (55). These cells are then able to leave the secondary lymphoid organs and home to sites of inflammation.

7.1.7. T cell subsets

$CD8^+$ T cells can exert their function by directly interacting with targets, for example cells infected by a virus or malignant cells presenting mutated peptides. An initial contact of the $CD8^+$ T cell to a target cell is mediated by the binding of the T cells Lymphocyte function-associated antigen 1 (LFA-1) and CD2 to a target cell's intercellular adhesion molecule 1 (ICAM; CD54) and CD58. After recognition of the target peptide presented on a fitting MHC, $CD8^+$ T cells form a supramolecular activation cluster (SMAC), also called an immune synapse, a dynamic structure of concentric rings of protein clusters containing CD2, CD4, CD8, CD28, T cell-specific tyrosine kinases and the θ isoform of protein kinase C (PKC) in the centre, while proteins like LFA-1, talin, CD43, and CD45 cluster in the periphery. TCRs cluster in the central part of the SMAC as well as in the periphery in microclusters (56-59). The $CD8^+$ T becomes polarized and focuses the secretion of soluble effector molecules at the site of contact. These can be divided into cytotoxins and cytokines. Cytotoxins are stored in exocytotic vesicles, and they include perforin, granzymes and granulysin. Perforin can perforate a target-cell's membrane, while granzymes initiate apoptosis through activation of the caspase cascade (60). A second mode of action is mediated by membrane-bound proteins of the death receptor family, such as Fas ligand (CD95L) and CD40 ligand, binding to their counterparts Fas (CD95) and CD40 on target cells and initiating apoptosis (61-63). $CD8^+$ effector T cells also release cytokines which act locally and at a distance. The main effector cytokines released are interferon (IFN)γ and tumour necrosis factor (TNF)α. IFNγ induces expression of MHC class I and II, activates macrophages and inhibits viral replication (64-66). TNFα is a cytokine, activating the vascular endothelium, aiding mobilisation and extravasation of immune cells, modulating permeability of blood

vessels, and acting as an endogenous pyrogen. Both IFNγ and TNFα have been shown to promote tumour regression by causing ischaemia in tumours (67).

The term $CD4^+$ T cell covers a more diverse variety of subsets. $CD4^+$ T cells recognize their antigens bound to MHC class II on APC and play a central role in aiding other immune cells, controlling their growth and activation as well as guiding them to the site of inflammation. $CD4^+$ T cells polarize the immune response appropriate to the nature of an immunological insult via an array of soluble and membrane-bound effector molecules. Subsets of $CD4^+$ T cells include the classical subsets Th1, Th2 and regulatory T cells (Treg). Th1 effector molecules include IFNγ, TNFα and β, IL-2, IL-3, IL-10, and GM-CSF, supporting $CD8^+$ effector T cells directly and by activating other cells like macrophages. Th2 secrete IL-4, aiding T cell growth and survival, as well as B cell growth hormones such as IL-5, IL-9, and IL-13. Additionally, they express membrane-bound CD40L, inducing B cell proliferation and isotype switching (55, 68, 69). Treg differ from other $CD4^+$ T cells, as they fulfil an inhibitory role. Their main cytokines are IL-10 and TGFβ, and their roles include limiting an immune response, maintaining tolerance to self-antigens, as well as modulating and suppressing T cell differentiation and proliferation (70).

A minority called natural killer T cells (NK T cells) express a limited diversity of α:β TCR and play a role in early infections, and they recognize CD1 rather than MHC molecules. NK T cells are classified as T cells that react to α-galactosylceramide loaded onto CD1d multimers, while earlier definitions were limited to T cells co-expressing NK cell markers such as CD161 (71-73).

A second minority, γ:δ T cells, express a different kind of TCR, a heterodimer of a γ- and a δ-chain. Recent research has implied a broad spectrum of roles in tissue homeostasis and surveillance of infection (45, 46).

7.2. Cancer immunotherapies

The notion that the immune system is a powerful ally in the fight against cancer has been established for a long time. One of the oldest cancer immunotherapies was established at the end of the 19^{th} century. W. Coley demonstrated the effectiveness of using heat-inactivated bacterial extracts of *Staphylococcus pyogenes* and *Serratia marcescens* (Coley's toxins), to boost immunity, generating favourable results in a variety of cancers (74, 75). A distant cousin of Coley's toxins, that is still in use today, was published in 1976, showing the effectiveness of

bacillus Calmette-Guérin (BCG), an attenuated strain of *Mycobacterium bovis*, in the treatment of bladder cancer (76). Early experiments in the 20th century showed that mice from Germany inoculated with cancer cells derived from a sarcoma of a mouse from Japan resisted subsequent challenges of the same tumour, if they rejected the tumour initially (77). This was later attributed to MHC mismatches (78). A powerful new tool in the research of cancer immunotherapies was the use of inbred mice, established between 1909-1920, enabling researchers to rule out non-tumour specific effects, and leading to the discovery of tumour antigens in the following decades (79, 80). Experiments between 1943 and 1957 using methylcholanthrene-induced tumours provided major evidence that tumours express antigens, allowing them to be recognized by the adaptive immune system, and that immunization against them is feasible (81-83).

In 1959 and 1970 the theory of immune surveillance of cancer was proposed by L. Thomas and F. Burnet. This hypothesis claims that cancer cells constantly arise and are recognized and rejected by the immune system (84). Since then, this hypothesis has been challenged and modified several times, emphasizing the complex interplay between tumorigenesis and the immune system (85, 86). To this day, it is debated whether naturally arising tumours, in contrast to transplanted ones, are able to elicit an immune response capable of rejecting a tumour (87).

7.2.1. Checkpoint-inhibitor therapy

T cell activation is followed by negative regulation by potent inhibitory proteins called checkpoint molecules. The two most prominent examples are cytotoxic T lymphocyte antigen 4 (CTLA4) and programmed cell death 1 (PD1). CTLA4 is induced after T cell activation and inhibits T cells through several mechanisms, including binding to CD80/CD86 with higher avidity and affinity than CD28, thereby competing for co-stimulatory ligands (88, 89). The first antibody targeting CTLA4 approved for clinical use in the treatment of melanoma was Ipilimumab in 2011, and approval for renal cell carcinoma, non-small cell lung cancer (NSCLC), mesothelioma and microsatellite instability-high- or mismatch repair-deficient colon cancer followed, either as mono- or combination therapies, with several more active studies as of 2021 (90-93). PD1 is expressed on T cells after activation, and it binds to PDL1 and 2, both being homologous to B7. The primary inhibitory function of

PD1 is realized by dephosphorylation of the CD3 ζ-subunit and ZAP70, interfering with T cell activation and CD28 signalling (94-97). PD1/PDL1 engagement can lead to apoptosis, or a state called T cell exhaustion, a loss of function induced by chronic low antigen stimulation, although the exact mechanism is an active research topic (98, 99). While PDL1 or PDL2 overexpression have been shown in cancer cell lines to hamper $CD8^+$ T cell anti-tumour response, PD1 blockade has been shown to promote tumour rejection and, in mouse models, limit metastasis (100, 101). Pembrolizumab and Nivolumab were the first anti-PD1 monoclonal antibodies (mAbs) approved for clinical use in the treatment of refractory, unresectable melanoma in 2014 (102-105). In subsequent years, successful trials expanded the indications for pembrolizumab and nivolumab. Indications for pembrolizumab now include NSCLC, Hodgkin's lymphoma, gastric and gastroesophageal carcinoma, and urothelial carcinoma (106-108). Likewise, nivolumab is used in treating renal cell carcinoma, hepatocellular carcinoma, head and neck squamous cell carcinoma, Hodgkin's lymphoma, urothelial carcinoma and several others, along with even more ongoing trials (109-113). PDL1 has also been targeted successfully with atezolizumab, approved in 2016 for the treatment of urothelial carcinoma, with more recent indications being expanded to NSCLC, small-cell lung cancer (SCLC) and triple-negative breast cancer treatment (114-117). In 2017, two more mAbs targeting PDL1 - avelumab and durvalumab - entered the market. Duvalumab can be used in treating NSCLC and urothelial carcinoma, while avelumab is indicated in treating renal cell carcinoma, urothelial carcinoma, and Merkel cell carcinoma (118-122).

7.3. Adoptive T cell therapy

7.3.1. Unmodified T cells

Adoptive cell therapy (ACT) is an active field of research, showing promise for a variety of different malignancies. One of the earliest publications concerning the use of cell-based therapy for the treatment of tumours showed that tumour regression can be induced by autologous co-transplantation of leukocytes and tumour tissue (123). The first clinical use of ACT came with the advent of allogeneic haematopoietic stem cell transplantation (allo-SCT) in chronic myeloid leukaemia (CML), where an immune effect, called graft-versus-leukaemia (GVL) cleared residual malignant T cells. It was later shown that GVL can be attributed mainly to T cells, since donor grafts depleted them of increased risk of relapse (124, 125). This

immune response can also manifest as a systemic autoimmune disorder, mainly involving the skin, intestine and liver, termed graft-versus-host disease (GVHD), representing one of the most serious and difficult to treat complications of allo-SCT (126). Studies concerning allo-SCT corroborated the duality of T cell response in the setting of monozygotic twins and led to the identification of minor histocompatibility antigens (MiHA) presented on leukaemia cells being the targets for T cells (127, 128). The prognosis of patients suffering relapse after allo-SCT is very poor and therapeutic options are limited. Donor Lymphocyte infusions (DLI) can induce partial responses (PR) and complete responses (CR) in this dire setting. A drawback of DLI therapy is a high rate of complications in the form of GVHD (129-131).

7.3.2. Tumour-infiltrating lymphocytes

ACT employing tumour-infiltrating lymphocytes (TILs) was pioneered in the treatment of metastatic melanoma in 1988. TILs were isolated from melanoma biopsies, expanded using IL-2 and reinfused autologously with concomitant systemic IL-2 treatment of the patient. Patients thus treated had a response rate of 34%, but median responses lasted only 4 months, with few patients reaching a CR (132). These results were improved markedly in 2011 by the same group by pairing IL-2-expanded TIL-based therapy with lymphodepletion in metastatic melanoma, reaching CR in 22% of patients, with 19/20 of those in CR three years after treatment (133). More recent approaches employ TILs screened for recognition of neoantigens and knockdown of negative regulators of TCR signalling like cytokine-inducible SH2-containing protein (Cish) (134, 135). Strategies using TIL are limited to treating the tumour entities harbouring them. T cells expanded *in vitro* have been shown to have impaired effector function *in vivo*, despite excellent effector function *in vitro*. Progress has been made employing IL-15 and IL-21 to achieve T cell culture, generating a less differentiated T cell phenotype with enhanced *in vivo* persistence and anti-tumour efficacy (136-138).

7.3.3. Receptor-modified T cells

The specificity of a T cell is determined by its TCR; the transfer of a new receptor specific for a defined antigen can redirect the immunological function of T cells and employ them to treat malignancies (139). The two main strategies to genetically modify T cells are with a chimeric antigen receptor (CAR) or a new TCR. The manufacturing process for a CAR- or TCR-engineered

T cell product starts with leukapheresis from a patient, and the product is then cryopreserved and shipped to a manufacturing facility. The cells are thawed, T cell enriched and activated. The transgene encoding for the CAR or TCR is generally transduced via a viral vector, i.e., adenovirus, retrovirus, or lentivirus (LV), of which lentivirus has become the most common method. It has also been shown that transient expression of a receptor via electroporation using mRNA or stable integration into the genome using a transposon vector system termed *Sleeping Beauty* (SB) is feasible (140, 141). T cells are expanded *ex vivo,* and after sufficient expansion, the resulting cells are frozen in adequate numbers for therapy. After a conditioning chemotherapy regimen, the cells can be thawed and immediately transfused intravenously into the patient (142). Nonmyeloablative chemotherapy regimens have been shown to lead to higher rates of responses and improved engraftment of the transfused T cell product (143). The ideal T cell subsets to be used, due to their lytic capacity and ability to propagate, seem to be central memory or naïve T cells (144-146).

The main difference between both strategies is that CARs are synthetic receptors targeting antigenic molecules presented on the surface of malignant T cells and independent of MHC, while TCR-engineered T cells detect epitopes bound to MHC molecules. The lack of a restriction to specific MHC molecules makes CARs applicable for a broader spectrum of possible patients, but is limited to surface molecules, while TCR-engineered T cells can target epitopes derived from intracellular proteins as well. TCR-engineered cells are fully integrated into the T cells' physiological signal transduction pathways, encompassing more subunits in their receptor structure and encompassing a variety of co-stimulatory receptors, including CD3, CD4/CD8 and CD28. TCR-engineered T cells can therefore be capable of more extended cytosolic signalling than CAR T cells (see 7.1.3).

TCR-engineered T cells may have an advantage over CAR T cells, especially in treating solid tumours - these often lack unique surface markers, but even when this is the case, CAR T cells mainly home to the periphery of a solid malignancy to access surface antigen (147, 148). The ability of TCR-engineered T cells to recognize intracellular tumour associated antigens (TAA) may enable them to penetrate deeper into the tumour, an ability which may prove useful in addressing solid tumours in future clinical trials.

7.3.4. CAR T cells

The synthetic CAR typically consists of an extracellular single-chain variable fragment (scFv) derived from an antibody linked to signalling domains of a TCR - in the case of the first generation of CARs, the CD3 ζ-chain. In the second and third generations, intracellular co-stimulatory molecules, like CD28 and/or CD137, are linked additionally (99). Fourth generation CARs are referred to as 'T cells redirected for antigen-unrestricted cytokine-initiated killing' (TRUCKs). They are engineered to release transgenic cytokines upon CAR signalling, creating a pro-inflammatory milieu aiming to disrupt the inhibitory tumour microenvironment in solid malignancies. The panel of cytokines being explored includes IL-7, IL-12, IL-15, IL-18, and IL-23, with several being tested in early trials and a broader variety of therapeutically active molecules being developed (149). Efforts have also been made to enhance the therapy by co-delivering a PD-1-blocking scFv with CAR T cells (150). CAR T cell therapy targeting CD19 has found its way into the clinic for the treatment of refractory or relapsed B-cell lymphoma and refractory or relapsed B-cell acute lymphoblastic leukaemia (ALL), with the approval of the U.S. Food and Drug Administration (FDA) in 2017 for axicabtagen ciloleucel and tisagenlecleucel (151, 152). Two more CARs targeting CD19 were approved in 2020 and 2021, namely brexucabtagene autoleucel for relapsed or refractory mantle cell lymphoma based on the ZUMA-2 trial, and the latest, lisocabtagene maraleucel, for relapsed or refractory large B cell lymphoma after evaluation in the TRANSCEND trial. In this trial, 54% of patients reached CR, of which 62% had remission lasting at least 9 months (153, 154). Recently, in March 2021, the FDA approved the first CAR in the treatment of relapsed or refractory multiple myeloma. Idecabtagene vicleucel is a second-generation CAR targeting B cell maturation antigen (BCMA) containing a CD137 motif and a CD3-zeta signalling domain (155, 156).

Other targets investigated include CD20, CD22, CD276, G protein–coupled receptor, mesothelin, GD2 and many more (157-159). Despite the identification of numerous suitable targets, the therapeutic success of CAR T cell therapy could not be reproduced in solid tumours, where a broad immunosuppressive response was observed. A major strategy in further development is the disruption of this inhibitory milieu (149).

7.3.5. TCR-engineered T cells

In TCR-engineered T cells, a transgene encoding for α- and β-chain of an antigen-specific TCR is introduced. With a TCR, it is possible to target virtually any antigen, regardless of it being expressed solely intracellularly. The idea to employ tumour antigen-specific TCR in the treatment of cancer was formulated as early as publications concerning TCR function emerged (48). The first clinical trial of TCR-engineered T cells used the TCR DMF4 and DMF5 derived from TIL of melanoma patients targeting melanoma-associated antigen recognized by T cells (MART-1). MART-1 is overexpressed in melanoma cells, but also expressed on cells of melanocyte lineage in the skin and retina. The recognized epitope for both TCRs, 27-35 aa, is presented on HLA-A*02:01. DMF4 has a lower affinity to pMHC class I than DMF5. In the trial, either DMF4 or DMF5 TCR-engineered T cells were transfused in combination with high-dose IL-2 treatment. In the case of DMF4, only 2/17 patients had a PR; response in the case of DMF5 was better, with PR in six out of 20 patients, but at the cost of severe on-target side effects (160, 161).

Severe on-target toxicity and poor response rates were also reported in subsequent trials targeting the TAA gp100 and carcinoembryonic antigen (CEA). Although clinical response was low, these trials illustrated the potency of TCR-engineered T cells to overcome peripheral tolerance mechanisms (162).

On-target toxicity is caused by expression of the targeted antigen in normal tissue, while off-target toxicity is caused by cross-reactivity of the therapeutic TCR with other epitopes. This was tragically demonstrated in a clinical study where the affinity-enhanced, HLA-A*01-restricted TCR specific for melanoma antigen (MAGE) A3 peptide (EVDPIGHLY) caused lethal cardiotoxicity days after transfusion. Later studies revealed that the four introduced substitutions in CDR2α led to cross-reactivity targeting a peptide expressed by the titin gene in contracting heart muscle cells (163, 164). In 2011, results were published of the most successful trial yet, wherein patients with refractory metastatic melanoma or synovial cell sarcoma expressing the New York oesophageal squamous cell carcinoma 1 (NY-ESO-1) cancer/testis antigen were treated using affinity-enhanced TCR-engineered T cells. The TCR originated from a melanoma patient and was enhanced by substitution of two amino acids in the α-chain of the HLA-A*02 restricted NY-ESO-1 specific TCR (165). Four out of six patients with synovial cell sarcoma and five out of eleven patients with melanoma showed tumour

regression. Two out of eleven patients with melanoma even reached CR, lasting for over a year, and no major off- or on-target side effects were reported (166). TCR binding TAA with optimal affinity is a bottleneck of ACT, since T cells bearing high-affinity TCR specific for TAA are deleted in the thymus during T cell development. Transgenic mice harbouring the entire human TCRα and β gene loci and HLA-A*0201, called ABabDII mice, were published in 2010, enabling the generation of high-affinity human TCR recognizing self-antigens, like TAA. This was expanded upon in 2015, when it was shown that high-affinity TCR recognizing cancer/testis antigen MAGE-A1 showing an anti-tumour effect *in vivo* could be isolated using ABabDII mice (167, 168). A phase 1, single-centre, single-arm, open-label, dose-escalation trial is currently being conducted using this TCR in relapsed/refractory multiple myeloma. Four cohorts of patients, with three to six patients each, receive an autologous product of IMP T1367 T cells engineered with the MAGE-A1 specific TCR T1367 recognizing the MAGE-A1 derived nonamer epitope MAGE-A1(278-286) presented on HLA-A*02:01 (DRKS-ID: DRKS00020221).

7.4. Limitations of *ex vivo* cultured T cells

The major therapeutic limitations of current TCR-engineered T cell products include the manufacturing time needed, the effector function of T cells in the finished product and manufacturing failures. The socioeconomic limitations of this patient-specific therapy design include the availability being restricted to specialized centres and the often prohibitive cost of receptor engineered T cells. The CAR T cell therapies tisagenlecleucel and axicabtagen ciloleucel have an estimated cost of US$475,000 and US$373,000 per patient, which can even, in the case of complications, be significantly higher (169). Many patients fail to receive a finished T cell product, either due to disease progression during manufacturing or due to manufacturing failure, commonly caused by insufficient apheresis, issues during T cell activation and inadequate expansion of engineered T cells (170). T cell therapeutics are approved only for the treatment of refractory/relapsed malignancies. Time passing between the apheresis of T cells and the transfusion of the adoptive T cell product is critical for the success of therapy. In these late stages of tumour disease, often after second, third or an even later line of therapy, responses to bridging therapy are short lived, and tumour progress and clinical deterioration can be a contraindication for T cell therapy. T cell culture *in vitro* for

extended periods of time has been shown to hamper T cell effector functions and their ability to home and proliferate sufficiently. The efficacy of the T cell product is decreased even further by freeze-thaw cycles during production (136, 170) (see 7.3.3, page 13).

7.5. Viral vectors

Viral vectors have been used in research and in clinical trials for 40 years. Early trials focused on the treatment of single gene defects, these being deemed the most approachable targets. The main classes of viral vectors can be divided into two categories according to whether they can integrate transgenes into the host cellular chromatin - thereby enabling long-term transgene expression, or if they transiently persist in the cell as extrachromosomal episomes. RV vectors and LV vectors convey long-term transgene expression, while others such as adenoviral, adeno-associated viral and viral vectors derived from Herpes virus convey a short-term transgene expression (171). Gene therapy employing viral vectors experienced severe setbacks in early trials due to side effects. In 2002, an 18-year-old male was treated with adenovirus vectors for ornithine transcarbamylase deficiency and consequently suffered a fatal systemic inflammatory response syndrome (SIRS) (172). In 2000, a gene therapy employed a defective Moloney gamma-retrovirus-derived vector in treating X-linked severe combined immunodeficiency (SCID), a life-threatening disorder in which T and B cells cannot mature due to the absence of the common γ-subunit of the IL-2 receptor. Treatment was successful in 9 out of 10 patients, but it was overshadowed by a publication in 2003, followed by another in 2008, reporting the triggering of T cell leukaemia in four out of nine treated patients. This has been attributed to insertional mutagenesis causing aberrant expression of LIM domain only 2 (LMO2), a known T-cell oncogene (173-175). Despite these setbacks, efforts in vector engineering improving delivery and safety as well as the use of viral vectors have experienced a renaissance, with widespread use in research and clinical settings. Voretigen neparvovec, the first virally-delivered gene therapy, was approved in 2017. This adeno-associated virus vector-based gene therapy is indicated for treatment of patients with biallelic RPE65 mutation-associated retinal dystrophy (176, 177). Recently, in 2019, the FDA approved another adeno-associated virus vector-based gene therapy, onasemnogene abeparvovec-xioi, for treating spinal muscular atrophy caused by mutation of biallelic mutations in the survival motor neuron 1 (SMN1) gene (178-180). RV, either gRV or

LV vectors, are routinely used in a clinical setting in the transduction of T cells for CAR T cell therapy (181) (see 7.3.4, page 15).

7.5.1. Gammaretroviral vectors

Gammaretroviruses (gRV) are complex enveloped RNA viruses with a diploid single-stranded (ss) RNA genome consisting of at least four genes, i.e., gag, pro, pol, and env. Gag encodes the primary structural polyprotein, pro encodes the viral protease and the pol gene encodes for reverse transcriptase, RNase H, and integrase. The env gene is responsible for the virus's envelope, viral surface glycoprotein and transmembrane proteins, and responsible for binding to cellular receptors and membrane fusion (182-184). gRV have been used extensively in gene therapy and the treatment of monogenic disorders, cancer, and even infectious diseases, presenting the classic approach for long-term gene therapy. gRV can infect a wide variety of human and mouse cell types, and can accommodate up to 8 kb of foreign inserts which they can integrate into the host genome for long-term transgene expression (171, 185). gRV have been engineered extensively to facilitate high transgene expression and can be produced effectively via producer cell lines (185, 186). The broad tropism is an advantage for its application in *ex vivo* transduction, but a major obstacle for use in *in vivo* transduction. For *ex vivo* transduction protocols, the desired cell type can simply be selected for and transduced, while in *in vivo* transduction it is necessary to limit the tropism, ideally to a single desired cell type, to increase transduction efficiency, drastically reduce the number of viral vectors needed and avoid side effects.

7.5.2. Pseudotyping

The tropism of a gRV is receptor dependent and determined by its envelope. A method called pseudotyping operates on this principle by combining the envelope of a given virus with a gRV vector to transfer its specificity for target host T cells (187-189). Viruses with envelopes specific only for a desired cell type or receptor are exceedingly rare. Previous research succeeded in introducing a new specificity of a viral envelope by using scFv and detargeting it from its original receptors. These attempts resulted in several drawbacks - impaired membrane-fusion ability, inconsistent specificity, and low titres of viral vectors (190-195). Later research focused on two-component envelopes. Sindbis virus, an alphavirus, encodes

for two transmembrane envelope proteins called E1 and E2. E1 is responsible for pH-dependent fusion, and E2 for receptor binding with the fusion being independent of the binding of E2. gRV and LV were successfully pseudotyped using the Sindbis virus envelope and retargeted using scFv, in combination with mutated E2 protein, reducing its endogenous tropism (196-198).

7.5.3. Pseudotyping of lentiviral vectors using *Measles* virus envelope

A virus capable of pH-independent fusion with a two-component envelope is the *Measles* virus (MV). MVs only natural hosts are humans; it belongs to the *Morbillivirus* genus within the family of *Paramyxoviridae*. MV codes for two transmembrane envelope glycoproteins called hemagglutinin (H) and membrane fusion protein (F). H forms tetramers assembled from two disulphide-linked homodimers and is responsible for receptor binding. Four endogenous receptors for MV have been identified, i.e., CD46, CD150, nectin-4 and CD46, with CD46 not being targeted by wild MV strains typically, but acquired during years of *in vitro* culture (199). The synthesis of F is a multistep process. First, the inactive precursor F0 is cleaved by furin into two subunits. These subunits, F1 and F2, are disulphide linked and they oligomerize as homotrimers. Upon binding of H, engagement of F is triggered, resulting, after a series of irreversible conformational changes, in membrane fusion (200, 201). A LV vector pseudotyped with MV H and F and retargeted to CD20 was described in 2009. The detargeting of H for its endogenous specificities was achieved by point mutation of Y418A, R533A, S548L, and F549S in the H ectodomain. To yield high titres of viral vectors, truncated tail variants of H and F had to be used (202-204). This system has been translated to many different target receptors, including human CD8 and CD4, and has been proven to be capable of transduction *in vitro* and *in vivo* (205-207).

7.5.4. Pseudotyping of gammaretroviral vectors using *Measles* virus envelope

LV vectors have the ability to transduce a variety of human and murine cells, but murine T cells are exceedingly difficult to transduce using them. The MV-envelope-based pseudotyped LV system was transferred to gRV vectors by I. Edes (Max Delbrück Centre for Molecular Medicine in the Helmholtz Association, Berlin, Germany). Its capability to transduce murine T cells specific to their subset was demonstrated *in vitro* and *in vivo*. For this project, truncated H and

F variants were generated and tested in combinations in order to yield high titres of gRV vectors. ScFv specific for murine CD4 and CD8 (mCD4 and mCD8) were generated and cloned to be presented on H proteins.

The two targeting vectors specific for murine CD4 (MVm4) or CD8 (MVm8) were shown to be able to transduce $CD4^+$ and $CD8^+$ reporter cells specifically in mixed cultures delivering distinct transgenes. Primary C57BL/6 (B6)-derived $CD8^+$ T cells were transduced *in vitro* by MVm8, but C57BL/6 (B6)-derived $CD4^+$ T cells were not transduced by MVm4. Both targeting vectors were able to transduce their specific subset of primary BALB/c-derived T cells. The MVm8 vector had the capability to transfer T cell specificity against ovalbumin (OVA)-positive cancer cell lines by delivering the transgene of the TCR OT-I to B6-derived $CD8^+$ T cells. Finally, this project demonstrated the ability of MVm8 to deliver a large transgene, coding for OT-I and a luciferase, to $CD8^+$ T cells *in vivo*. RAG2-deficient mice were repopulated with polyclonal T cells derived from B6 mice, or monoclonal T cells derived from P14-TCR transgenic mice. After *in vivo* transduction, T cells demonstrated homing, expansion and contraction, and were able to convey resistance against infection in a challenge with OVA-transgenic *Listeria monocytogenes* (208).

8. Aims of the thesis

The aim of this thesis was to establish a tumour model on BALB/c-background, transferring the gRV system pseudotyped with a MV-based envelope (MVm8 and MVm4) from B6 and showing specific transduction of $CD8^+$ T cells and $CD4^+$ T cells *in vitro* and *in vivo*.

The gRV vector system was adapted from a LV vector system established in a previous project. It was shown to be capable of transducing C57BL/6-derived $CD8^+$ T cells *in vitro* and *in vivo,* but not $CD4^+$ T cells.

The first part of the project focused on selecting, sequencing, optimising, and cloning a set of TCRs targeting the same antigen - *Influenza* A/PR/8/34 hemagglutinin (HA). The TCRs used were two MHC class I H-$2K^d$-restricted TCRs called Clone 1 and Clone 4 as well as the MHC class II H2-IE^d-restricted SFE TCR.

The second part showed the stable transfection via electroporation of two suitable progressor cancer cell lines, named AB1 and 4T1, using the *Sleeping Beauty* transposon system. AB1 and 4T1 were stably transfected with the transgene coding for the TCR's target antigen HA and thus derivative cell lines were generated. The cell lines were then characterised, and a staining protocol was established.

The third part was related to the transduction of cell lines and primary BALB/c-derived splenocytes *in vitro* and the characterisation of T cells transduced with the TCRs in co-culture settings with peptide presented on splenocytes, APC and the established HA-presenting cell lines.

Lastly, the MVm8- and MVm4-pseudotyped gRV system was used to demonstrate for the first time that targeted and simultaneous *in vivo* transduction of primary murine T cells with MHC class I and MHC class II-restricted TCRs is feasible. The transduced T cells expressed a TCR which was linked to a luciferase and *in vivo* imaging was performed to visualize their stable transduction, proliferation, homing and retraction.

9. Materials and Methods

9.1. TCR chain subtype and CDR3 identification

Cryopreserved splenocytes of three different mouse strains, harbouring three HA-specific TCR transgenes coding for the MHC class I-restricted Clone 1 TCR and Clone 4 TCR as well as the MHC class II-restricted SFE TCR, were kindly provided by L. Sherman (The Scripps Research Institute, La Jolla, California, USA). The TCRs are discussed in depth later (see 10.1, page 35). The mouse strains from which the splenocytes were isolated are listed in Table 1. $1*10^7$ splenocytes of each strain were thawed, pelleted, and lysed. Total RNA was extracted, and cDNA was synthesized.

Table 1 Mouse strains harbouring TCR transgenes

Mouse strain	**TCR transgene**	**Reference**
CBy.Cg-Thy1a Tg(TcraCl1,TcrbCl1)1Shrm/J	Clone 1	(209-211)
B10.Cg-H2d Tg(TcraCl4,TcrbCl4)1Shrm/ShrmJ	Clone 4	(211-213)
C.Cg-Tg(Tcra/Tcrb)1Vbo/AjcaMmjax	SFE	(214-220)

The primers listed in Table 2 were designed to amplify and identify the TCR α- and β-chain allele of the TCRs, as well as the complementarity-determining region 3 (CDR3). Sequences were analysed (Eurofins Genomics) and compared to the IMGT/V-QUEST reference directory (221).

Table 2 List of primers used for TCR chain subtype and CDR3 identification

Name	**Sequence**	**Purpose**
Clone1alpha-forward	ATTTCCCTAGTGGTCCTGTGGC	Identification of Clone 1 α-chain subtype and CDR3
Clone4alpha-forward	TGAAGAGGCTGCTGTGCTCTC	Identification of Clone 4 α-chain subtype and CDR3
SFEalpha_1-forward (TRAV6)	TGAACTCTTCTCCAGGCTTCGTG	Identification of SFE α-chain subtype CDR3

SFEalpha_2-forward (TRAV6-5)	TGGAGACTCGGTGACTCAGAC	Identification of SFE α-chain subtype and CDR3
Vbeta8.2-forward	ATGGGCTCCAGGCTCTTCTTC	Identification of Clone 1, Clone 4, SFE β-chain subtype and CDR3
TRAC-reverse	TCGGTGAACAGGCAGAGGGT	Identification of Clone 1, Clone 4, SFE α-chain subtype and CDR3
TRBC-reverse	CAAGCACACGAGGGTAGCCTTT	Identification of Clone 1, Clone 4, SFE β-chain subtype and CDR3

9.2. Techniques of molecular biology

RNA extraction was performed using the RNeasy Mini Kit (Qiagen, Hilden, Germany) according to the manufacturer's instructions. cDNA was transcribed using SuperScript II Reverse Transcriptase (Thermo Fisher Scientific) and Oligo(dT)20 (Thermo Fisher Scientific) according to the manufacturer's instructions. Polymerase chain reaction (PCR) was performed according to manufacturer's information using the Phusion High-Fidelity or Taq PCR Kit with the provided GC- or HF-buffer (all Thermo Fisher Scientific). PCR Products underwent gel electrophoresis and were purified via Invisorb Fragment CleanUp (Stratec Biomedical, Berlin, Germany). Restriction digests were performed using enzymes listed in Table 3 (all Thermo Fisher Scientific). All restriction enzymes create sticky ends, except Bst1107I which creates a blunt end. Religation of plasmid backbones was prevented by two rounds of dephosphorylation via Calf Intestinal Alkaline Phosphatase (CIP, Roche, Basel, Switzerland) according to the manufacturer's details. For blunt-end cloning of 506-SB-HA-IRES-GFP DNA polymerase I, Large (Klenow) Fragment (New England Biolabs, Ipswich, Massachusetts, USA) was used before ligation was performed using the Rapid DNA Ligation Kit (Roche) as specified by the supplier. Verification of products was performed via Sanger sequence analysis (Eurofins Genomics, Ebersberg, Germany). Amplification of plasmid DNA was achieved by heat-shock

transformation of chemo-competent bacteria MACH-1 (Thermo Fisher Scientific). Plasmid DNA was isolated using the Invisorb Spin Plasmid Mini Two Kit (Stratec) and for large quantities the Plasmid Maxi Kit (Qiagen).

9.3. Construction of MP71- and 506-SB-plasmids

Clone 1, Clone 4, and SFE TCR constructs flanked by the desired restriction enzyme recognition sites and codon optimized were planned using Clone Manager (Sci-Ed, North Carolina, USA), custom ordered using GeneArt (Thermo Fisher Scientific) and cloned into MP71-plasmid sites (Table 3). Plasmids intended for production of viral vectors used in *ex vivo* transduction were derived from the MP71-OT1. Plasmids destined for *in vivo* transduction were derived from either MP71-OT1-P2A-FLuc or MP71-OT1-P2A-RLuc. MP71-OT1-P2A-FLuc and MP71-OT1-P2A-RLuc contain a P2A element linking the TCR construct to one of two *in vivo* reporter genes, FLuc or RLuc, and were supplied by I. Edes (208).

The DNA sequence of *Influenza* A/PR/8/34 H1N1 HA was obtained from the NIAID Influenza Research Database (IRD); the nucleotide sequence of *Influenza* A/PR/8/34 H1N1 (GCA_000865725.1) was first published by G. Winter et al. in 1981 and was available from the European Nucleotide Archive (ENA) (222, 223). A plasmid was custom ordered using GeneArt (Thermo Fisher Scientific) and cloned into MP71-IRES-GFP, linking hemagglutinin via an internal ribosomal entry site (IRES) to a green fluorescent protein (GFP) reporter gene. The transgene was subsequently cloned into a *Sleeping Beauty* (SB) transposon plasmid for electroporation. The 506-SB-GFP plasmid was kindly supplied by J. Clauss (Max-Delbrück-Centrum, Berlin, Deutschland) (224).

Table 3 List of generated Plasmids

Plasmid	**Origin**	**Restriction enzymes used**	**Purpose**
MP71-Clone 1	ordered plasmid, MP71-OT1	Not1, EcoR1	*ex vivo* transduction
MP71-Clone 1-P2A-FLuc	ordered plasmid, MP71-OT1-P2A-Fluc	Ade1, EcoR1	*in vivo* transduction

MP71-Clone 4	ordered plasmid, MP71-OT1	Not1, EcoR1	*ex vivo* transduction
MP71-Clone 4-P2A-FLuc	ordered plasmid, MP71-OT1-P2A-Fluc	Ade1, EcoR1	*in vivo* transduction
MP71-SFE	ordered plasmid, MP71	Not1, EcoR1	*ex vivo* transduction
MP71-SFE-P2A-RLuc	ordered plasmid, MP71-OT1-P2A-RLuc	BstX1, EcoR1	*in vivo* transduction
506-SB-HA-IRES-GFP	506-SB-GFP, MP71-HA-IRES-GFP	Not1, EcoR1, Sal1, Bst1107I	AB1HA, 4T1HA

9.4. Cell culture

The AB1 cell line (CBA-0144, CellBank Australia, Westmead, New South Wales, Australia) was kindly provided by D. Klatzmann (225). It is a BALB/c-derived mesothelioma cell line. AB1 cells were harvested from peritoneal fluid after stimulation with crocidolite asbestos; they are fibroblast-like and tumorigenic in immunocompetent BALB/c mice (see 10.2, page 37). The AB1 cell line and its derivative AB1 HA were cultured in Roswell Park Memorial Institute 1640 medium (RPMI, Thermo Fisher Scientific), supplemented with 10% FCS (PAN-Biotech, Aidenbach, Germany) and 100 IU/ml of penicillin/streptomycin (P/S, Thermo Fisher Scientific).

The 4T1 cell line (ATCC CRL-2539, American Type Culture Collection, Manassas, Virginia, USA) was also provided by D. Klatzmann. It is a derivative of 410.4, formerly referred to as 4T01 (226, 227). 410.4 was isolated from a spontaneously arising mammary tumour of a BALB/cfC3H mouse. The 4T1 line grows aggressively and spreads metastatically in immunocompetent BALB/c mice. The 4T1 cell line and its derivative 4T1 HA were cultured in Dulbecco's Modified Eagles Medium (DMEM, Thermo Fisher Scientific), supplemented with 10% FCS (PAN-Biotech) and 100 IU/ml of P/S (Thermo Fisher Scientific) (see 10.2, page 37).

293T (ATCC: CRL-3216), a variant of the Human Embryonic Kidney 293 cell line (HEK-293) expressing the SV40 Large T-antigen, was cultured in DMEM supplemented with 10% FCS and 100 IU/ml of P/S, unless otherwise specified.

The 6.5 hybridoma producing the clonotypic 6.5 mAb was kindly provided by L. Klein, thanks to the recommendation of H. von Boehmer (214). It secretes a clonotypic mAb specific for the SFE TCR. It was cultured in RPMI (Life Technologies) supplemented with 5% FCS (PAN-Biotech) and 100 IU/ml P/S (Life Technologies), unless otherwise specified (see 10.4, page 42).

The $CD4^+$ $CD8^-$ 58m4 and the $CD4^-$ $CD8^+$ 58m8 cell lines were established and provided by I. Edes (208). They are derivatives of the 58 α^- β^- T cell line, which itself is a TCR-deficient derivate of the $CD4^-$ $CD8^-$ BW5147 thymoma cell line (228, 229). They were cultured in T cell medium (TCM, RPMI, 1% P/S, 1% Sodium pyruvate, 1% non-essential amino acids [all Thermo Fisher Scientific] and 10% FCS [PAN-Biotech]). All cell lines were cultured at 37°C, 5% CO_2.

9.4.1. Generation of AB1 HA and 4T1 HA

The cancer cell lines AB1 HA and 4T1 HA were derived from AB1 and 4T1 cells via electroporation (see 10.2, page 37). The Amaxa human T-cell Nucleofector Kit (Lonza, Basel, Switzerland) was used according to the manufacturer's instructions. AB1 or 4T1 cells ($1*10^6$ cells each) were suspended in 100 µL of electroporation buffer, supplemented with 10 µg of 506-SB-HA-IRES-GFP DNA and 7 µg of *Sleeping Beauty* transposase SB100X RNA prepared from pcDNA3.1 (Thermo Fisher Scientific, Dreieich, Germany) and kindly provided by J. Clauss.

For the generation of AB1-HAiGFP program A023 was used, and for 4T1-HAiGFP it was program T024. Electroporated cells were resuspended in TCM and incubated for 72 h. The electroporated cells were single-cell sorted based on GFP expression into 96-well plates.

9.5. Large scale virus production

Substantial amounts of virus were required for *in vivo* transduction. This was achieved by transient transfection of 293T cells. $1.4*10^7$ 293T cells were seeded into T175 flasks 20 h prior to transfection. Once a confluence of 80% was reached, the culture medium was exchanged for 11 ml of DMEM without supplements to achieve minimal coverage of cells. The transfection protocol was performed at room temperature in sterile conditions. 70 µl of 18 mM branched polyethylenimine (PEI, average Mw ~25,000 by LS, average Mn ~10,000, branched, Sigma Aldrich, Seelze, Germany) were added to 310 µl of 5% glucose (Merck,

Darmstadt, Germany). For each batch, four different plasmids were used (see Table 4 and below).

Table 4 Plasmids used in large scale virus production

Plasmid	**Properties**	**Ratio of plasmid DNA used in large scale virus production**	**Provided by**
MVm4/MVm8	mouse CD4 or CD8-alpha-specific MV-derived H variant HΔ21A	0.06	I. Edes, MDC, Berlin, Germany
MV FΔ24	MV-derived F variant FcΔ24	0.31	I. Edes, MDC, Berlin, Germany
TCR/TCR-Luciferase retroviral vector	constructs listed in Table 3	0.95	Generated in this thesis (Table 3)
pcDNA3.1-MLVg/p	gag/pol	1	C. Baum, Medical School Hannover, Hannover, Germany

1. The MVm4 or MVm8 plasmid encoding for the retargeted MV hemagglutinin HΔ21A variant specific for murine CD4 and murine CD8α.
2. The FΔ24 plasmid, encoding for the FΔ24 variant of the MV fusion protein.
3. pcDNA3.1-MLVg/p encoding the Moloney MLV gag/pol genes kindly provided by C. Baum (Medical School Hannover, Hannover, Germany).
4. One of the TCR/TCR-Luciferase retroviral vector constructs listed in Table 3.

The plasmids were mixed in a ratio of 0.06:0.31:0.95:1 for a total 35 µg of DNA, to which 310 µl of 5% glucose (Merck) were added. The glucose solutions containing PEI and DNA were vortexed separately at low revolutions for 1 min and incubated for 10 min, then mixed for 1 min and incubated for an additional 10 min. DMEM without supplements was added to a

total volume of 3 ml, which was added to the cell flask. After six hours of incubation, FCS was added to a concentration of 10%. After 48 h of incubation, the supernatant was harvested and passed through a 0.45 µm filter into ice-cooled thin wall polypropylene tubes (Beckman-Coulter, Brea, CA, USA). A layer of 4.5 ml of 20% sucrose (Sigma, Kawasaki, Japan) was underlayed and the tubes were placed in a pre-cooled (4°C) SW 32 Ti swinging-bucket rotor in an Optima XPN-80 Ultracentrifuge (both Beckman-Coulter, Brea, CA, USA). The supernatant was centrifuged at 100 000g, 4°C for 3 h and discarded. The pellet was gently resuspended by pipetting 40 times in 100 µl of DPBS (Gibco, Thermo Fisher Scientific).

9.5.1. Titration of MVm8- and MVm4-vectors

Titres of MVm8- and MVm4-pseudotyped gRV vector batches were tested by transduction of duplicates of 58m8 or 58m4 cells in serial dilution. Titrations were performed in 96 round-bottom well plates. In the first row of wells, 5 µl of virus particles suspended in DPBS were added to 195 µl of T cell medium. The following well contained 100 µl of T cell medium which was mixed with 100 µl of medium from the first well. This serial dilution was performed 9 times. To each well, $1*10^4$ 58m4 or 58m8 cells in 100 µl TCM enriched with protamine sulfate in a concentration of 8 µg/ml (Sigma Aldrich) were added. After 48 h of incubation, cells were stained using the mouse anti-Vβ8.1/8.2 antibody (Table 5). Transduction rates between 1% and 30%, determined by FACS analysis, were used to calculate the titre of the batch.

9.6. Antibodies

9.6.1. Anti-SFE TCR antibody production

The 6.5 hybridoma cell line was cultivated in RPMI containing 5% FCS and 1% P/S. A culture of 6.5 cells was kept for 10 weeks. The concentration of FCS in the culture medium was lowered every two weeks to 4%, 3% and 2%. After expanding at 2% FCS concentration for a month, the cells were transferred into RPMI medium without additives (0% FCS) and cultivated for four days. The cells were pelleted by centrifugation (10,000 g for 20 min) and discarded. The resulting 1.5 l of supernatant was mixed with 4.1 M saturated ammonium sulfate solution to a final saturation of 45% ammonium sulfate and cooled to 4°C for 12 h. The precipitate was pelleted by centrifugation (4,000 g for 20 min at 4°C) and dissolved in 300 ml PBS. The antibodies were further purified by Protein A column (Thermo Fisher Scientific) according to

the manufacturer's instructions. As the elution buffer, 0.1 M glycine-HCL (pH 2.8) was used, and tris-HCL (pH 9) was used to neutralise the resulting antibody solution. Sodium azide was added to a final concentration of 0.01% as a preservative. The concentration was determined using absorbance at 280 nm and diluted to 0.2 mg/ml.

9.6.2. Antibody staining and flow cytometry

Cells were stained with antibodies, or the tetramer listed in Table 5. Surface antigens were stained by incubating up to $1*10^6$ cells in 100-200 µl of PBS with 1 µg of antibody for 30 min at 4°C. Antibodies were conjugated to fluorophores as listed, except for the HA-specific PY102, kindly provided by P. Palese (Icahn School of Medicine at Mount Sinai, New York, USA), and the clonotypic 6.5 antibody specific for SFE TCR (see 10.4, page 42). These were stained with 1 µg of secondary antibodies for an additional 30 min at 4°C. The fluorophores used were allophycocyanin (APC), fluorescein (FITC), and phycoerythrin (PE). Staining of the Clone 1 and Clone 4 TCR with the H-$2K^d$-Influenza-HA-tetramer-IYSTVASSL-PE (MBL International, Woburn, Massachusetts, USA) was performed for 1 h at 4°C according to the manufacturer's instructions. To discriminate living from dead cells, a staining with SYTOX Blue Dead Cell Stain (Thermo Fisher Scientific) was performed. Before analysis, cells were washed in PBS twice. Flow cytometry was performed using MACSQuant (Miltenyi Biotec, Teterow, Germany). Flow cytometry data was analysed using FlowJo v10.07 (BD Biosciences).

Table 5 Antibodies and tetramer used in flow cytometry

Specificity	**Type**	**Specification**	**Clone**	**Conjugated fluorophore**	**Supplier/ origin**
Mouse CD4	Primary antibody	Rat IgG2a	RM4-5	APC/PE	BioLegend
Mouse CD8	Primary antibody	Rat IgG2a	53-6.7	APC/PE	BD Biosciences
Mouse TRBC	Primary antibody	Hamster IgG	H57-597	APC	BioLegend

Mouse Vβ8.1/2	Primary antibody	Rat IgG2a	KJ16-133.18	APC/PE	BioLegend
HA (A/PR8/1934)	Primary antibody	Mouse Ig	PY102		
SFE-TCR	Primary antibody	Rat IgG2b	6.5		
Rat IgG2b	Secondary antibody	Mouse IgG1	MRG2b-85	FITC	BioLegend
Mouse IgG / mouse IgM	Secondary antibody	Goat Ig	Polyclonal	FITC/APC	BD Biosciences
H-2K^d-YISTVASSL specific TCRs (Clone 1 and Clone 4)	Tetramer	MHC class I H-2K^d tetramer		PE	MBL

9.7. Co-culture and ELISA assays

Effector cells were BALB/c-derived primary T cells transduced with the MV-pseudotyped gRV encoding for Clone 1, Clone 4 or SFE TCR. For each assay, $5*10^4$ effector cells in 100 µl of TCM were seeded into the wells of 96-well round-bottom plates. Target T cells for the MHC class I-restricted TCR-transduced T cells were peptide-loaded BALB/c-derived-splenocytes, AB1 HA- or 4T1 HA-lysate-loaded-splenocytes, and AB1 HA or 4T1 HA cancer cells. For T cells transduced with the MHC class II-restricted SFE-TCR, peptide-loaded, AB1 HA-loaded or 4T1 HA-lysate-loaded DCs were used. DCs differentiated from BALB/c bone marrow were kindly provided by M.-C. Ku.

Co-culture assay target cells and effector cells were seeded in a 1:1 ratio. 1 µmol of ^{518}IYSTVASSL^{526}-peptide (Table 6) was added and seven sequential steps of 1:10 dilution were performed. For SFE-peptide co-culture assays, 1 µmol of ^{518}IYSTVASSL^{526} (Table 6) was added

and seven sequential steps of 1:10 dilution were performed. DC were incubated with peptide for 24 h at 37°C and 5% CO_2 prior to the co-culture assay. For HA-bearing cancer cell lysate co-cultures, DC were incubated with cancer cell lysate for 24 h prior to co-culture assay. The lysate was produced by subjecting $1*10^4$ cancer cells in 100 µl of TCM, either AB1 HA or 4T1 HA, to three freeze-thaw cycles in liquid nitrogen and a 37°C water bath. Then, five sequential steps of 1:3 dilution were performed. Untransduced effector cells, effector cells transduced with an irrelevant TCR, and target cells without antigen were used as negative controls. T cells stimulated by 1 µM ionomycin (Calbiochem) and 5 ng/ml phorbol 12-myristate 13-acetate (PMA, Promega) were used as positive controls. Co-culture assays were incubated at 37°C and 5% CO_2. The resulting supernatant was harvested after 24 h and analysed for either IFNγ- or IL-2-secretion. IFNγ- or IL-2- Enzyme-linked Immunosorbent Assay (ELISA, BD Biosciences) was performed according to the manufacturer's protocol.

Table 6 Peptides used in co-culture assays

Recognizing TCR	**Amino acid-sequence**	**Origin**	**Restriction**	**Supplier**
Clone 1/Clone 4-peptide	IYSTVASSL	*Influenza* A/PR/8/34 H1N1, Hemagglutinin 533-541	H-2K^d	MBL
SFE-peptide	SFERFEIFPK	*Influenza* A/PR/8/34 H1N1, Hemagglutinin 107–119	I-E^d	Biomatik

9.8. BALB/c-derived splenocytes

Mouse experiments were performed according to the mouse experiment application G0131/14 approved by the State Office for Health and Social Affairs (LAGeSo) on 10.07.2014.

9.8.1. Isolation of splenocytes

BALB/c mice (Taconic, Boston, Massachusetts, USA) were bred in house and kept under specific pathogen-free (SPF) conditions. Mice were sacrificed and the spleen was removed and passed through a 40 µm cell strainer (BD Biosciences); the cell strainer was rinsed with 5 ml RPMI (Thermo Fisher Scientific). The single cell solution was centrifuged at 300 g for 6 min, the supernatant was discarded, and 2 ml Ammonium-Chloride-Potassium (ACK) Lysing Buffer

(1 mM KHCO3, 100 nM EDTA [both Roth, Karlsruhe, Germany] 50 mM NH4Cl [Merck]) was added. After 5 minutes, 9 ml of RPMI were added followed by centrifugation. The supernatant was replaced with RPMI and the cell pellet was resuspended for further purpose.

9.8.2. Magnetic-activated cell sorting (MACS)

To isolate $CD4^+$ or $CD8^+$ T cells from total splenocytes, anti-mouse-CD4 or -CD8 antibodies were employed (Table 5). MACS was performed using EasySep Magnet and EasySep Mouse PE Positive Selection Kit (both Miltenyi Biotec, Bergisch Gladbach, Germany) according to the manufacturer's instructions.

9.8.3. BALB/c-derived splenocyte culture

Primary murine splenocytes were cultured in T cell medium supplemented with 0.1 µg/ml anti-mouse CD28, 1 µg/ml anti-mouse CD3 (both BD Biosciences, Pharmingen, Heidelberg, Germany), and 10 U/ml recombinant IL-2 (Chiron, Marburg, Germany) and kept at $2*10^6$ cells/ml. After 24 h of incubation, the cells were transduced *in vitro* or used for repopulating BALB/c $Rag2^{-/-}$ mice for later *in vivo* transduction.

9.9. Transduction

9.9.1. *In vitro* transduction

24-well non-tissue culture plates were coated with 0.5 ml/well RetroNectin (12.5 µg/ml, TaKaRa, Saint-German-en-Laye, France) overnight at 4°C. The activated splenocytes were seeded at $1.2*10^6$/well/ml. Dynabeads Mouse T-Activator anti-CD3/anti-CD28 (Thermo Fisher Scientific) was added to a concentration of $1*10^4$/ml. 1 ml virus supernatant supplemented with protamine sulfate (8 µg/ml) and IL-2 (40 U/ml) was added. After centrifugation for 90 min at 800 g, 32°C, the plates were incubated at 37°C and 5% CO_2. The efficiency of transduction was determined 48-56 h later via flow cytometry, and co-culture assays were performed 10-12 days after.

9.9.2. *In vivo* transduction

BALB/c-derived splenocytes were isolated and cultured as described above. After one day of culture, the splenocytes were washed in PBS twice and injected into BALB/c $Rag2^{-/-}$ i.v.

retro-orbitally. Inhalational anaesthesia using isofluran-O_2-mixture was used for all injections. The isolated splenocytes were pooled; on average one spleen yielded enough splenocytes to repopulate two BALB/c Rag2$^{-/-}$ mice. Approximately 6*10^6 splenocytes resuspended in 200 µl PBS were used to repopulate one mouse. Twenty-four hours after injection of splenocytes, mice were injected with 200 µl PBS containing approximately 2*10^6 viral vector particles of either MVm8/Clone 1-FLuc, MVm8/Clone 4-FLuc or MVm4/SFE-RLuc, or 200 µl PBS without viral vectors. The priming was performed 5 days later by injecting irradiated AB1 HA cells subcutaneously (s.c.) into the right flank; per mouse 5*10^6 AB1 HA cells in 200 µl were irradiated with 65 Gy. Priming was defined as day 0; an antigenic boost was performed on day 65, using 5*10^6 AB1 HA cell/200 µl irradiated with 65 Gy and injected s.c. into the contralateral flank.

9.9.3. *In vivo* imaging

Mice were sedated by inhalational anaesthesia using isofluran-O_2 mixture. Mice transduced with MVm8/Clone 1-FLuc or MVm8/Clone 4-FLuc were injected i.v. retro-orbitally with luciferin (Biosynth, Staad, Switzerland) at a concentration of 300 mg/g body weight in PBS for a total volume of 100 µl. Mice transduced with MVm4/SFE-RLuc were injected in the same manner with 100 µl of coelenterazin (Biosynth) dissolved in DMSO at a concentration of 1 µg/µl. Mice were imaged under anaesthesia lying on their backs and using the Xenogen In Vivo Imaging System (IVIS) 200 (Caliper Life Science, Hopkinton, Massachusetts, USA). The exposure time was set for 60 sec. LivingImage analysis software (Caliper Life Science) was used for analysis. For the region of interest (ROI), the whole mouse was selected excluding only the mouse head and tail.

9.10. Data analysis

Tumour growth, co-culture and *in vivo* transduction data was analysed using GraphPad Prism 9 (GraphPad, La Jolla, California, USA). Co-Culture data is shown as mean and the standard error of the mean (SEM). Mean functional avidity (EC50), was calculated as a non-linear fitting of an asymmetric five parameter logistic model.

10. Results

10.1. Detection of TCR chain subtypes and CDR3 regions

To transfer the MV-envelope-based pseudotyped gRV system to BALB/c mice and to verify its transduction capability *in vitro* and *in vivo,* a tumour model had to be established. This involved the identification and characterisation of a set of TCRs that recognize the same antigen restricted to MHC alleles present in BALB/c mice. To show specific transduction and functionality of $CD8^+$ T cells and $CD4^+$ T cells, at least one TCR had to be restricted to MHC class I and another to MHC class II.

The set of TCRs used in this project recognize the same antigen, HA of *Influenza* A/PR/8/34 H1N1. All of the chosen TCRs recognize their epitopes restricted to MHC molecules found in BALB/c mice. A literature search was performed to determine the characteristics and structure of the TCRs. It was needed to know at least part of the α- and β-chain to design suitable primers for the sequencing of the TCRs. Clone 1 and Clone 4 TCR recognize the same epitope on HA (^{518}IYSTVASSL^{526}), which is presented on mouse MHC class I H-$2K^d$. Clone 1 is a low-avidity TCR generated by L. Sherman et al. in 1999 by intraperitoneal immunization of D2 mice with HA. The TCRs' α-chain was reported as being encoded by Vα1 and Jα11, the beta chain of Vβ8.2/D/Jβ2.4 (211). In 2005, a mouse transgenic for Clone 1 TCR was generated to study low avidity, self-specific T cells directed against insulin-producing β cells of the pancreatic islets in mice transgenic for HA (Ins-HA) (209, 210). Clone 4 is a high-avidity TCR, which was obtained from a B10.D2 mouse derived T cell clone previously immunized with *Influenza* A/PR/8/34 H1N1, and is composed of Vα10 and Vβ8.2 (211). Clone 4 transgenic mice were first described in 1996 by L. Sherman et al. They were generated by microinjection of TCR-α- and TCR-β-chain shuttle vectors into H-2^{bxd} (C57BL/6 X BALB/c) F1 mouse zygotes. Clone 4 transgenic mice were mated with Ins-HA mice to study T cell tolerance mechanisms in the setting of autoimmune diabetes (212, 213). The SFE TCR recognizes a different peptide (^{110}SFERFEIFPK^{119}) presented on MHC class II I-E^d. It was derived in 1983 from a monoclonal BALB/c $CD4^+$ T cell line called Vir-2 by Hackett et al. (216). A hybridoma cell line called 14.3.d was derived from Vir-2 clone $V_{2\text{-}15}$ by fusion with thymoma BW5147. Its TCR was determined to be encoded by Vα4/Jα2B4 and Vβ8.2/Jβ2.1 (215). The name for this TCR has changed several times during the almost 40 years

in which it has been researched - the first references name it as 14.3.d TCR and V2.1 TCR (216, 220). Its encoding TCR gene segments were confirmed when it was used by J. Kirberg and H. von Boehmer et al. to create TCR transgenic mice for experiments in thymic selection in 1990. It was stained using an anti-clonotypic mAb called 6.5, which earned it the name 6.5 TCR (214, 216, 217) (see 10.4, Page 42). The 6.5 antibody was initially produced by B. Riwar and H. Kishi (unpublished). The TCR was used by L. Sherman et al. in tumour models studying $CD4^+$ T cell response and autoimmunity; due to its recognition of HA, it was later referred to as HA TCR, and as SFE TCR because of the recognized epitope (218, 219). The data provided in the literature is summarised in Table 7. In most listed publications, the regions of the TCR chains were determined via antibody staining and the information is incomplete - no data was available regarding α- or β-chain subtype, TRAJ, TRBD or CDR3 region. The primers were designed to cover α- and β-chain segment subtypes (Table 2, page 23). Primary splenocytes derived from TCR-transgenic mice were kindly provided by L. Sherman (The Scripps Research Institute, La Jolla, California, USA). The mouse strains are listed in Table 1 on page 23. RNA isolation, cDNA synthesis and TOPO cloning were performed. The TCRs were sequenced and aligned to the IMGT database (221, 230). A summary of the alleles and CDR3s constituting the TCRs determined by sequencing is given in

Table 8. TRAV and TRAJ, or TRBV, TRBD and TRBJ sequences were linked via a P2A element and codon optimised, with suitable restriction enzyme recognition motifs implemented, and were subsequently inserted into the MP71 vector (231) (see 9.3, page 25).

Table 7 TCR chain segments reported in the literature

TCR	**V-region**	**D-region**	**J-region**	**references**
Clone 1 α-chain	Vα1		Jα11	(210, 211)
Clone 1 β-chain	Vβ8.2	D	Jβ2.4	(210, 211)
Clone 4 α-chain	Vα 10			(211-213)
Clone 4 β-chain	Vβ 8.2			(211-213)
SFE α-chain	Vα4		Jα2B4	(214-220)
SFE β-chain	Vβ8.2		Jβ2.1	(214-220)

Table 8 TCR chain segments and CDR3 regions determined by sequencing

TCR	V-region	D-region	J-region	CDR3
Clone 1 α-chain	TRAV7-2*02		TRAJ13*01	CAANSGTYQRF
Clone 1 β-chain	TRBV13-2*01	TRBD2*01	TRBJ2-4*01	CASGDGGARQNTLYF
Clone 4 α-chain	TRAV13D-4*01		TRAJ42*01	CASNSGGSNAKLTF
Clone 4 β-chain	TRBV13-2*01	TRBD1*01	TRBJ1-4*02	CASGETGTNERLFF
SFE α-chain	TRAV6-5*01		TRAJ56*01	CALSGGNNKLTF
SFE β-chain	TRBV13-2*01	TRBD1*01	TRBJ2-1*01	CASGGGRGSYAEQFF

The TCRs listed provided two TCRs restricted to MHC class I and one TCR restricted to MHC class II. They were chosen as tools to analyse subset-specific transduction and for further analysis *in vitro* and *in vivo*.

10.2. Generation of cell lines expressing HA

The T cells transduced with TCRs using the MV-envelope-based pseudotyped gRV system had to be tested *in vitro* and *in vivo*. Strategies exist to test TCR-transgenic T cell functionality *in vitro* and *in vivo,* circumventing the need for an antigen-presenting cell line. Antigenic epitopes can be loaded onto MHC to test transduced T cells *in vitro,* or epitopes or full-length HA can be *in vivo* injected into mice. These and other assays are used later in this project, but they do not represent the complete immune response of a tumour model. The generation of cell lines expressing the model antigen HA allows for a better model of adoptive T cell therapy to show the recognition of cancer cells *in vitro* and *in vivo.* The availability of cell lines expressing HA enables *in vivo* tumour rejection experiments. A suitable cell line had to be a progressor cancer cell line, and capable of tumorigenesis when injected into immune competent BALB/c mice. In addition, it had to express MHC class I H-2K^{d} to enable recognition by Clone 1 and Clone 4 TCR. AB1 [mouse mesothelioma] (RRID:CVCL_4403) is a cell line derived from malignant mesothelial cells in 1992. Female BALB/c mice were exposed to crocidolite asbestos through intraperitoneal injection and fibroblast-like mesothelioma cells were obtained from ascites fluid. AB1 cells are tumorigenic in syngeneic immunocompetent

mice (225). The AB1 cell line was a generous gift from D. Klatzmann (Pierre & Marie Curie University and Medical school, Paris, France). 4T1 [mouse mammary carcinoma] (CRL-2539, ATCC) is a BALB/c-derived cancer cell line. It was derived in 1992 by F. Miller et al. from a single spontaneously arising mammary tumour from a BALB/cfC3H mouse (232). Clonal subpopulations were generated; among these is 410.4, from which the thioguanine-resistant variant 4T1 was selected (233). 4T1 is characterised by being exceptionally tumorigenic and spontaneously metastasizing to both the lung and liver. 4T1 parallels highly invasive, metastatic human stage IV breast cancer in its immunogenicity, metastatic properties, and growth characteristics, and is used frequently as a model for the disease (234, 235). The 4T1 cell line was generously provided by D. Klatzmann. Both cell lines were chosen as appropriate models for HA recognition by the selected TCRs. As they were not expressing the target antigen endogenously, derivate cell lines had to be generated.

10.2.1. Electroporation of AB1 and 4T1

In order to test the processing of the antigen and recognition by TCRs on the cell surface, derivatives of AB1 and 4T1 expressing HA of *Influenza* A/PR/8/34 H1N1 were generated using electroporation and the *Sleeping Beauty* transposon system. The nucleotide sequence of *Influenza* A/PR/8/34 H1N1 (GCA_000865725.1) was first published by G. Winter et al. in 1981 and was available from the European Nucleotide Archive (ENA) (222). The cell lines AB1 and 4T1 were electroporated with a transgene encoding for HA linked via IRES to the reporter gene green fluorescent protein (GFP) (Figure 1). GFP was used as a reporter since no commercial antibody was available for staining of HA at the time of cloning. The plasmid, 506-SB-HAiGFP, is a derivative of the *Sleeping Beauty* transposon plasmid pT2/HB modified to carry the MP71-promoter and was, together with RNA coding for the required transposase, kindly provided by J. Clauss (Max Delbrück Center for Molecular Medicine in the Helmholtz Association, Berlin, Germany) (224, 231, 236). The resulting cells were single-cell sorted, and for each cell line, 40 clones were raised in 96-well plates.

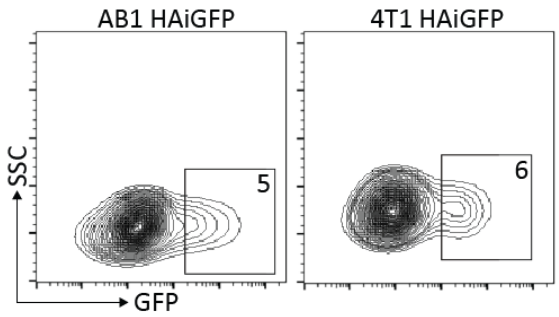

Figure 1 AB1 and 4T1 express GFP after electroporation with 506-SB-HAiGFP.

AB1 and 4T1 were analysed and sorted by flow cytometry 48 h after electroporation with 506-SB-HAiGFP. The non-transgenic parental cell lines AB1 and 4T1 were used as controls. Numbers indicate the percentage of GFP-positive cells in the gate.

10.2.2. AB1 HA and 4T1 HA

Subsequently, AB1-HAiGFP and 4T1-HAiGFP clones were selected for high and uniform expression of GFP. The clones selected were AB1-HAiGFP Clone 4 and 4T1-HAiGFP clone 23, hereafter referred to as AB1 HA and 4T1 HA (Figure 2A). Later, the surface expression of HA was shown to correlate with GFP expression using the PY102 mAb (Figure 2B). The PY102 mAb was kindly provided by P. Palese (Icahn School of Medicine at Mount Sinai, New York, USA).

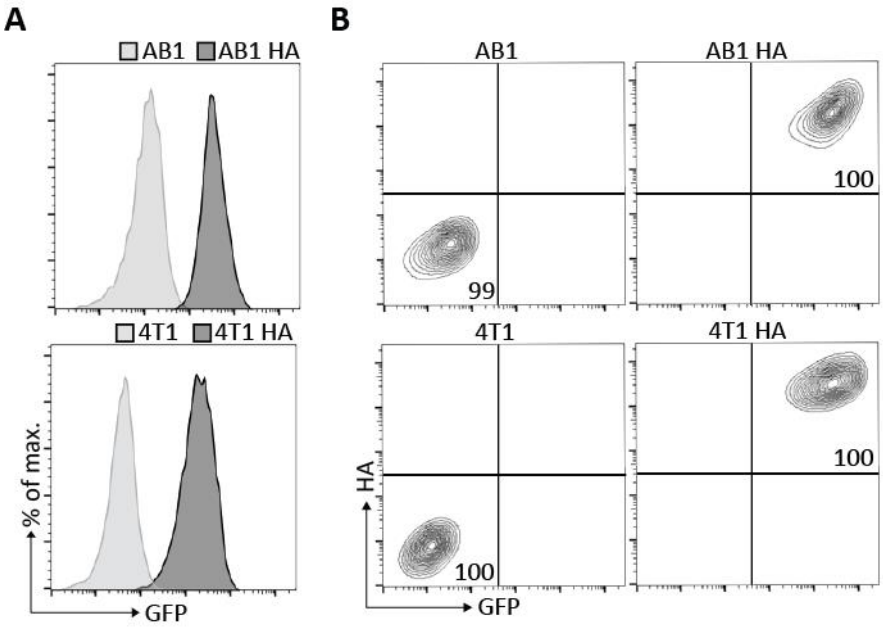

Figure 2 AB1 and 4T1 single cell clones AB1 HA and 4T1 HA show expression of HA and GFP.
(A) AB1-HAiGFP Clone 4 and 4T1-HAiGFP clone 23 were analysed by flow cytometry and selected for highest uniform GFP expression after electroporation with 506-SB-HAiGFP. AB1-HAiGFP Clone 4 was in culture for 28 days, and 4T1-HAiGFP clone 23 for 21 days. (B) AB1, AB1 HA (AB1-HAiGFP clone 4), 4T1 and 4T1 HA (4T1-HAiGFP clone 23) cells were stained with anti-HA mAb PY102 labelled with APC and analysed for expression levels of HA by flow cytometry. The non-electroporated parental cell lines AB1 and 4T1 were used as controls. Numbers indicate the percentage of positive cells. The results shown are representative and were repeated in experiments involving AB1, 4T1, AB1 HA or 4T1 HA.

10.2.3. Growth of cancer cell lines and derivatives in BALB/c mice

As any kind of modification can alter the growth kinetics of cancer cell lines, the generated derivate cell lines had to be analysed for their *in vivo* growth, to ensure comparability with their respective parental cell line. Therefore, the cancer cell lines AB1 and 4T1, as well as their antigen-expressing derivatives AB1 HA and 4T1 HA, were injected s.c. into the flanks of BALB/c mice. Three mice were injected with $5*10^5$ cells of one of the cell lines suspended in 200 µl PBS. Tumours developed in 2/3 mice injected with AB1, 3/3 with AB1 HA, 3/3 with 4T1 and 2/3 with 4T1 HA. The resulting tumours were measured daily for 16 days. Mice injected with AB1 or AB1 HA developed palpable tumours, first reaching a size larger than 10 mm^3 on day 10 (5/5), and then larger than 50 mm^3 on day 14 (4/5) and day 15 (1/5). 4T1 and 4T1 HA were highly tumorigenic, with palpable tumours that first reached a size larger than 10 mm^3 on

day 7 (4/5) and day 8 (1/5), and then larger than 50 mm³ on day 8 (2/5) and day 9 (3/5). Growth curves for parental cell lines were comparable to their respective derivatives (

Figure 3). Both derivative cell lines were therefore deemed to be appropriate models to test the TCRs *in vitro* and *in vivo*.

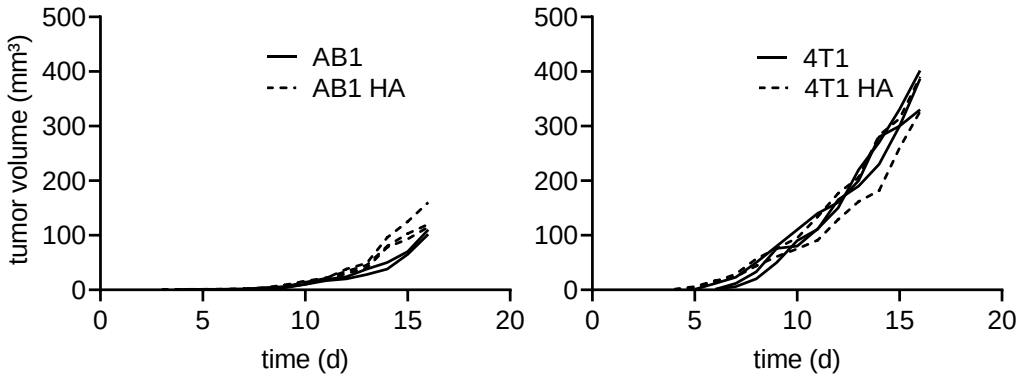

Figure 3 AB1 HA and 4T1 HA grow similarly to their respective parental cell lines AB1 and 4T1 in BALB/c mice. Tumour sizes of mice inoculated s.c. with the parental cell lines AB1 (n=2) and 4T1 (n=3) compared to their respective HA-expressing derivative cell line AB1 HA (n=3) or 4T1 HA (n=2), measured daily for a total of 16 days.

10.3. Transduction of 58m4 and 58m8 and titration of viral supernatants

In order to analyse and confirm the subset-specific transduction capability of the pseudotyped viral supernatants to mouse CD4 and CD8, two cell lines derived from BW5147 cells were employed that either express CD4 or CD8. BW5147 (RRID:CVCL_3896) is a cell line derived from a spontaneous AKR/J mouse thymoma mouse established in 1980 by A. Conzelmann et al., which is deficient for CD4 and CD8 (237, 238). The 58 T cell line is a TCR-deficient derivative of BW5147 established by F. Letourner et al. in 1989 (228). The 58m4 ($CD4^+CD8^-TCR^-$) and 58m8 ($CD4^-CD8^+TCR^-$) daughter cell lines were established by I. Edes. The specificity of MVm4- and MVm8-pseudotyped gRV to mouse CD4 and CD8, respectively, was shown by I. Edes in mixed cell culture and confirmed by experiments using blocking antibodies (208). In order to test the pseudotyped gRV vectors for Clone 1, Clone 4 and SFE, supernatants containing pseudotyped gRV vectors were generated by transient transfection of 293T cells (see 9.5, page 27). The resulting supernatants were enriched by ultracentrifugation and resuspended in 100 µl DPBS. MVm8/Clone 1 and MVm8/Clone 4 were used to transduce 58m8 cells and MVm4/SFE was used to transduce 58m4 cells.

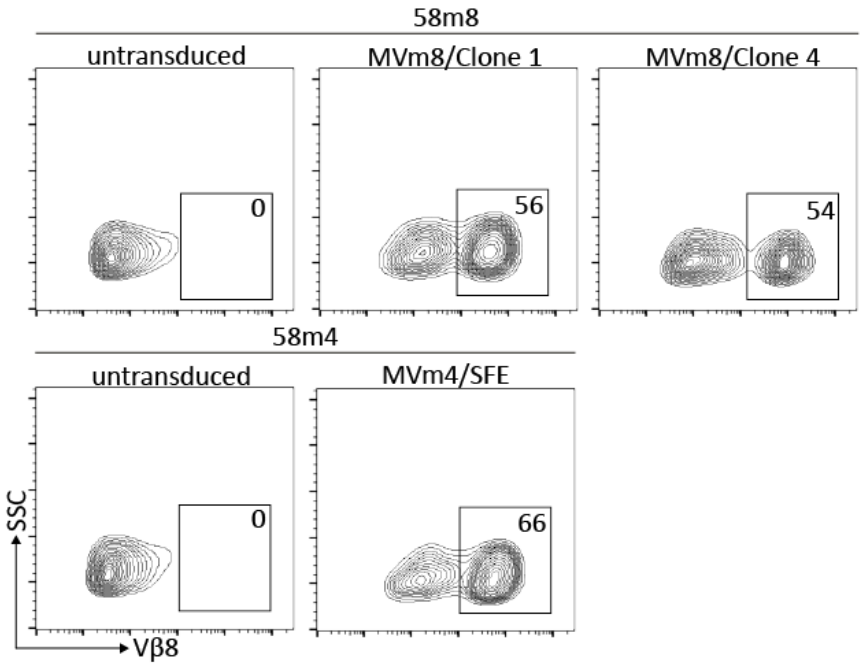

Figure 4 MVm8/Clone 1 and MVm8/Clone 4 transduce 58m8 and MVm4/SFE transduces 58m4.
$CD8^+$ 58m8 and $CD4^+$ 58m4 were stained with mAb anti-mouse-Vβ8 labelled with PE, after transduction with MV-envelope-pseudotyped gRV targeted to either mouse CD4 (MVm4) or mouse CD8 (MVm8) and analysed by flow cytometry. Untransduced 58m4 and 58m8 were used as controls. Numbers indicate the percentage of positive cells. The results shown are representative of the third to fourth step in dilution for titrations of viral supernatants, depending on the yield, and were repeated routinely.

Transduction efficiency and surface TCR expression were determined by staining with an anti-mouse-Vβ8-antibody labelled with PE and subsequent flow cytometry analysis (Figure 4). This experiment confirmed the transduction efficiency of 58m4- and 58m8-pseudotyped vectors carrying the transgenes coding for the TCRs Clone 1, Clone 4 and SFE. From here on, the transductions of 58m4 and 58m8 cells were used in a serial dilution of supernatants containing MVm8/Clone 1, MVm8/Clone 4 or MVm4/SFE to determine viral titre of the batch.

10.4. Production of the 6.5 antibody for TCR-specific staining

A large percentage of T cells in the repertoire of BALB/c express a TCR β-chain encompassing Vβ8 - a share of 20% or even higher is reported in the literature and mirrored in the findings of this thesis (Figure 7, page 46). This also holds true for all three TCRs used in this project, demanding suitable staining methods to differentiate between T cells endogenously expressing Vβ8 and transduced T cells. TCR-specific staining was needed to enable the verification of the surface expression of TCRs and transduction efficacy in transduced T cells. An MHC-peptide-tetramer, H-$2K^d$-IYSTVASSL-PE (MBL International, Woburn, Massachusetts,

USA), to be used to confirm the surface expression and specificity of Clone 1 and Clone 4 TCR, was commercially available (Figure 6, page 44). For the SFE TCR, no MHC-tetramer was commercially available or described in the literature. In 1994, H. von Boehmer et al. used a clonotype-specific antibody called mAb 6.5 for the staining of the SFE TCR, referred to as 'TCR specific for 110-119 HA'. The mAb 6.5 was originally produced by B. Riwar and H. Kishi (unpublished) following a process previously described by S. Weber et al. This involved immunizing rats using a solubilized form of the SFE TCR and generating a mAb-producing hybridoma (214, 217). The hybridoma producing the clonotypic 6.5 was kindly provided by L. Klein (Ludwig-Maximilians-University, Munich, Germany) thanks to the recommendation of H. von Boehmer (Harvard Medical School, Boston, United States). To generate a supply of the clonotypic mAb, the 6.5 hybridoma was cultured for 10 weeks, gradually lowering the fetal calf serum (FCS) concentration. The hybridoma was kept at 0% FCS for 4 days, and the resulting supernatant was precipitated using ammonium sulfate and purified by Protein A chromatography (see 9.6.1, page 29). The clonotypic 6.5 mAb was stained with anti-rat-IgG2b mAb labelled with FITC in a second step and analysed by flow cytometry.

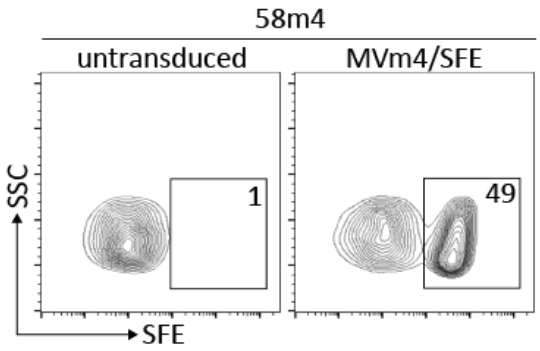

Figure 5 Staining using clonotypic 6.5 mAb on 58m4 transduced with MVm4/SFE.
$CD4^+$ 58m4 were transduced using MVm4/SFE and stained using anti-CD4 mAb and the clonotypic 6.5 mAb specific for the SFE TCR produced by purification of 6.5. hybridoma supernatant. The 6.5 mAb was stained with anti-rat-IgG2b mAb labelled with FITC in a second step and analysed by flow cytometry. Non-transduced 58m4 were used as controls. Numbers indicate the percentage of positive cells. The results shown are representative for two experiments.

It showed specific staining of the SFE TCR on 58m4, comparable to the staining using anti-C mAb and anti-Vβ mAb. The results established the 6.5 mAb as an invaluable staining method and confirmed surface expression of the SFE TCR on transduced cells (Figure 5).

10.5. Transduction of primary BALB/c-derived T cells *in vitro*

10.5.1. Transduction of BALB/c-derived CD8$^+$ T cells by MVm8 *in vitro*

The first *in vitro* transduction of primary cells using MVm8-pseudotyped gRV encoding for Clone 1 and Clone 4 TCR was performed on splenocytes derived from BALB/c mice. Both TCRs are MHC class I-restricted (H-2k^d) and recognize the same epitope of HA (^{518}IYSTVASSL^{526}). Splenocytes were isolated on day 0 and activated by anti-CD3- and anti-CD28-stimulation, and additionally the culture was supplemented with cytokines IL-2 and IL-15. Activation of the T cells was necessary because gRV are dependent on disaggregation of the T cells nuclear envelope for stable transduction. Transduction was performed on day 2 and the splenocytes were analysed for transduction efficiency two days later. The transduced cells were stained with anti-CD8 mAb and H-2K^d-tetramer-IYSTVASSL-PE and analysed by flow cytometry. The transduction rate for MVm8/Clone 1 and MVm8/Clone 4 was 31% and 25% of CD8$^+$ cells, respectively. These results validated the surface expression of the TCRs on primary transduced CD8$^+$ T cells (Figure 6). Due to difficulties acquiring the H-2K^d-tetramer-IYSTVASSL-PE and the prohibitive costs, later experiments were, in part, repeated after Vβ8-depletion before transduction using magnetic activated cell sorting (MACS), and the transduction rate was determined by Vβ8-expression (see 9.8.2, page 33).

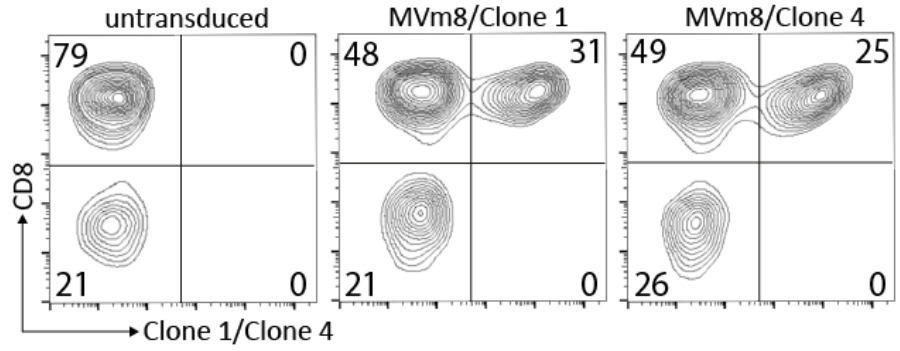

Figure 6 MVm8/Clone 1 and MVm8/Clone 4 transduce BALB/c-derived CD8$^+$ splenocytes efficiently and exclusively.

Unsorted BALB/c-derived CD8$^+$ splenocytes were transduced using MVm8-pseudotyped gRV/Clone 1 and MVm8-pseudotyped gRV/Clone 4 and were stained for TCR surface expression using H-2K^d-tetramer-IYSTVASSL-PE. Untransduced splenocytes were used as controls. Numbers indicate the percentage of positive cells. The results are representative and were repeated in co-culture experiments involving MVm8/Clone 1- and Clone 4-transduced splenocytes.

10.5.2. Transduction of BALB/c-derived CD4$^+$ T cells by MVm4 *in vitro*

in vitro transduction of primary cells using MVm4-pseudotyped gRV encoding for the SFE TCR was performed on splenocytes derived from BALB/c mice. The SFE TCR is MHC class II-restricted (I-E^d) and recognizes the epitope ^{110}SFERFEIFPK^{119} of HA. Splenocytes were isolated on day 0 and activated by anti-CD3- and anti-CD28-stimulation, and in contrast to the culturing of CD8$^+$ T cell culture, only IL-2 was added to the culture medium. Omitting IL-15 thwarted overgrowth by CD8$^+$ T cells, which would have been detrimental for later co-culture experiments. Transduction was performed on day 2 and transduced splenocytes were analysed two days later. Staining was performed with anti-CD4, anti-Vβ mAb and 6.5 mAb purified from 6.5 hybridoma supernatant, and analysed by flow cytometry (see 10.4, page 42; and 9.6.1, page 29). MVm4-gRV/SFE achieved a transduction rate of 17% in total splenocytes, which equated to 42% of the CD4$^+$ population. These results validated the surface expression of the SFE TCR on primary transduced CD4$^+$ T cells. Analysis of the transduction rate using anti-Vβ8 mAb was impeded by high endogenous Vβ8-expression (Figure 7). Transduced CD4$^+$ splenocytes were cultured and used on day 8-10 in co-culture experiments, and repeated analyses by flow cytometry showed comparable transduction rates, thereby confirming stable transduction (208) (see 10.5.4, page 48).

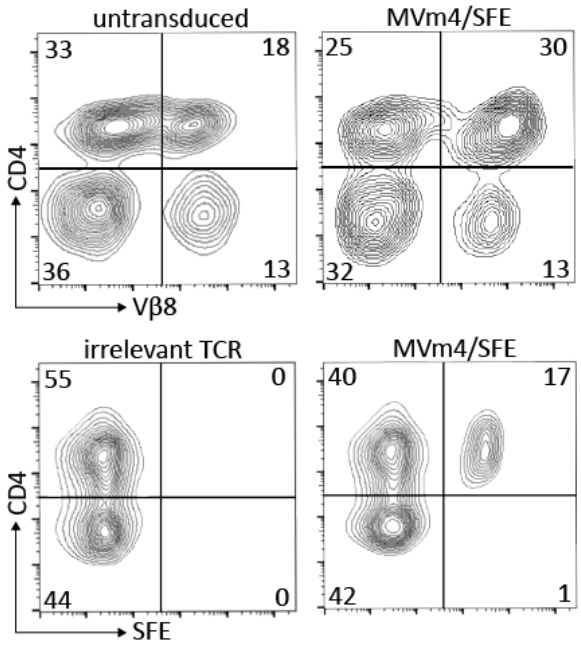

Figure 7 MVm4-pseudotyped gRV/SFE transduces BALB/c-derived CD4$^+$ splenocytes effectively and exclusively. Unsorted BALB/c-derived CD4$^+$ splenocytes were transduced using MVm4-pseudotyped gRV/SFE and stained for TCR surface expression using anti-Vβ8 mAb and clonotypic 6.5 mAb. Untransduced splenocytes and splenocytes transduced with an irrelevant TCR (MVm4/OT-1) were used as controls. Numbers indicate the percentage of positive cells. The results are representative and were repeated in co-culture experiments involving MVm4/SFE transduced splenocytes.

10.5.3. Co-culture assays using MVm8/Clone 1- and Clone 4-transduced T cells

MVm8/Clone 1- and Clone 4-transduced CD8$^+$ T cells were evaluated in co-culture assays to verify the functionality of transduced T cells, to characterise the TCR and to verify the stability of transduction. Both TCRs are restricted to MHC class I H-2K^d and recognize the same epitope (^{518}IYSTVASSL^{526}) of HA. A detailed description of both TCRs was given earlier (10.1, page 35). After isolation of splenocytes on day 0 and transduction on day 2, the T cells were cultured until days 10-14 when co-culture assays were performed. Transduced CD8$^+$ splenocytes were analysed on day 4 and reanalysed on day**s** 10-14, showing comparable transduction rates, thereby confirming the stable transduction previously shown by I. Edes (208). CD8$^+$ T cells transduced with either of the TCRs showed specific recognition of their target antigen as determined by IFNγ secretion. T cells transduced by MVm8/Clone 4 showed higher IFNγ-release compared to T cells transduced with MVm8/Clone 1. The mean functional avidity (EC50) calculated by non-linear fitting of an asymmetric 5 parameter logistic model of Clone 1 TCR to peptide ^{518}IYSTVASSL^{526} was $10^{-8,12}$ mol/l, and the EC50 of Clone 4 was

$10^{-10,73}$ mol/l. These results confirm Clone 4 TCR as the TCR of higher avidity, as reported in the literature, and a TCR capable of co-receptor independent recognition of HA on MHC class I H-2K^{d} (210-213) (Figure 8).

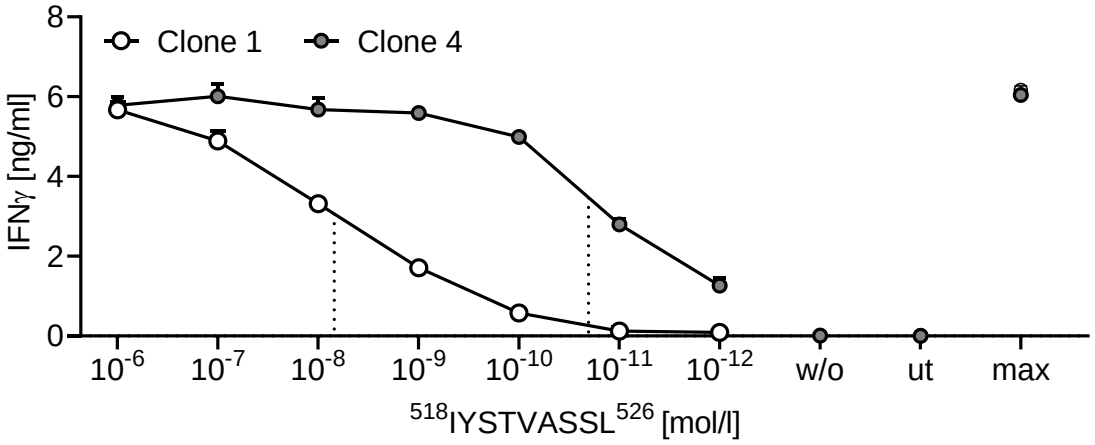

Figure 8 MVm8/Clone 1- and MVm8/Clone 4-transduced BALB/c-derived CD8^{+} T cells recognize their epitope presented on unsorted splenocytes.

CD8^{+} BALB/c-derived T cells were transduced with either MVm8/Clone 1 or MVm8/Clone 4 and co-cultured with splenocytes loaded with the HA-peptide (^{518}IYSTVASSL^{526}) in decreasing concentrations. Splenocytes without peptide (w/o) and untransduced CD8^{+} T cells (ut) were used as negative controls. T cells stimulated independently of their TCR by incubation with ionomycin and PMA to show maximum IFNγ secretion were used as positive controls (max). The supernatant was analysed for concentration of IFNγ by ELISA. The EC50 values of TCRs are indicated by dotted lines. One representative experiment out of two is shown, and results are shown as mean and standard deviation (SD) of technical quadruplicates.

In later experiments, the transduced T cells were co-cultured with the cancer cell lines AB1 HA and 4T1 HA generated previously (10.2, page 37). T cells transduced with MVm8/Clone 1 or MVm8/Clone 4 were cultured with either of the HA-expressing cancer cell lines AB1 HA or 4T1 HA, or with the parental cell lines not transduced with HA. T cells and cancer cells were seeded in a 1:1 ratio and cultured for 24h. The supernatant was analysed for secreted IFNγ via ELISA. Specific recognition of the HA antigen on the cancer cells was shown, confirming stable expression of the transgenic HA, the intact MHC-loading machinery, and the sufficient MHC class I surface expression for recognition by Clone 1- and Clone 4-transduced T cells. As expected, the high-avidity TCR Clone 4 triggered a considerably higher release of IFNγ, being more than 6-fold higher for AB1 HA and 9-fold higher for 4T1 HA (Figure 9).

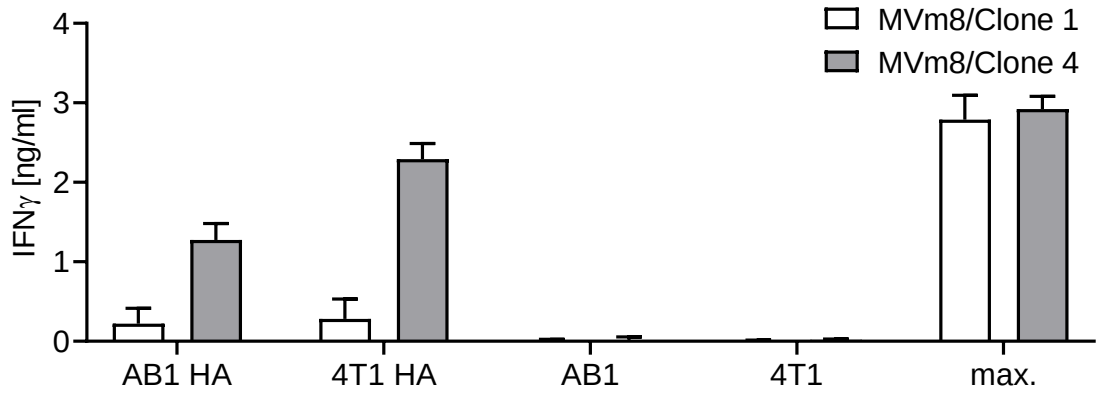

Figure 9 MVm8/Clone 1- and MVm8/Clone 4-transduced BALB/c-derived $CD8^+$ T cells recognize the antigen expressing cell lines AB1 HA and 4 T1 HA.

$CD8^+$ BALB/c-derived T cells were transduced with either MVm8/Clone 1 or MVm8/Clone 4 and co-cultured with the HA expressing cancer cell lines AB1 HA or 4T1 HA. The parental cancer cell lines AB1 and 4T1 do not express the TCRs' cognate antigen and were used as controls. T cells stimulated independently of their TCR by incubation with ionomycin and PMA to show maximum IFNγ secretion were used as positive controls (max). The supernatant was analysed for concentration of IFNγ via ELISA. The results are shown as mean and standard deviation (SD) of technical duplicates.

10.5.4. Co-culture assays using MVm4/SFE-transduced T cells

MVm4/SFE-transduced $CD4^+$ T cells were evaluated in co-culture assays to verify the functionality of transduced T cells, to characterise the TCR and to verify the stability of transduction. The SFE TCR is restricted to MHC class II $I\text{-}E^d$ and recognizes the epitope ^{110}SFERFEIFPK^{119} of HA. A detailed description was given earlier (10.1, page 35). Prior co-culture experiments using unsorted splenocytes loaded with peptide showed only minimal release of IL-2 and IFNγ - this was attributed to the difficulty in replacing the endogenously presented peptides on MHC class II (data not shown). To address this challenge, professional APCs were chosen as target cells. DCs differentiated from BALB/c bone marrow were kindly provided by M.-C. Ku (Max Delbrück Center for Molecular Medicine in the Helmholtz Association, Berlin, Germany). $CD4^+$ T cells transduced with MVm4/SFE were co-cultured with DCs differentiated from BALB/c bone marrow. DCs were incubated in a serial dilution of decreasing concentrations of ^{110}SFERFEIFPK^{119} 24h prior to co-culture with T cells. Transduced T cells and DCs were seeded in a 1:1 ratio and the supernatant was harvested after 24h and analysed for IL-2 secretion via ELISA. The SFE TCR showed specific recognition of its target antigen on DCs in a concentration-dependent manner (Figure 10).

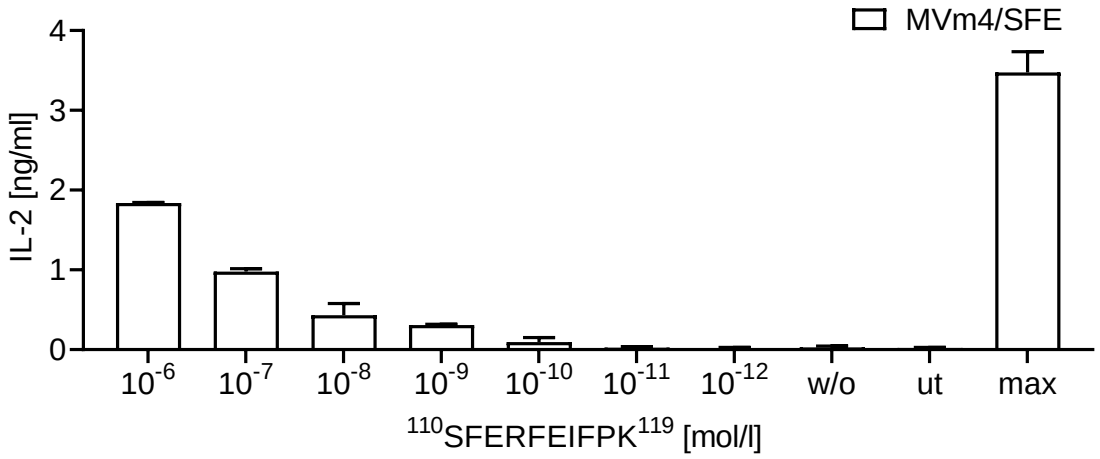

Figure 10 MVm4/SFE-transduced BALB/c-derived CD4$^+$ T cells recognize peptide presented on DCs.
CD4$^+$ BALB/c-derived T cells were transduced with MVm4/SFE and co-cultured with DCs loaded with HA-peptide (^{110}SFERFEIFPK^{119}) in decreasing concentrations 24h previously. DCs without peptide (w/o) and untransduced CD4$^+$ T cells (ut) were used as negative controls. T cells stimulated independently of their TCR by incubation with ionomycin and PMA to show maximum IL-2 secretion were used as positive controls (max). The supernatant was analysed for concentration of IL-2 via ELISA. The results are shown as mean and standard deviation (SD) of technical duplicates.

To expand on this, a similar experiment was repeated in the setting of CD4$^+$ T cells transduced with MVm4/SFE recognizing processed antigen on DCs obtained from tumour cell lysate. The lysate was generated by freeze-thaw cycles of either 10^5 AB1 HA or 4T1 HA cells. The resulting lysate was diluted in 5 serial 1:3 steps and added to the cell medium of DCs 24h prior to the co-culture experiment. Transduced T cells and DCs were again seeded in a 1:1 ratio and the supernatant was harvested after 24h and analysed for IL-2 secretion via ELISA. It was shown that the target antigen processed by DC was recognized in a dose-dependent manner by the SFE-transduced T cells (Figure 11). In higher concentrations, namely 1:1 and 1:3, there was no clear correlation between antigen dose and IL-2 secretion. This was attributed to the significant toxicity of the tumour cell lysate on DCs, indicated by their aberrant phenotype revealed by microscopy (data not shown). It was therefore concluded that MVm4/SFE-transduced CD4$^+$ T cells recognize their naturally processed target antigen in a concentration-dependent manner.

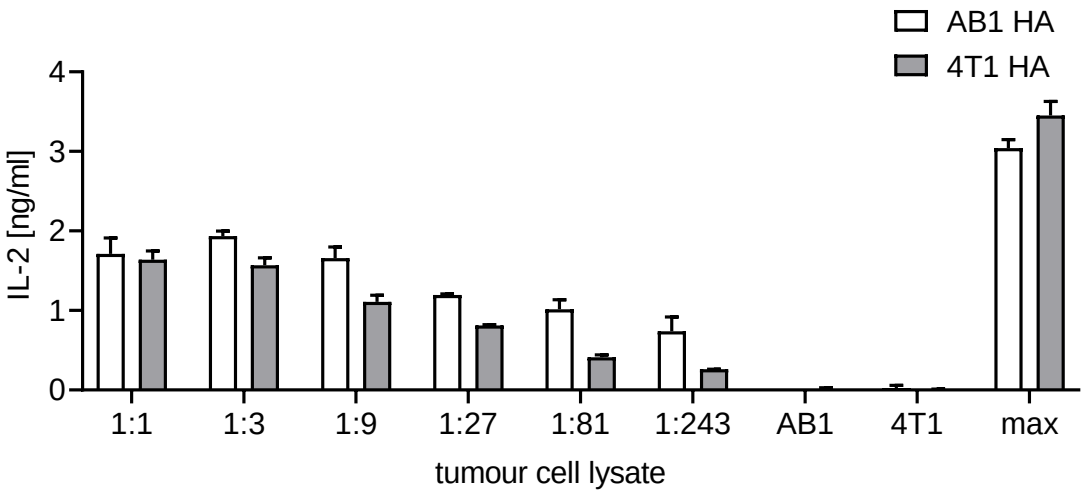

Figure 11 MVm4/SFE-transduced BALB/c-derived CD4$^+$ T cells recognize their epitope presented on DCs after processing of antigen derived from cell lysate.

CD4$^+$ BALB/c-derived T cells were transduced with MVm4/SFE and co-cultured with DCs loaded with a cell lysate of AB1 HA or 4T1 HA in decreasing concentrations 24h previously. The lysate was generated by repeated freeze-thaw cycles of 1000 cells per 100µl. 10^5 T cells and DCs were cultured in each well in 100µl; in the first well, 100µl cell lysate was added and a serial dilution of 1:3 in 5 steps was performed. T cells and DCs loaded with 100µl of AB1 or 4T1 cell lysate were used as controls. T cells stimulated independently of their TCR by incubation with ionomycin and PMA to show maximum IL-2 secretion were used as positive controls (max). The supernatant was analysed for concentration of IL-2 via ELISA. The results are shown as mean and standard deviation (SD) of technical duplicates.

10.6. Transduction of BALB/c lymphocytes *in vivo*

After showing the capacity of MVm8 and MVm4 viral vectors to transduce BALB/c-derived splenocytes *in vitro* specific to their subset, the next step was to show transduction *in vivo*. BALB/c-derived splenocytes were isolated, activated for 24 h, and injected i.v. retro-orbitally to repopulate RAG2$^{-/-}$ mice. The MVm8-pseudotyped vectors encoded for the two MHC class I-restricted TCRs, Clone 1 and Clone 4, while the MVm4-pseudotyped vector encoded for the MHC class II-restricted TCR SFE. Each of the TCRs was linked to a luciferase for *in vivo* imaging. Clone 1 and Clone 4 were linked to *Firefly* luciferase (FLuc), and SFE was linked to *Renilla* luciferase (RLuc). In the experiment, 4 groups of three mice each were analysed. The constructs MVm8/Clone 1-FLuc, MVm8/Clone 4-FLuc and MVm4/SFE-RLuc were each injected i.v. via the tail vein. Mice injected with phosphate-buffered saline (PBS) were used as controls (Figure **12**A). Five days after transduction (day 0), the mice were immunized with irradiated AB1 HA cells, injected s.c. into their right flanks. Mice were imaged

after retro-orbital luciferin or coelenterazine injection starting on day 3. Luciferin served as a substrate for MVm8/Clone 1-FLuc and MVm8/Clone 4-FLuc, while coelenterazine served as a substrate for MVm4/SFE-RLuc. Short intervals of imaging were chosen when the strongest dynamic in immune response was anticipated and the lowest frequency after the signal largely subsided, as well as before the boost. On day 65, mice were boosted by injection of irradiated AB1 HA cells into the contralateral flank, and imaging resumed three days later (Figure 12B and Figure 13A). Specific luciferase levels were detected in all mice injected with MV-pseudotyped gRV (9/9), while mice repopulated with untransduced T cells showed only background levels of luminescence signal after luciferin or coelenterazine injection. Mice injected with MVm8/Clone 1-FLuc showed the weakest signals out of the three vectors, with distinct signals appearing on day 8. The luminescence quickly weakened but was measurable in distinct spots, mostly in the flanks, until day 31. Until the boost on day 65, the luminescence signal was in the range of the background of the untransduced mice, with a few higher measurements of less well-defined signals of the upper abdomen (Figure 13A, day 51, day 64). After the boost, mice transduced with MVm8/Clone 1-FLuc showed distinct activation, but mice transduced with other vectors showed markedly higher luminescence. The luminescence exhibited by mice transduced with MVm8/Clone 1-FLuc was more spread out and less intense, and therefore not visible in the heat map shown in Figure 13A. When singled out and shown with a lower luminescence threshold of 20 [(p/s)/(cm^2/sr)x10^2], areas where almost no luminescence signal was visible before became identifiable. A representative example comparing two different thresholds of mice transduced with MVm8/Clone 1-FLuc on day 68 is shown in Figure 13B. As expected, mice repopulated with the high-avidity TCR Clone 4 showed a much higher luciferase signal than mice repopulated with the low-avidity Clone 1 TCR. Between days 8-14 the left- and rightmost mice showed homing to the site of antigen stimulus, with a pronounced dynamic in the intensity of luminescence signal (Figure 13A, days 8-14). The rightmost mouse showed an unexpectedly high and enduring luminescence signal for the rest of the experiment (Figure 13, days 31-73). The difference between both MHC class I-restricted TCRs correlated with prior *in vitro* experiments, showing lower release of IFNγ upon contact of antigen (Figure 8 and Figure 9).

The highest luciferase signals were measurable in all mice transduced with MVm4/SFE-RLuc, showing a signal at the earliest on day 3, and reaching the highest signals of the experiment around day 8 (Figure 13A, days 3-14). Mice transduced with MVm4/SFE-RLuc showed a distinct

nodal luminescence signal after priming and boost. In conclusion, $CD4^+$ and $CD8^+$ T cell subsets were transduced in BALB/c mice *in vivo* by all MV-pseudotyped gRV vectors. Transduced T cells exhibited several desired characteristics - they showed homing, expansion, and contraction, and remained transduced stably and measurably for a time span of more than 10 weeks. The different dynamics of the TCRs, and especially of the MHC class I-restricted TCRs of low and high avidity, i.e., Clone 1 and Clone 4, mirrored the results of prior *in vitro* co-culture experiments.

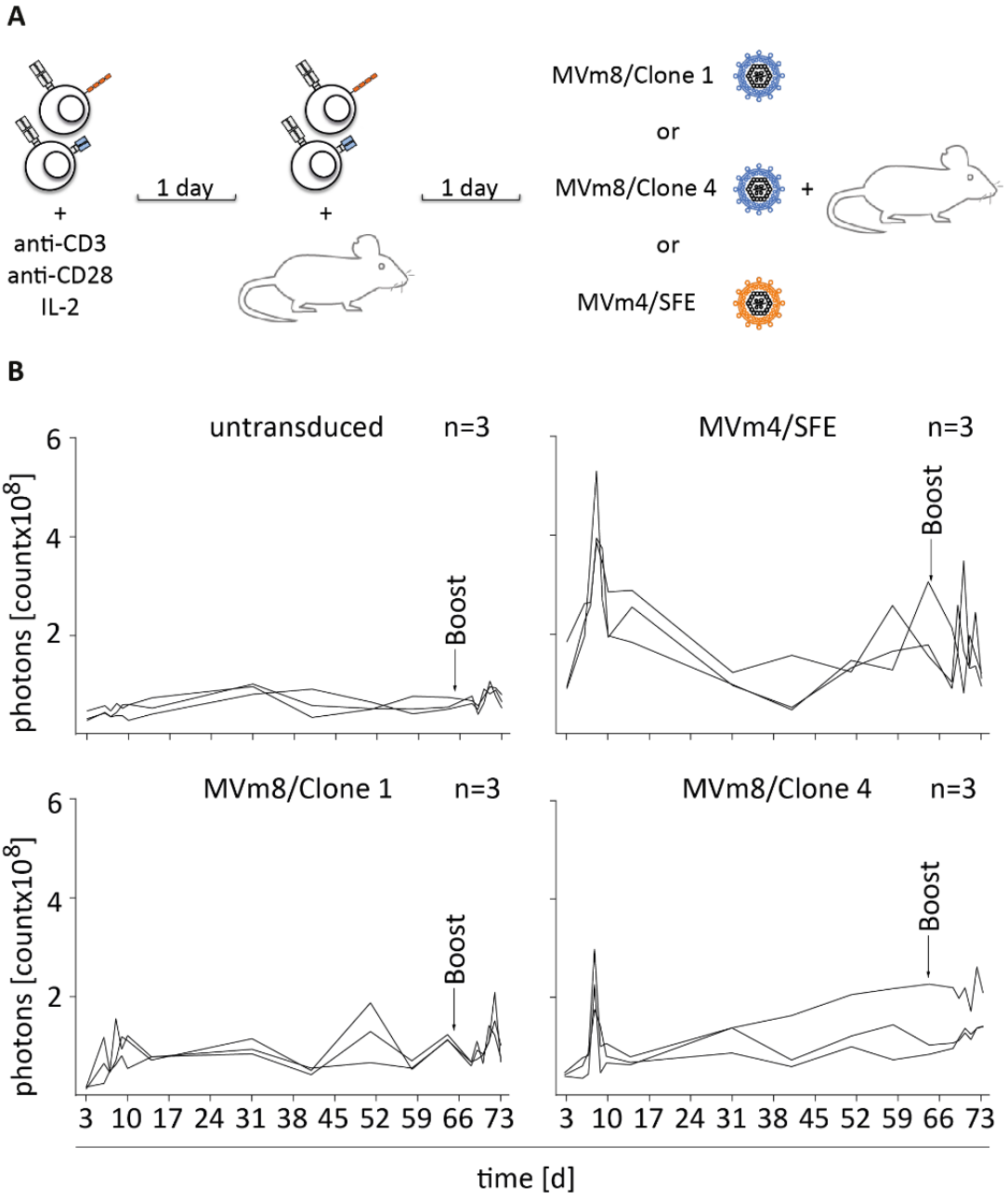

Figure 12 *In vivo* transduction of BALB/c mice, synopsis.

(A) BALB/c-derived splenocytes were isolated and activated for 24 h. BALB/c Rag2$^{-/-}$ were repopulated with the activated unsorted splenocytes. After one day, three mice were each injected i.v. with MVm8/Clone 1-FLuc, MVm8/Clone 4-FLuc, and MVm4/SFE-RLuc for *in vivo* transduction. (B) Mice were primed by s.c. application of irradiated AB1 HA cells into the right flank on day 0. Mice received an antigenic boost by s.c. application of irradiated AB1 HA cells into the contralateral flank on day 65. Luminescence was measured for a total of 73 days. *in vivo* imaging measured transduced T cells indirectly via reporter luciferases after i.v. application of luciferin or coelenterazine in a dark chamber using Xenogen IVIS 200. Untransduced T cells-repopulated BALB/c Rag2$^{-/-}$ were used as controls. MVm8/Clone 1, MVm8/Clone 4, and MVm4/SFE refer to MV-pseudotyped gRV coding for a TCR linked to a reporter luciferase, i.e., MVm8/Clone 1-FLuc, MVm8/Clone 4-FLuc, and MVm4/SFE-RLuc, respectively.

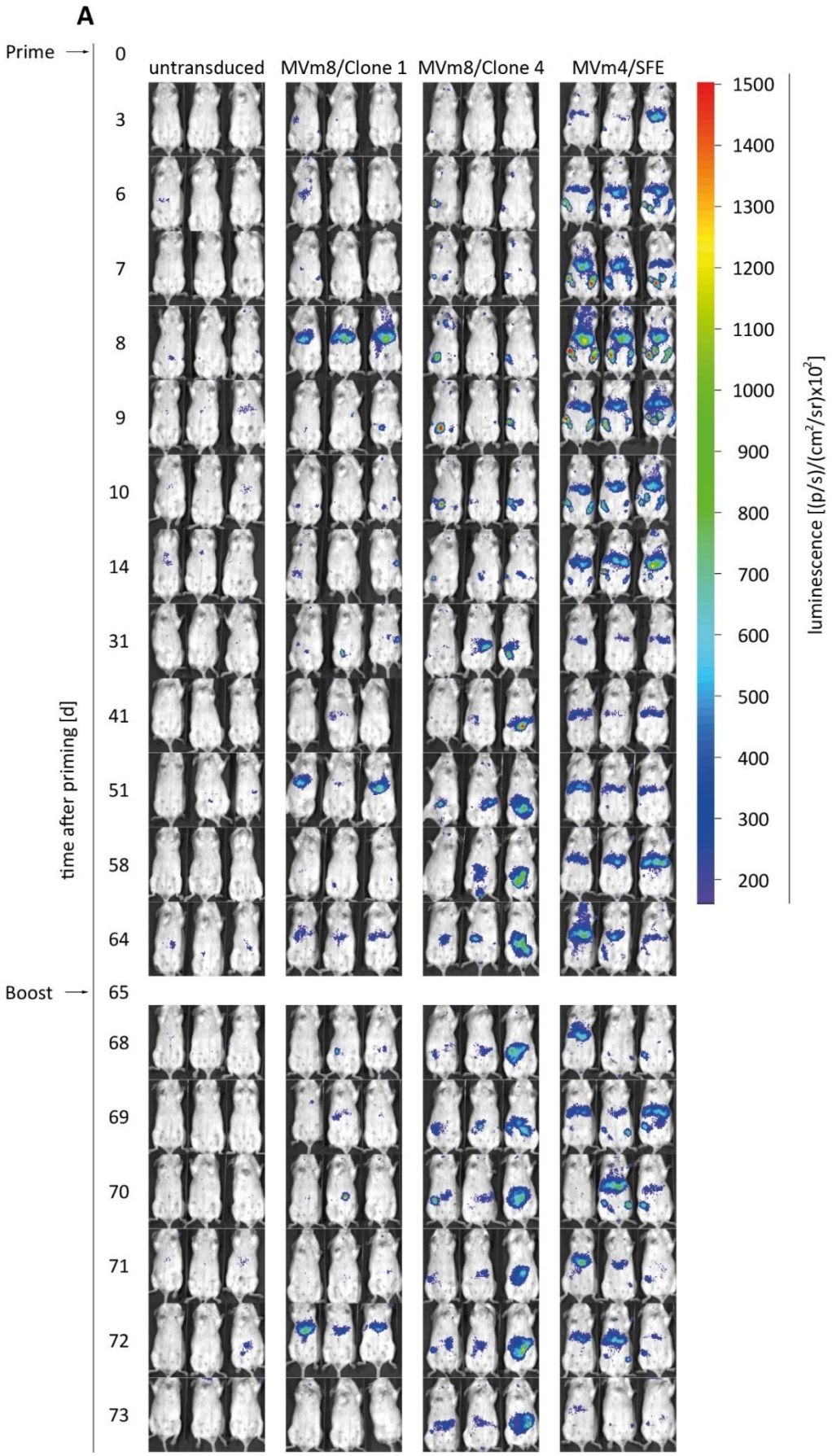
A
Prime
Boost
time after priming [d]
0
3
6
7
8
9
10
14
31
41
51
58
64
65
68
69
70
71
72
73
untransduced
MVm8/Clone 1
MVm8/Clone 4
MVm4/SFE
1500
1400
1300
1200
1100
1000
900
800
700
600
500
400
300
200
luminescence [(p/s)/(cm²/sr)x10²]

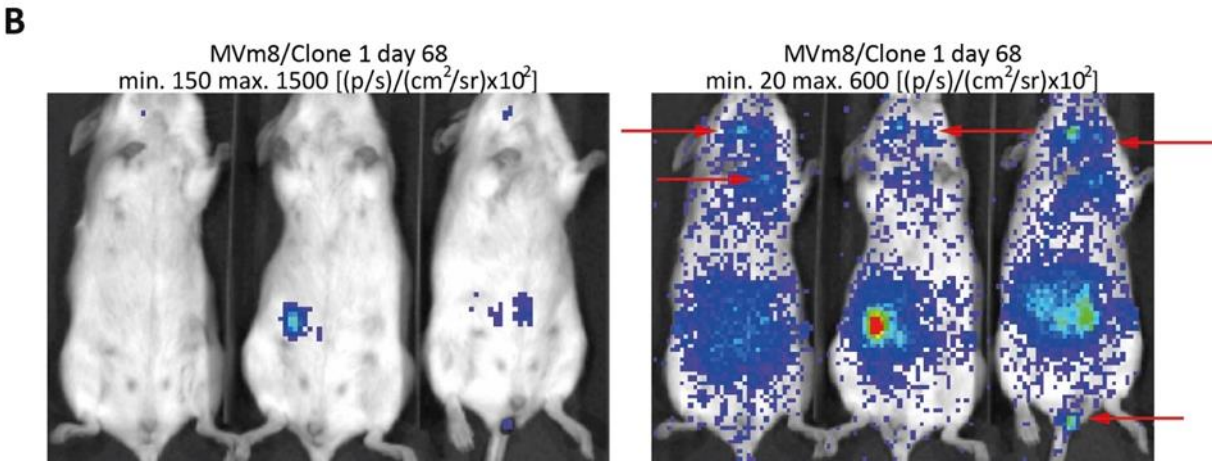

Figure 13 *In vivo* transduction of BALB/c mice, detailed.

(A) Detailed view of all mice transduced with MVm8/Clone 1-FLuc, MVm8/Clone 4-FLuc or MVm4/SFE-RLuc. Mice were primed by s.c. application of irradiated AB1 HA cells into the right flank on day 0. Mice received an antigenic boost by s.c. application of irradiated AB1 HA cells into the contralateral flank on day 65. *in vivo* imaging measured transduced T cells indirectly via reporter luciferases after i.v. application of luciferin or coelenterazine in a dark chamber using Xenogen IVIS 200. IVIS-parameters: min=150 and max=1500 [(p/s)/(cm^2/sr)x10^2]. Luminescence was measured for a total of 73 days. Untransduced T cells-repopulated BALB/c Rag2$^{-/-}$ were used as controls. (B) Comparison of two threshold settings for IVIS-imaging for the mice transduced by MVm8/Clone 1-FLuc showing the lowest luminescence of the used vectors. Arrows indicate areas of luminescence excluded by the threshold used in (A). MVm8/Clone 1, MVm8/Clone 4, and MVm4/SFE refer to MV-pseudotyped gRV coding for a TCR linked to a reporter luciferase, i.e., MVm8/Clone 1-FLuc, MVm8/Clone 4-FLuc, and MVm4/SFE-RLuc, respectively.

11. Discussion

11.1. Limitations of *ex vivo* manufacturing of T cell-based immunotherapies

T cell immunotherapy is one of the most promising advances in cancer therapy. The introduction of therapeutic TCRs and CARs can convey new specificities to redirect a patient's immune system and induce a potent anti-tumour response. The major drawbacks of T cell-based therapies are inherent to the current manufacturing process, which requires patient-individual apheresis, *ex vivo* activation, transduction and expansion to generate a therapeutic product. The first difficulty of this process stems from the quality and quantity of cells available for apheresis. T cell-based therapeutics are currently only approved for relapsed and refractory malignancies. Eligible patients have commonly undergone several regimens of chemotherapy, often resulting in leukopenia and insufficient T cell quality. Problems in T cell activation and transduction as well as inadequate expansion of engineered T cells may result in manufacturing failures. The final T cell products' efficacy is further reduced by repeated freeze-thaw cycles, comprising at least two, after apheresis and before infusion of the finished product (136, 170). This is further complicated by an excessive time demand, in a setting where the patient's response to bridging therapy is often short-lived and patients are prone to clinical deterioration due to progressive disease, complications and comorbidities. Long *ex vivo* culture time can impede T cell effector functions, and their ability to home and proliferate adequately (136). Advances in *in vitro* culture counteract this by focusing on less differentiated phenotypes like naïve and central memory T cells (239-241). Implementation of these new approaches is hampered by the complexity of T cell product manufacturing, and all the while threatening to further increase complexity, costs, and manufacturing time. Clinically approved T cell therapies focus on generating $CD8^+$ cytotoxic T cells, to which the efficacy of adoptive cell therapy has most often been attributed. Recent studies have shown that $CD4^+$ CAR T cells demonstrated similar cytolytic efficacy *in vitro* and *in vivo.* They showed slower initial tumour killing capacity, but were less prone to activation-induced cell death and exhaustion (242-244).

Extrapolating these findings to TCR-engineered T cells, it is likely that combining MHC class I-restricted TCR in $CD8^+$ T cells and MHC class II-restricted TCR in $CD4^+$ T cells would result in a more potent and longer lasting anti-tumour response. Current gene transfer protocols do not differentiate between T cell subsets, including state-of-the-art stable

non-viral transfection methods like electroporation, magnetofection, laser- or ultrasound-assisted protocols employing the *Sleeping Beauty* transposon/transposase system, the clustered regularly interspersed short palindromic repeat (CRISPR)-Cas9 system, ZINC finger nucleases (ZFNs) or Transcription Activator-Like Effector Endonucleases (TALENs) (224, 245-248). Strategies to employ subset-specific gene transfer would have to include an additional step of prior separation, e.g., by FACS or MACS, potentially losing a portion of cells and reducing viability. The highly specialized manufacturing process of T cell products for clinical use must abide by GMP guidelines and undergoes thorough testing before approval is granted. Specialized centres are approved for the use of cellular therapies in an involved review process (carried out in the United States of America by the Foundation for the Accreditation of Cellular Therapy (FACT) and by their European equivalent, the Joint Accreditation Committee ISCT-Europe & EBMT (JACIE)). This further limits the availability of this technology and drastically increases its price. As an example, the use of the CAR T cell products tisagenlecleucel and axicabtagen ciloleucel have an estimated cost of US$475,000 and US$373,000 per patient, which can even, in the case of complications, be significantly higher (169).

11.2. The synergy of $CD4^+$ and $CD8^+$ T cells and their clinical application

In this thesis, the potent capabilities of a MV-envelope-based pseudotyped gRV system to transduce T cell subsets *in vivo* specifically, efficiently, and stably were demonstrated. The vector system could not only solve many issues related to the state-of-the-art manufacture of T cell therapies but also further T cell therapies by establishing an uncomplicated yet flexible tool to introduce emergent findings to clinical application. One major development in the field of T cell therapies is the renaissance of $CD4^+$ T cells as a mediator in anti-tumour responses. Most cell-based cancer immunotherapies are focused on $CD8^+$ T cells. Though the success of these therapies is undeniable and the critical role $CD8^+$ T cells play in effectuating a tumour response should not be understated, emergent observations have illustrated the potent and synergistic anti-tumour effects of $CD4^+$ T cells. The tumour microenvironment (TME) in solid malignancies poses a daunting challenge for T cell therapies. Aberrant tumour vasculature, and cancer-associated cells like tumour-associated macrophages and fibroblasts can inhibit T cell extravasation. The effector function of T cells is blunted by the expression of checkpoint molecules, and the proliferation and activation of T cells is diminished by a lack of DCs or their

impaired function. In solid malignancies, the access to surface antigen is often limited to the periphery, hindering CAR T cells especially, in contrast to TCR-engineered T cells (147, 148). The hypoxic environment as well as many metabolites, like lactate and reactive oxygen species, have been implicated in aggravating these conditions, with new publications broadening the spectrum of inhibitory mechanisms of the TME every year (249-252). Common approaches to overcome this inhibitory environment are the implementation of checkpoint inhibitors or the generating of a T cell product which can thrive in these conditions. Examples of these approaches include the selection of T cell subtypes, enhanced signalling mechanisms, co-delivery of transgenes coding for cytokines, or PD-1-blocking scFv (99, 144-146, 149, 150). The clinical success of $CD8^+$ T cell-based immunotherapies, as well as the more easily available tools to monitor them and established read-outs like $CD8^+$ T cell infiltration for anti-tumour immunity, have long eclipsed the role of $CD4^+$ T cells in an anti-tumour response. Recently, the varied and potent mechanisms by which $CD4^+$ T cells initiate and sustain an effective anti-tumour effect have been highlighted, even in immunotherapy specifically designed to elicit a $CD8^+$ T cell response (253-256). The eponymous function of $CD4^+$ T helper cells describes their ability to initiate and assist many anti-tumour effects. $CD4^+$ T cells can secrete IL-2, which leads to the activation, differentiation, proliferation of $CD8^+$ T cells (51-54). They can maintain an inflammatory milieu by CD40L upregulation, thereby supporting DC activation and cross-presentation (257). The interplay of antigens recognized by $CD4^+$ and $CD8^+$ T cells is a prerequisite for bystander elimination of antigen-negative cancer cells, disrupting the TME and countering a mechanism of immune escape (258, 259). CD40L signalling to B cells has been described to also induce a humoral response against solid tumours in tumour-adjacent tertiary lymphoid structures (260, 261). $CD4^+$ T cells also facilitate a direct anti-tumour effect by the secretion of IFNγ and TNFα (64-67). The synergy of $CD4^+$ and $CD8^+$ T cells targeting model antigens was demonstrated in several tumour models. It was shown that the co-transfer of $CD8^+$ and $CD4^+$ T cells targeting the antigen SIYRYYGL on PRO4L, a fibrosarcoma cell line, was able to eradicate a tumour, whereas $CD8^+$ T cells alone only inhibited tumour growth (262). It was shown that for optimal synergy, $CD4^+$ T cells must be antigen-specific and act locally to promote recruitment and proliferation in the induction phase of an anti-tumour response. Furthermore, Schietinger et al. demonstrated the necessity of cooperation between $CD4^+$ and $CD8^+$ T cells during the effector phase to eliminate a tumour (258, 261). Li et al. presented data of $CD8^+$ and $CD4^+$ T cells targeting ovalbumin presented by B16 cells. While

adoptive cell therapy with $CD8^+$ T cells alone was highly effective in mediating regression, it achieved only low tumour-free survival rates. The co-transfer of $CD4^+$ T1 cells and $CD8^+$ T cells induced a synergistic and lasting anti-tumour response (263). Current manufacturing of T cell products is focused only on $CD8^+$ T cells, with an already excessive demand of cost and time needed for production. The inclusion of $CD4^+$ T cells would necessitate the manufacturing of a second product, due to the different culture conditions and times required by each T cell subtype, further complicating an already involved process. The MV-envelope-based pseudotyped gRV system used in this thesis is a promising approach which could not only introduce a new specificity to $CD8^+$ T cells, but simultaneously also introduce this to the previously neglected $CD4^+$ T cells. It is a tool that could dramatically simplify the process of generating a functional T cell product *in vivo*. This could lower costs and save time, while, due to its simple process, being able to adapt to advances in the field of T cell-based immunotherapy more quickly. Examples of this could include the downregulation of checkpoint molecules, e.g., employing RNA interference, or the co-delivery of transgenes coding for cytokines. New TCRs targeting emergent tumour-associated antigens might get approved for clinical application much more quickly. The vision for the clinical application of this vector technology shall be explored in more detail later.

11.3. Cell lines and immune escape

To explore the capabilities of the MV-envelope-based gRV vector system, three TCRs were chosen that recognize epitopes of the same antigen. Two of them are restricted to MCH class I and the other to MHC class II. To lay the foundation for future *in vivo* experiments, cell lines expressing the model antigen HA had to be established and characterised. Transduced T cells were challenged with the cancer cell lines harbouring their recognized model antigen, first *in vitro* and later *in vivo*. The cell lines AB1 and 4T1 were chosen because they are progressor cell lines, capable of reliably establishing a solid tumour in immunocompetent BALB/c mice, thus enabling *in vivo* tumour experiments. The added immunogenicity of the antigen HA expressed on the derivatives AB1 HA and 4T1 HA was a concern, as injected cancer cells might be rejected or a change in the growth kinetic might lessen the value of parental cell lines as negative controls in future experiments. AB1 and 4T1 and their HA-transgenic derivatives were shown to be capable of reliably generating tumours in immunocompetent BALB/c mice, with no significant difference in growth kinetics between the parental and derivative cell lines.

4T1 and 4T1 HA showed exceptional tumorigenicity, matching previously published data in which it was used to model highly invasive, metastatic stage IV breast cancer. The unchanged growth kinetics indicated the cell lines' high immune escape competence. A variety of mechanisms have been described, including downregulation of MHC molecules, overexpression of checkpoint receptors and CD47, loss of antigen and defects in antigen presentation (264-270). Future *in vivo* experiments could leverage the availability of different cell lines further to evaluate the capabilities of the gRV vector system discussed in this thesis, e.g., comparing their anti-tumour effect to directly administered T cells and the synergy of $CD4^+$ and $CD8^+$ T cells like in the work of Li et al. and Arina et al. discussed earlier (11.2) (262). The *in vivo* experiment of this thesis was a proof of principle, employing irradiated cancer cells as a target to show T cell expansion and homing. Subsequent experiments attempting to immunize mice against a tumour challenge or treating an already established tumour by *in vivo* transduction using the highly aggressive cell lines described in this thesis would be daunting. Conversely, the MV-pseudotyped gRV vector system's ability to transduce $CD4^+$ and $CD8^+$ T cells selectively and simultaneously might be capable of overcoming this challenge by generating a synergistic T cell response. A different but not mutually exclusive approach would be to combine *in vivo* engineered T cells with checkpoint therapies, which have been shown to be effective in tumour challenges employing AB1 and 4T1 cells (264-267).

11.4. TCR avidity and co-culture

The three different TCRs employed in this thesis target the model antigen HA. Clone 1 and Clone 4 recognize an epitope restricted to MHC class I H-$2k^d$, with Clone 4 described in the literature as a TCR of decidedly higher avidity. SFE is a high-avidity TCR recognizing a different epitope - restricted MHC class II I-E^d (see 10.1, page 35) (209-220). The difference in reported avidity mirrored the results of *in vitro* co-culture assays, where the mean functional avidity of Clone 1 TCR to ^{518}IYSTVASSL^{526} was $10^{-8,12}$ mol/l, while Clone 4 TCR showed an EC50 of $10^{-10,73}$ mol/l. These differences between Clone 1 and Clone 4 TCR were also apparent in *in vivo* transduction experiments. Clone 4 TCR-transduced T cells exhibited higher avidity and superior homing capabilities. The interplay of TCRs of different avidities can be investigated further in future experiments in the setting of *in vivo* transduction.

11.5. TCR-engineering by subset-specific *in vivo* transduction of $CD4^+$ and $CD8^+$ T cells

In the scope of this thesis, BALB/c T cells were transduced *in vivo* by systemic application of MVm8- or MVm4-pseudotyped gRV vectors conveying a new specificity for HA antigen. Their effector functions were analysed by *in vivo* imaging using a bioluminescence reporter assay. Sufficient proliferation of the target cells was necessary to achieve high transduction rates using gRV vectors. We opted for a setting in which BALB/c derived splenocytes were used to repopulate BALB/c $Rag2^{-/-}$ mice prior to transduction. A luciferase signal was detected in all mice after systemic application of either MVm8-Clone 1-FLuc, MVm8-Clone 4-FLuc or MVm4-SFE-RLuc and consecutive antigenic stimulus. Bioluminescence showed strong dynamics indicating T cell effector functions such as proliferation and homing. For all vectors, *in vivo* transduction was stable for a long period of time, lasting for over 70 days with no indication of transience of transduction or loss of transduced cells as determined by signal intensity after the boost. Moreover, a faster increase in luminescence detected after a second antigenic boost on day 65 indicated a T cell memory response. After the first antigenic stimulus, the maximum luciferase signal exhibited by mice transduced with one of the MHC class I-specific TCRs, Clone 1 or Clone 4, showed pronounced differences. The luminescence detected in mice transduced with the high-affinity Clone 4 TCR was higher by an average factor of approximately 2.5 on days 7 and 8. Despite the striking and correlating data of *in vitro* co-culture assays, these differences must be interpreted cautiously, as a number of factors influence the intensity of the detected bioluminescence signal. In the experimental setup, the initial *in vivo* transduction efficiency was unknown, so either T cells transduced with the low- or high-avidity TCR might have started out with a larger pool of redirected cells. Furthermore, shortly after transduction, T cells cannot be reliably detected using *in vivo* imaging. In the case of transduction using MVm8-Clone 1 and Clone 4, a pronounced difference was detected earliest on day 6 after stimulus. Transduced T cells might not have homed and accumulated or proliferated sufficiently yet to be detected. Other factors include differences of depth in tissue of antigenic stimulus, in the hair of mice, and in the amount of luciferin injected, as well as differences in instrumentation, angle of detection and background noise (271). In future experiments, some of these factors could be controlled. *In vivo* transduction efficiency could be judged using TCR analysis of circulating T cells in the blood, sampling of tumour or site of antigenic stimulus. To increase the detected

bioluminescence signal, mice could be shaven, or if a future project required a very low threshold of detection, a more invasive approach could be chosen, like window chamber implantation surgery or intravital microscopy (272).

The strongest bioluminescence was detected in mice transduced with $CD4^+$-specific MVm4-SFE-RLuc vector. As a caveat, for this vector *Renilla* luciferase was used as a reporter rather than *Firefly* luciferase, so direct comparison between mice transduced with MVm4-SFE-RLuc and $CD8^+$-specific vectors is limited. Conversely, this enables future *in vivo* imaging of co-transduction experiments using MVm4 and MVm8 gRV vectors in tandem. The luminescence signal in mice transduced with MVm4-SFE-RLuc was exceptionally strong in nodal regions of draining lymph nodes after antigenic stimulus, which could be indicative of the priming of naïve transduced T cells. This was corroborated by a consecutive increase of luminescence at the site of antigenic stimulus, which was followed by retraction of transduced cells. This dynamic was highly suggestive of a T cell response, showing homing, proliferation and contraction, and is further supported by the faster dynamic of onset and extinction of the T cell's luminescence signal following a second antigenic stimulus.

11.6. Titre and variety of pseudotyped retroviral vectors

Viral envelopes consisting of two components, for which binding and membrane fusion are mediated by separate glycoproteins, are ideally suited for retargeting of retroviral vectors. MV codes for two transmembrane envelope glycoproteins called hemagglutinin (H) and membrane fusion protein (F). Modifying the specificity of H does not impede membrane fusion, as is the case for most viral vectors. A challenge of pseudotyping is the yield of viral vectors; in prior experiments, MV-envelope was used to pseudotype LV vectors, resulting in a minimal yield, being likely due to steric interferences between the intracellular domain of H and F, and LV matrix proteins. The yield was dramatically increased through the use of variants of H and F, differing in the length and sequence of the cytoplasmatic tail (273). The same process was employed in the work of I. Edes and transferred to gRV, determining a different set of variants as optimal for MV-envelope-pseudotyped gRV (208). The titres of viral vectors generated in this thesis were sufficient to transduce T cells *in vitro* and *in vivo*. For the *in vivo* experiment, viral vector particles were injected into each mouse. The generated MV-pseudotyped gRV vectors' titres decrease with the increasing size of the transgene, and in a clinical or different experimental setting, a higher titre can be achieved by omitting the

reporter luciferases (208). To upscale this technology to humans, an even higher yield would be advantageous. In humans, though the restriction of volume of injection is less challenging than in mice, the current manufacturing process of transient transfection is still labour- and cost-intensive. It could be streamlined by generating a stable packaging cell line, and upscaled by flow-through or steady-state systems coupled to downstream concentration of viral particles like ultrafiltration and continuous flow centrifugation. Different members of the paramyxovirus family share the feature of MV of distinct glycoproteins mediating binding and fusion and have been shown to be suitable for pseudotyping of LV vectors. *Nipah* virus (NV) envelope-pseudotyped LV, showing promise of a higher achievable titre, might be a suitable choice for application in humans. Additionally, NV infections are exceedingly rare in humans, making the existence of a humoral immunity interfering with gene transfer highly unlikely (274, 275).

11.7. Conclusion and outlook

This doctoral thesis expands on the work of I. Edes, who generated a gRV system pseudotyped with a MV-based envelope capable of transducing B6-derived $CD8^+$ and $CD4^+$ T cells *in vitro,* and demonstrated for the first time that *in vivo* transduction of $CD8^+$ T cells by systemic application of targeting vectors leads to functionally engineered T cells (208). This gRV system was successfully transferred from B6 to BALB/c mice, confirming the targeted *in vivo* transduction of $CD8^+$ T cells, and expanding on this by providing the first evidence of targeted *in vivo* transduction of $CD4^+$ T cells leading to a functional MHC class II-restricted T cell response. This technology and its successors have a vast potential of application in cancer therapy. The drawbacks of currently employed T cell-based therapy, namely its limited choice of cell types and its demands on manufacturing costs and time, have been outlined. Although CAR T cell therapies are currently the main clinical focus, recent developments in TCR-engineered T cells show great promise. The choice of antigen to target is a cardinal aspect of T cell therapy; common types of tumour antigen include TAA and cancer-germline antigens, with neither being entirely restricted to malignancies, raising concerns about on-target toxicity and a blunted therapeutic effect due to tolerance mechanisms. Tumour neoantigens, truly foreign proteins absent entirely in healthy tissue, offer an ideal target for T cell therapies. CAR T cell therapy is severely limited in targeting this category due to the rarity of surface-expressed neoantigens that are not presented as epitopes on MHC. TCR-engineered

T cells have great potential in targeting these intracellular antigens in the context of MHC complexes (276-278). Since these neoantigens show considerable variation in different patients and a suitable TCR has to be matched to a patient's HLA repertoire, in the near future a personalized approach to generating a TCR-engineered T cell therapy would likely have to be taken. It has been shown that the identification of neoantigen-specific TCRs and generation of TCR-engineered T cells is feasible in short time periods (279-281). In this approach, the time needed for generation of a personalized T cell therapy is critical for success and might be reduced by employing an *in vivo* transduction approach offered by MV-envelope-pseudotyped vectors or their successors. Powerful tools to quickly generate TCRs of optimal affinity to target cancer antigens have emerged, e.g., AB*ab*DII mice transgenic for human TCR gene loci and HLA-A2 enabling the isolation of human TCRs (168, 282). Currently, TCR gene transfer therapy focuses on a personalized approach using diverse methods for rapid identification of therapeutic TCRs, with particular success for MHC class I-restricted TCRs. The vector system described in this thesis aims at simplifying the manufacturing of T cell therapeutics and including $CD4^+$ T cells simultaneously. Advances in the identification and engineering of TCRs, and the analysis and prediction of tumour antigens might enable the generation of comprehensive libraries of TCRs targeting suitable antigens and restricted to an array of different HLA-alleles, albeit despite major advances, the detection of therapeutic MHC class II-restricted TCRs remains challenging (283). This library could be translated to clinical use by having the transgenes available as MV-pseudotyped vectors to use for *in vivo* transduction, akin to off-the-shelf products like checkpoint inhibitors, or to be quickly produced using packaging cell lines and the desired transgene. The simplicity and flexibility of this vector system would enable advances in TCR engineering as well as the co-delivery of cytokines or checkpoint-inhibition to be included, thereby promptly introducing advances in the field into clinical application.

12. References

1. Brubaker SW, Bonham KS, Zanoni I, Kagan JC. Innate immune pattern recognition: a cell biological perspective. Annu Rev Immunol. 2015;33:257-90.
2. Mogensen TH. Pathogen recognition and inflammatory signaling in innate immune defenses. Clin Microbiol Rev. 2009;22(2):240-73.
3. Akira S, Uematsu S, Takeuchi O. Pathogen recognition and innate immunity. Cell. 2006;124(4):783-801.
4. Jin MS, Lee JO. Structures of the toll-like receptor family and its ligand complexes. Immunity. 2008;29(2):182-91.
5. Kawai T, Akira S. Innate immune recognition of viral infection. Nat Immunol. 2006;7(2):131-7.
6. Ahmed R, Gray D. Immunological memory and protective immunity: understanding their relation. Science. 1996;272(5258):54-60.
7. McHeyzer-Williams LJ, McHeyzer-Williams MG. Antigen-specific memory B cell development. Annu Rev Immunol. 2005;23:487-513.
8. Rajewsky K. Clonal selection and learning in the antibody system. Nature. 1996;381(6585):751-8.
9. Hedrick SM, Nielsen EA, Kavaler J, Cohen DI, Davis MM. Sequence relationships between putative T-cell receptor polypeptides and immunoglobulins. Nature. 1984;308(5955):153-8.
10. Yanagi Y, Yoshikai Y, Leggett K, Clark SP, Aleksander I, Mak TW. A human T cell-specific cDNA clone encodes a protein having extensive homology to immunoglobulin chains. Nature. 1984;308(5955):145-9.
11. Garcia KC, Degano M, Stanfield RL, Brunmark A, Jackson MR, Peterson PA, Teyton L, Wilson IA. An alphabeta T cell receptor structure at 2.5 A and its orientation in the TCR-MHC complex. Science. 1996;274(5285):209-19.
12. Garboczi DN, Ghosh P, Utz U, Fan QR, Biddison WE, Wiley DC. Structure of the complex between human T-cell receptor, viral peptide and HLA-A2. Nature. 1996;384(6605):134-41.
13. Falk K, Rotzschke O, Rammensee HG. Cellular peptide composition governed by major histocompatibility complex class I molecules. Nature. 1990;348(6298):248-51.
14. Rotzschke O, Falk K, Deres K, Schild H, Norda M, Metzger J, Jung G, Rammensee HG. Isolation and analysis of naturally processed viral peptides as recognized by cytotoxic T cells. Nature. 1990;348(6298):252-4.
15. Ziegler K, Unanue ER. Identification of a macrophage antigen-processing event required for I-region-restricted antigen presentation to T lymphocytes. J Immunol. 1981;127(5):1869-75.
16. Allen PM, Strydom DJ, Unanue ER. Processing of lysozyme by macrophages: identification of the determinant recognized by two T-cell hybridomas. Proc Natl Acad Sci U S A. 1984;81(8):2489-93.
17. Babbitt BP, Allen PM, Matsueda G, Haber E, Unanue ER. Binding of immunogenic peptides to Ia histocompatibility molecules. Nature. 1985;317(6035):359-61.
18. Chien Y, Becker DM, Lindsten T, Okamura M, Cohen DI, Davis MM. A third type of murine T-cell receptor gene. Nature. 1984;312(5989):31-5.
19. Saito H, Kranz DM, Takagaki Y, Hayday AC, Eisen HN, Tonegawa S. Complete primary structure of a heterodimeric T-cell receptor deduced from cDNA sequences. Nature. 1984;309(5971):757-62.
20. Yanagi Y, Chan A, Chin B, Minden M, Mak TW. Analysis of cDNA clones specific for human T cells and the alpha and beta chains of the T-cell receptor heterodimer from a human T-cell line. Proc Natl Acad Sci U S A. 1985;82(10):3430-4.
21. Minami Y, Weissman AM, Samelson LE, Klausner RD. Building a multichain receptor: synthesis, degradation, and assembly of the T-cell antigen receptor. Proc Natl Acad Sci U S A. 1987;84(9):2688-92.

22. Reth M. Antigen receptor tail clue. Nature. 1989;338(6214):383-4.
23. Wang H, Kadlecek TA, Au-Yeung BB, Goodfellow HE, Hsu LY, Freedman TS, Weiss A. ZAP-70: an essential kinase in T-cell signaling. Cold Spring Harb Perspect Biol. 2010;2(5):a002279.
24. Chan AC, Desai DM, Weiss A. The role of protein tyrosine kinases and protein tyrosine phosphatases in T cell antigen receptor signal transduction. Annu Rev Immunol. 1994;12:555-92.
25. Siegel JN, Egerton M, Phillips AF, Samelson LE. Multiple signal transduction pathways activated through the T cell receptor for antigen. Semin Immunol. 1991;3(5):325-34.
26. Letourneur F, Klausner RD. A novel di-leucine motif and a tyrosine-based motif independently mediate lysosomal targeting and endocytosis of CD3 chains. Cell. 1992;69(7):1143-57.
27. Starr TK, Jameson SC, Hogquist KA. Positive and negative selection of T cells. Annu Rev Immunol. 2003;21:139-76.
28. Klein L, Kyewski B, Allen PM, Hogquist KA. Positive and negative selection of the T cell repertoire: what thymocytes see (and don't see). Nat Rev Immunol. 2014;14(6):377-91.
29. Zinkernagel RM, Callahan GN, Klein J, Dennert G. Cytotoxic T cells learn specificity for self H-2 during differentiation in the thymus. Nature. 1978;271(5642):251-3.
30. Derbinski J, Schulte A, Kyewski B, Klein L. Promiscuous gene expression in medullary thymic epithelial cells mirrors the peripheral self. Nat Immunol. 2001;2(11):1032-9.
31. Surh CD, Sprent J. T-cell apoptosis detected in situ during positive and negative selection in the thymus. Nature. 1994;372(6501):100-3.
32. Gotter J, Brors B, Hergenhahn M, Kyewski B. Medullary epithelial cells of the human thymus express a highly diverse selection of tissue-specific genes colocalized in chromosomal clusters. J Exp Med. 2004;199(2):155-66.
33. Gallegos AM, Bevan MJ. Central tolerance to tissue-specific antigens mediated by direct and indirect antigen presentation. J Exp Med. 2004;200(8):1039-49.
34. Kappler JW, Roehm N, Marrack P. T cell tolerance by clonal elimination in the thymus. Cell. 1987;49(2):273-80.
35. Picca CC, Caton AJ. The role of self-peptides in the development of CD4+ CD25+ regulatory T cells. Curr Opin Immunol. 2005;17(2):131-6.
36. Hsieh CS, Lee HM, Lio CW. Selection of regulatory T cells in the thymus. Nat Rev Immunol. 2012;12(3):157-67.
37. Van Laethem F, Sarafova SD, Park JH, Tai X, Pobezinsky L, Guinter TI, Adoro S, Adams A, Sharrow SO, Feigenbaum L, Singer A. Deletion of CD4 and CD8 coreceptors permits generation of alphabetaT cells that recognize antigens independently of the MHC. Immunity. 2007;27(5):735-50.
38. Schatz DG, Oettinger MA, Baltimore D. The V(D)J recombination activating gene, RAG-1. Cell. 1989;59(6):1035-48.
39. Oettinger MA, Schatz DG, Gorka C, Baltimore D. RAG-1 and RAG-2, adjacent genes that synergistically activate V(D)J recombination. Science. 1990;248(4962):1517-23.
40. van Gent DC, Ramsden DA, Gellert M. The RAG1 and RAG2 proteins establish the 12/23 rule in V(D)J recombination. Cell. 1996;85(1):107-13.
41. Mombaerts P, Iacomini J, Johnson RS, Herrup K, Tonegawa S, Papaioannou VE. RAG-1-deficient mice have no mature B and T lymphocytes. Cell. 1992;68(5):869-77.
42. Shinkai Y, Rathbun, G., Lam, K. P., Oltz, E. M., Stewart, V., Mendelsohn, M., Charron, J., Datta, M., Young, F., Stall, A. M. . RAG-2-deficient mice lack mature lymphocytes owing to inability to initiate V(D)J rearrangement. Cell. 1992;68(5):855-67.
43. Saint-Ruf C, Ungewiss K, Groettrup M, Bruno L, Fehling HJ, von Boehmer H. Analysis and expression of a cloned pre-T cell receptor gene. Science. 1994;266(5188):1208-12.
44. Malissen M, Trucy J, Jouvin-Marche E, Cazenave PA, Scollay R, Malissen B. Regulation of TCR alpha and beta gene allelic exclusion during T-cell development. Immunol Today. 1992;13(8):315-22.

45. Ribot JC, Lopes N, Silva-Santos B. Gammadelta T cells in tissue physiology and surveillance. Nat Rev Immunol. 2021;21(4):221-32.
46. Kalliolias GD, Ivashkiv LB. TNF biology, pathogenic mechanisms and emerging therapeutic strategies. Nature Reviews Rheumatology. 2016;12(1):49-62.
47. Komori T, Okada A, Stewart V, Alt FW. Lack of N regions in antigen receptor variable region genes of TdT-deficient lymphocytes. Science. 1993;261(5125):1171-5.
48. Davis MM, Bjorkman PJ. T-cell antigen receptor genes and T-cell recognition. Nature. 1988;334(6181):395-402.
49. Li S, Lefranc MP, Miles JJ, Alamyar E, Giudicelli V, Duroux P, Freeman JD, Corbin VD, Scheerlinck JP, Frohman MA, Cameron PU, Plebanski M, Loveland B, Burrows SR, Papenfuss AT, Gowans EJ. IMGT/HighV QUEST paradigm for T cell receptor IMGT clonotype diversity and next generation repertoire immunoprofiling. Nat Commun. 2013;4:2333.
50. Fischer DS, Wu Y, Schubert B, Theis FJ. Predicting antigen specificity of single T cells based on TCR CDR3 regions. Molecular Systems Biology. 2020;16(8):e9416.
51. Schwartz RH. Models of T cell anergy: is there a common molecular mechanism? J Exp Med. 1996;184(1):1-8.
52. Murphy K, Weaver C, Janeway C. Janeway's immunobiology 9th Edition. New York2017.
53. Bour-Jordan H, Blueston JA. CD28 function: a balance of costimulatory and regulatory signals. J Clin Immunol. 2002;22(1):1-7.
54. Gonzalo JA, Delaney T, Corcoran J, Goodearl A, Gutierrez-Ramos JC, Coyle AJ. Cutting edge: the related molecules CD28 and inducible costimulator deliver both unique and complementary signals required for optimal T cell activation. J Immunol. 2001;166(1):1-5.
55. Zhu J, Yamane H, Paul WE. Differentiation of effector CD4 T cell populations (*). Annu Rev Immunol. 2010;28:445-89.
56. Freiberg BA, Kupfer H, Maslanik W, Delli J, Kappler J, Zaller DM, Kupfer A. Staging and resetting T cell activation in SMACs. Nat Immunol. 2002;3(10):911-7.
57. Lee KH, Holdorf AD, Dustin ML, Chan AC, Allen PM, Shaw AS. T cell receptor signaling precedes immunological synapse formation. Science. 2002;295(5559):1539-42.
58. Monks CR, Freiberg BA, Kupfer H, Sciaky N, Kupfer A. Three-dimensional segregation of supramolecular activation clusters in T cells. Nature. 1998;395(6697):82-6.
59. Monks CR, Kupfer H, Tamir I, Barlow A, Kupfer A. Selective modulation of protein kinase C-theta during T-cell activation. Nature. 1997;385(6611):83-6.
60. Liu X, Lieberman J. Knocking 'em Dead: Pore-Forming Proteins in Immune Defense. Annu Rev Immunol. 2020;38:455-85.
61. Guicciardi ME, Gores GJ. Life and death by death receptors. Faseb j. 2009;23(6):1625-37.
62. Barry M, Bleackley RC. Cytotoxic T lymphocytes: all roads lead to death. Nat Rev Immunol. 2002;2(6):401-9.
63. Rouvier E, Luciani MF, Golstein P. Fas involvement in Ca(2+)-independent T cell-mediated cytotoxicity. J Exp Med. 1993;177(1):195-200.
64. Wheelock EF. Interferon-Like Virus-Inhibitor Induced in Human Leukocytes by Phytohemagglutinin. Science. 1965;149(3681):310-1.
65. Carswell EA, Old LJ, Kassel RL, Green S, Fiore N, Williamson B. An endotoxin-induced serum factor that causes necrosis of tumors. Proc Natl Acad Sci U S A. 1975;72(9):3666-70.
66. Guidotti LG, Chisari FV. Cytokine-mediated control of viral infections. Virology. 2000;273(2):221-7.
67. Kammertoens T, Friese C, Arina A, Idel C, Briesemeister D, Rothe M, Ivanov A, Szymborska A, Patone G, Kunz S, Sommermeyer D, Engels B, Leisegang M, Textor A, Fehling HJ, Fruttiger M, Lohoff M, Herrmann A, Yu H, Weichselbaum R, Uckert W, Hubner N, Gerhardt H, Beule D, Schreiber H, Blankenstein T. Tumour ischaemia by interferon-gamma resembles physiological blood vessel regression. Nature. 2017;545(7652):98-102.
68. Mosmann TR, Sad S. The expanding universe of T-cell subsets: Th1, Th2 and more. Immunol Today. 1996;17(3):138-46.

69. Caza T, Landas S. Functional and Phenotypic Plasticity of CD4(+) T Cell Subsets. Biomed Res Int. 2015;2015:521957.
70. Kondělková K, Vokurková D, Krejsek J, Borská L, Fiala Z, Ctirad A. Regulatory T cells (TREG) and their roles in immune system with respect to immunopathological disorders. Acta Medica (Hradec Kralove). 2010;53(2):73-7.
71. Godfrey DI, MacDonald HR, Kronenberg M, Smyth MJ, Van Kaer L. NKT cells: what's in a name? Nat Rev Immunol. 2004;4(3):231-7.
72. Gumperz JE, Brenner MB. CD1-specific T cells in microbial immunity. Curr Opin Immunol. 2001;13(4):471-8.
73. Hong S, Scherer DC, Singh N, Mendiratta SK, Serizawa I, Koezuka Y, Van Kaer L. Lipid antigen presentation in the immune system: lessons learned from CD1d knockout mice. Immunol Rev. 1999;169:31-44.
74. Coley WB. The treatment of malignant tumors by repeated inoculations of erysipelas. With a report of ten original cases. . Am J Medical Sciences. 1893(105):487-511.
75. Coley WB. The Treatment of Inoperable Sarcoma by Bacterial Toxins (the Mixed Toxins of the Streptococcus erysipelas and the Bacillus prodigiosus). Proc R Soc Med. 1910;3(Surg Sect):1-48.
76. Morales A, Eidinger D, Bruce AW. Intracavitary Bacillus Calmette-Guerin in the treatment of superficial bladder tumors. J Urol. 1976;116(2):180-3.
77. Loeb L. Ueber Entstehung eines Sarkoms nach Transplantation eines Adenocarcinoms einer japanischen Maus. Zeitschrift für Krebsforschung. 1908;7(1):80-110.
78. Oiseth SJ, Aziz MS. Cancer immunotherapy: a brief review of the history, possibilities, and challenges ahead. Journal of Cancer Metastasis and Treatment. 2017;3:250-61.
79. Strong LC. INBRED MICE IN SCIENCE. In: Morse HC, editor. Origins of Inbred Mice: Academic Press; 1978. p. 45-67.
80. Old LJ, Boyse EA. Specific antigens of tumors and leukemias of experimental animals. Med Clin North Am. 1966;50(3):901-12.
81. Prehn RT, Main JM. Immunity to methylcholanthrene-induced sarcomas. J Natl Cancer Inst. 1957;18(6):769-78.
82. Gross L. Intradermal Immunization of C3H Mice against a Sarcoma That Originated in an Animal of the Same Line. Cancer Research. 1943;3(5):326.
83. Foley EJ. Antigenic properties of methylcholanthrene-induced tumors in mice of the strain of origin. Cancer Res. 1953;13(12):835-7.
84. Burnet FM. The concept of immunological surveillance. Prog Exp Tumor Res. 1970;13:1-27.
85. Rygaard J, Povlsen CO. The nude mouse vs. the hypothesis of immunological surveillance. Transplant Rev. 1976;28:43-61.
86. Penn I. Tumors of the immunocompromised patient. Annu Rev Med. 1988;39:63-73.
87. Blankenstein T. Do autochthonous tumors interfere with effector T cell responses? Semin Cancer Biol. 2007;17(4):267-74.
88. Intlekofer AM, Thompson CB. At the bench: preclinical rationale for CTLA-4 and PD-1 blockade as cancer immunotherapy. J Leukoc Biol. 2013;94(1):25-39.
89. Buchbinder EI, Desai A. CTLA-4 and PD-1 Pathways: Similarities, Differences, and Implications of Their Inhibition. Am J Clin Oncol. 2016;39(1):98-106.
90. Sheng IY, Ornstein MC. Ipilimumab and Nivolumab as First-Line Treatment of Patients with Renal Cell Carcinoma: The Evidence to Date. Cancer Manag Res. 2020;12:4871-81.
91. Motzer RJ, Tannir NM, McDermott DF, Arén Frontera O, Melichar B, Choueiri TK, Plimack ER, Barthélémy P, Porta C, George S, Powles T, Donskov F, Neiman V, Kollmannsberger CK, Salman P, Gurney H, Hawkins R, Ravaud A, Grimm MO, Bracarda S, Barrios CH, Tomita Y, Castellano D, Rini BI, Chen AC, Mekan S, McHenry MB, Wind-Rotolo M, Doan J, Sharma P, Hammers HJ, Escudier B. Nivolumab plus Ipilimumab versus Sunitinib in Advanced Renal-Cell Carcinoma. N Engl J Med. 2018;378(14):1277-90.

92. Rijavec E, Indini A, Ghidini M, Tomasello G, Cattaneo M, Barbin F, Grossi F. Nivolumab plus ipilimumab for the first-line treatment of metastatic NSCLC. Expert Rev Anticancer Ther. 2021;21(7):705-13.
93. Overman MJ, McDermott R, Leach JL, Lonardi S, Lenz HJ, Morse MA, Desai J, Hill A, Axelson M, Moss RA, Goldberg MV, Cao ZA, Ledeine JM, Maglinte GA, Kopetz S, André T. Nivolumab in patients with metastatic DNA mismatch repair-deficient or microsatellite instability-high colorectal cancer (CheckMate 142): an open-label, multicentre, phase 2 study. Lancet Oncol. 2017;18(9):1182-91.
94. Carreno BM, Collins M. The B7 family of ligands and its receptors: new pathways for costimulation and inhibition of immune responses. Annu Rev Immunol. 2002;20:29-53.
95. Ishida Y, Agata Y, Shibahara K, Honjo T. Induced expression of PD-1, a novel member of the immunoglobulin gene superfamily, upon programmed cell death. Embo j. 1992;11(11):3887-95.
96. Latchman Y, Wood CR, Chernova T, Chaudhary D, Borde M, Chernova I, Iwai Y, Long AJ, Brown JA, Nunes R, Greenfield EA, Bourque K, Boussiotis VA, Carter LL, Carreno BM, Malenkovich N, Nishimura H, Okazaki T, Honjo T, Sharpe AH, Freeman GJ. PD-L2 is a second ligand for PD-1 and inhibits T cell activation. Nat Immunol. 2001;2(3):261-8.
97. Hui E, Cheung J, Zhu J, Su X, Taylor MJ, Wallweber HA, Sasmal DK, Huang J, Kim JM, Mellman I, Vale RD. T cell costimulatory receptor CD28 is a primary target for PD-1-mediated inhibition. Science. 2017;355(6332):1428-33.
98. Barber DL, Wherry EJ, Masopust D, Zhu B, Allison JP, Sharpe AH, Freeman GJ, Ahmed R. Restoring function in exhausted CD8 T cells during chronic viral infection. Nature. 2006;439(7077):682-7.
99. Waldman AD, Fritz JM, Lenardo MJ. A guide to cancer immunotherapy: from T cell basic science to clinical practice. Nature Reviews Immunology. 2020;20(11):651-68.
100. Iwai Y, Ishida M, Tanaka Y, Okazaki T, Honjo T, Minato N. Involvement of PD-L1 on tumor cells in the escape from host immune system and tumor immunotherapy by PD-L1 blockade. Proc Natl Acad Sci U S A. 2002;99(19):12293-7.
101. He YF, Zhang GM, Wang XH, Zhang H, Yuan Y, Li D, Feng ZH. Blocking programmed death-1 ligand-PD-1 interactions by local gene therapy results in enhancement of antitumor effect of secondary lymphoid tissue chemokine. J Immunol. 2004;173(8):4919-28.
102. Robert C, Long GV, Brady B, Dutriaux C, Maio M, Mortier L, Hassel JC, Rutkowski P, McNeil C, Kalinka-Warzocha E, Savage KJ, Hernberg MM, Lebbe C, Charles J, Mihalcioiu C, Chiarion-Sileni V, Mauch C, Cognetti F, Arance A, Schmidt H, Schadendorf D, Gogas H, Lundgren-Eriksson L, Horak C, Sharkey B, Waxman IM, Atkinson V, Ascierto PA. Nivolumab in previously untreated melanoma without BRAF mutation. N Engl J Med. 2015;372(4):320-30.
103. Weber J, Mandala M, Del Vecchio M, Gogas HJ, Arance AM, Cowey CL, Dalle S, Schenker M, Chiarion-Sileni V, Marquez-Rodas I, Grob JJ, Butler MO, Middleton MR, Maio M, Atkinson V, Queirolo P, Gonzalez R, Kudchadkar RR, Smylie M, Meyer N, Mortier L, Atkins MB, Long GV, Bhatia S, Lebbe C, Rutkowski P, Yokota K, Yamazaki N, Kim TM, de Pril V, Sabater J, Qureshi A, Larkin J, Ascierto PA, CheckMate C. Adjuvant Nivolumab versus Ipilimumab in Resected Stage III or IV Melanoma. N Engl J Med. 2017;377(19):1824-35.
104. Weber JS, D'Angelo SP, Minor D, Hodi FS, Gutzmer R, Neyns B, Hoeller C, Khushalani NI, Miller WH, Jr., Lao CD, Linette GP, Thomas L, Lorigan P, Grossmann KF, Hassel JC, Maio M, Sznol M, Ascierto PA, Mohr P, Chmielowski B, Bryce A, Svane IM, Grob JJ, Krackhardt AM, Horak C, Lambert A, Yang AS, Larkin J. Nivolumab versus chemotherapy in patients with advanced melanoma who progressed after anti-CTLA-4 treatment (CheckMate 037): a randomised, controlled, open-label, phase 3 trial. Lancet Oncol. 2015;16(4):375-84.
105. Gong J, Chehrazi-Raffle A, Reddi S, Salgia R. Development of PD-1 and PD-L1 inhibitors as a form of cancer immunotherapy: a comprehensive review of registration trials and future considerations. J Immunother Cancer. 2018;6(1):8.
106. Fuchs CS, Doi T, Jang RW, Muro K, Satoh T, Machado M, Sun W, Jalal SI, Shah MA, Metges JP, Garrido M, Golan T, Mandala M, Wainberg ZA, Catenacci DV, Ohtsu A, Shitara K, Geva R, Bleeker J, Ko AH, Ku G, Philip P, Enzinger PC, Bang YJ, Levitan D, Wang J, Rosales M, Dalal RP, Yoon HH.

Safety and Efficacy of Pembrolizumab Monotherapy in Patients With Previously Treated Advanced Gastric and Gastroesophageal Junction Cancer: Phase 2 Clinical KEYNOTE-059 Trial. JAMA Oncol. 2018;4(5):e180013.

107. Bellmunt J, de Wit R, Vaughn DJ, Fradet Y, Lee JL, Fong L, Vogelzang NJ, Climent MA, Petrylak DP, Choueiri TK, Necchi A, Gerritsen W, Gurney H, Quinn DI, Culine S, Sternberg CN, Mai Y, Poehlein CH, Perini RF, Bajorin DF, Investigators K-. Pembrolizumab as Second-Line Therapy for Advanced Urothelial Carcinoma. N Engl J Med. 2017;376(11):1015-26.
108. Moskowitz AJ, Shah G, Schoder H, Ganesan N, Drill E, Hancock H, Davey T, Perez L, Ryu S, Sohail S, Santarosa A, Galasso N, Neuman R, Liotta B, Blouin W, Kumar A, Lahoud O, Batlevi CL, Hamlin P, Straus DJ, Rodriguez-Rivera I, Owens C, Caron P, Intlekofer AM, Hamilton A, Horwitz SM, Falchi L, Joffe E, Johnson W, Lee C, Palomba ML, Noy A, Matasar MJ, Pongas G, Salles G, Vardhana S, Sanin BW, von Keudell G, Yahalom J, Dogan A, Zelenetz AD, Moskowitz CH. Phase II Trial of Pembrolizumab Plus Gemcitabine, Vinorelbine, and Liposomal Doxorubicin as Second-Line Therapy for Relapsed or Refractory Classical Hodgkin Lymphoma. J Clin Oncol. 2021:JCO2101056.
109. El-Khoueiry AB, Sangro B, Yau T, Crocenzi TS, Kudo M, Hsu C, Kim TY, Choo SP, Trojan J, Welling THR, Meyer T, Kang YK, Yeo W, Chopra A, Anderson J, Dela Cruz C, Lang L, Neely J, Tang H, Dastani HB, Melero I. Nivolumab in patients with advanced hepatocellular carcinoma (CheckMate 040): an open-label, non-comparative, phase 1/2 dose escalation and expansion trial. Lancet. 2017;389(10088):2492-502.
110. Sharma P, Retz M, Siefker-Radtke A, Baron A, Necchi A, Bedke J, Plimack ER, Vaena D, Grimm MO, Bracarda S, Arranz JA, Pal S, Ohyama C, Saci A, Qu X, Lambert A, Krishnan S, Azrilevich A, Galsky MD. Nivolumab in metastatic urothelial carcinoma after platinum therapy (CheckMate 275): a multicentre, single-arm, phase 2 trial. Lancet Oncol. 2017;18(3):312-22.
111. Ferris RL, Blumenschein G, Jr., Fayette J, Guigay J, Colevas AD, Licitra L, Harrington K, Kasper S, Vokes EE, Even C, Worden F, Saba NF, Iglesias Docampo LC, Haddad R, Rordorf T, Kiyota N, Tahara M, Monga M, Lynch M, Geese WJ, Kopit J, Shaw JW, Gillison ML. Nivolumab for Recurrent Squamous-Cell Carcinoma of the Head and Neck. N Engl J Med. 2016;375(19):1856-67.
112. Ferris RL, Spanos WC, Leidner R, Goncalves A, Martens UM, Kyi C, Sharfman W, Chung CH, Devriese LA, Gauthier H, Chiosea SI, Vujanovic L, Taube JM, Stein JE, Li J, Li B, Chen T, Barrows A, Topalian SL. Neoadjuvant nivolumab for patients with resectable HPV-positive and HPV-negative squamous cell carcinomas of the head and neck in the CheckMate 358 trial. J Immunother Cancer. 2021;9(6).
113. Motzer RJ, Escudier B, George S, Hammers HJ, Srinivas S, Tykodi SS, Sosman JA, Plimack ER, Procopio G, McDermott DF, Castellano D, Choueiri TK, Donskov F, Gurney H, Oudard S, Richardet M, Peltola K, Alva AS, Carducci M, Wagstaff J, Chevreau C, Fukasawa S, Tomita Y, Gauler TC, Kollmannsberger CK, Schutz FA, Larkin J, Cella D, McHenry MB, Saggi SS, Tannir NM. Nivolumab versus everolimus in patients with advanced renal cell carcinoma: Updated results with long-term follow-up of the randomized, open-label, phase 3 CheckMate 025 trial. Cancer. 2020;126(18):4156-67.
114. Horn L, Mansfield AS, Szczesna A, Havel L, Krzakowski M, Hochmair MJ, Huemer F, Losonczy G, Johnson ML, Nishio M, Reck M, Mok T, Lam S, Shames DS, Liu J, Ding B, Lopez-Chavez A, Kabbinavar F, Lin W, Sandler A, Liu SV, Group IMS. First-Line Atezolizumab plus Chemotherapy in Extensive-Stage Small-Cell Lung Cancer. N Engl J Med. 2018;379(23):2220-9.
115. Schmid P, Chui SY, Emens LA. Atezolizumab and Nab-Paclitaxel in Advanced Triple-Negative Breast Cancer. Reply. N Engl J Med. 2019;380(10):987-8.
116. Rittmeyer A, Barlesi F, Waterkamp D, Park K, Ciardiello F, von Pawel J, Gadgeel SM, Hida T, Kowalski DM, Dols MC, Cortinovis DL, Leach J, Polikoff J, Barrios C, Kabbinavar F, Frontera OA, De Marinis F, Turna H, Lee JS, Ballinger M, Kowanetz M, He P, Chen DS, Sandler A, Gandara DR, Group OAKS. Atezolizumab versus docetaxel in patients with previously treated non-small-cell lung cancer (OAK): a phase 3, open-label, multicentre randomised controlled trial. Lancet. 2017;389(10066):255-65.

117. Rosenberg JE, Hoffman-Censits J, Powles T, van der Heijden MS, Balar AV, Necchi A, Dawson N, O'Donnell PH, Balmanoukian A, Loriot Y, Srinivas S, Retz MM, Grivas P, Joseph RW, Galsky MD, Fleming MT, Petrylak DP, Perez-Gracia JL, Burris HA, Castellano D, Canil C, Bellmunt J, Bajorin D, Nickles D, Bourgon R, Frampton GM, Cui N, Mariathasan S, Abidoye O, Fine GD, Dreicer R. Atezolizumab in patients with locally advanced and metastatic urothelial carcinoma who have progressed following treatment with platinum-based chemotherapy: a single-arm, multicentre, phase 2 trial. Lancet. 2016;387(10031):1909-20.
118. Antonia SJ, Ozguroglu M. Durvalumab in Stage III Non-Small-Cell Lung Cancer. N Engl J Med. 2018;378(9):869-70.
119. Powles T, van der Heijden MS, Castellano D, Galsky MD, Loriot Y, Petrylak DP, Ogawa O, Park SH, Lee JL, De Giorgi U, Bogemann M, Bamias A, Eigl BJ, Gurney H, Mukherjee SD, Fradet Y, Skoneczna I, Tsiatas M, Novikov A, Suarez C, Fay AP, Duran I, Necchi A, Wildsmith S, He P, Angra N, Gupta AK, Levin W, Bellmunt J, investigators Ds. Durvalumab alone and durvalumab plus tremelimumab versus chemotherapy in previously untreated patients with unresectable, locally advanced or metastatic urothelial carcinoma (DANUBE): a randomised, open-label, multicentre, phase 3 trial. Lancet Oncol. 2020;21(12):1574-88.
120. Motzer RJ, Penkov K, Haanen J, Rini B, Albiges L, Campbell MT, Venugopal B, Kollmannsberger C, Negrier S, Uemura M, Lee JL, Vasiliev A, Miller WH, Jr., Gurney H, Schmidinger M, Larkin J, Atkins MB, Bedke J, Alekseev B, Wang J, Mariani M, Robbins PB, Chudnovsky A, Fowst C, Hariharan S, Huang B, di Pietro A, Choueiri TK. Avelumab plus Axitinib versus Sunitinib for Advanced Renal-Cell Carcinoma. N Engl J Med. 2019;380(12):1103-15.
121. Patel MR, Ellerton J, Infante JR, Agrawal M, Gordon M, Aljumaily R, Britten CD, Dirix L, Lee KW, Taylor M, Schoffski P, Wang D, Ravaud A, Gelb AB, Xiong J, Rosen G, Gulley JL, Apolo AB. Avelumab in metastatic urothelial carcinoma after platinum failure (JAVELIN Solid Tumor): pooled results from two expansion cohorts of an open-label, phase 1 trial. Lancet Oncol. 2018;19(1):51-64.
122. Kaufman HL, Russell J, Hamid O, Bhatia S, Terheyden P, D'Angelo SP, Shih KC, Lebbe C, Linette GP, Milella M, Brownell I, Lewis KD, Lorch JH, Chin K, Mahnke L, von Heydebreck A, Cuillerot JM, Nghiem P. Avelumab in patients with chemotherapy-refractory metastatic Merkel cell carcinoma: a multicentre, single-group, open-label, phase 2 trial. Lancet Oncol. 2016;17(10):1374-85.
123. Southam CM, Brunschwig A, Levin AG, Dizon QS. Effect of leukocytes on transplantability of human cancer. Cancer. 1966;19(11):1743-53.
124. Weiden PL, Flournoy N, Thomas ED, Prentice R, Fefer A, Buckner CD, Storb R. Antileukemic effect of graft-versus-host disease in human recipients of allogeneic-marrow grafts. N Engl J Med. 1979;300(19):1068-73.
125. Apperley JF, Jones L, Hale G, Waldmann H, Hows J, Rombos Y, Tsatalas C, Marcus RE, Goolden AW, Gordon-Smith EC. Bone marrow transplantation for patients with chronic myeloid leukaemia: T-cell depletion with Campath-1 reduces the incidence of graft-versus-host disease but may increase the risk of leukaemic relapse. Bone Marrow Transplant. 1986;1(1):53-66.
126. Hill GR, Betts BC, Tkachev V, Kean LS, Blazar BR. Current Concepts and Advances in Graft-Versus-Host Disease Immunology. Annual Review of Immunology. 2021;39(1):19-49.
127. Horowitz MM, Gale RP, Sondel PM, Goldman JM, Kersey J, Kolb H-J, Rimm AA, Ringdén O, Rozman C, Speck B, Truitt RL, Zwaan FE, Bortin MM. Graft-versus-leukemia reactions after bone marrow transplantation. Blood. 1990;75(3):555-62.
128. Goulmy E. Minor histocompatibility antigens: allo target molecules for tumor-specific immunotherapy. Cancer J. 2004;10(1):1-7.
129. Patriarca F, Sperotto A, Lorentino F, Oldani E, Mammoliti S, Isola M, Picardi A, Arcese W, Saporiti G, Sorasio R, Mordini N, Cavattoni I, Musso M, Borghero C, Micò C, Fanin R, Bruno B, Ciceri F, Bonifazi F. Donor Lymphocyte Infusions After Allogeneic Stem Cell Transplantation in Acute Leukemia: A Survey From the Gruppo Italiano Trapianto Midollo Osseo (GITMO). Frontiers in Oncology. 2020;10(1959).

130. Kolb HJ, Mittermuller J, Clemm C, Holler E, Ledderose G, Brehm G, Heim M, Wilmanns W. Donor leukocyte transfusions for treatment of recurrent chronic myelogenous leukemia in marrow transplant patients. Blood. 1990;76(12):2462-5.
131. Porter DL, Roth MS, McGarigle C, Ferrara JL, Antin JH. Induction of graft-versus-host disease as immunotherapy for relapsed chronic myeloid leukemia. N Engl J Med. 1994;330(2):100-6.
132. Rosenberg SA, Packard BS, Aebersold PM, Solomon D, Topalian SL, Toy ST, Simon P, Lotze MT, Yang JC, Seipp CA, Simpson C, Carter C, Bock S, Schwartzentruber D, Wei JP, White DE. Use of tumor-infiltrating lymphocytes and interleukin-2 in the immunotherapy of patients with metastatic melanoma. A preliminary report. N Engl J Med. 1988;319(25):1676-80.
133. Rosenberg SA, Yang JC, Sherry RM, Kammula US, Hughes MS, Phan GQ, Citrin DE, Restifo NP, Robbins PF, Wunderlich JR, Morton KE, Laurencot CM, Steinberg SM, White DE, Dudley ME. Durable complete responses in heavily pretreated patients with metastatic melanoma using T-cell transfer immunotherapy. Clin Cancer Res. 2011;17(13):4550-7.
134. Cohen CJ, Gartner JJ, Horovitz-Fried M, Shamalov K, Trebska-McGowan K, Bliskovsky VV, Parkhurst MR, Ankri C, Prickett TD, Crystal JS, Li YF, El-Gamil M, Rosenberg SA, Robbins PF. Isolation of neoantigen-specific T cells from tumor and peripheral lymphocytes. J Clin Invest. 2015;125(10):3981-91.
135. Zacharakis N, Chinnasamy H, Black M, Xu H, Lu YC, Zheng Z, Pasetto A, Langhan M, Shelton T, Prickett T, Gartner J, Jia L, Trebska-McGowan K, Somerville RP, Robbins PF, Rosenberg SA, Goff SL, Feldman SA. Immune recognition of somatic mutations leading to complete durable regression in metastatic breast cancer. Nat Med. 2018;24(6):724-30.
136. Gattinoni L, Klebanoff CA, Palmer DC, Wrzesinski C, Kerstann K, Yu Z, Finkelstein SE, Theoret MR, Rosenberg SA, Restifo NP. Acquisition of full effector function in vitro paradoxically impairs the in vivo antitumor efficacy of adoptively transferred CD8+ T cells. J Clin Invest. 2005;115(6):1616-26.
137. Battram AM, Bachiller M, Lopez V, Fernández de Larrea C, Urbano-Ispizua A, Martín-Antonio B. IL-15 Enhances the Persistence and Function of BCMA-Targeting CAR-T Cells Compared to IL-2 or IL-15/IL-7 by Limiting CAR-T Cell Dysfunction and Differentiation. Cancers (Basel). 2021;13(14).
138. Bonte S, de Munter S, Billiet L, Goetgeluk G, Ingels J, Jansen H, Pille M, de Cock L, Weening K, Taghon T, Leclercq G, Vandekerckhove B, Kerre T. In vitro OP9-DL1 co-culture and subsequent maturation in the presence of IL-21 generates tumor antigen-specific T cells with a favorable less-differentiated phenotype and enhanced functionality. Oncoimmunology. 2021;10(1):1954800.
139. Dembic Z, Haas W, Weiss S, McCubrey J, Kiefer H, von Boehmer H, Steinmetz M. Transfer of specificity by murine alpha and beta T-cell receptor genes. Nature. 1986;320(6059):232-8.
140. Clauss J, Obenaus M, Miskey C, Ivics Z, Izsvák Z, Uckert W, Bunse M. Efficient Non-Viral T-Cell Engineering by Sleeping Beauty Minicircles Diminishing DNA Toxicity and miRNAs Silencing the Endogenous T-Cell Receptors. Hum Gene Ther. 2018;29(5):569-84.
141. Izsvák Z, Hackett PB, Cooper LJN, Ivics Z. Translating Sleeping Beauty transposition into cellular therapies: Victories and challenges. BioEssays. 2010;32(9):756-67.
142. Tyagarajan S, Spencer T, Smith J. Optimizing CAR-T Cell Manufacturing Processes during Pivotal Clinical Trials. Mol Ther Methods Clin Dev. 2020;16:136-44.
143. Dudley ME, Wunderlich JR, Robbins PF, Yang JC, Hwu P, Schwartzentruber DJ, Topalian SL, Sherry R, Restifo NP, Hubicki AM, Robinson MR, Raffeld M, Duray P, Seipp CA, Rogers-Freezer L, Morton KE, Mavroukakis SA, White DE, Rosenberg SA. Cancer regression and autoimmunity in patients after clonal repopulation with antitumor lymphocytes. Science. 2002;298(5594):850-4.
144. Klebanoff CA, Gattinoni L, Torabi-Parizi P, Kerstann K, Cardones AR, Finkelstein SE, Palmer DC, Antony PA, Hwang ST, Rosenberg SA, Waldmann TA, Restifo NP. Central memory self/tumor-reactive CD8+ T cells confer superior antitumor immunity compared with effector memory T cells. Proc Natl Acad Sci U S A. 2005;102(27):9571-6.

145. Berger C, Jensen MC, Lansdorp PM, Gough M, Elliott C, Riddell SR. Adoptive transfer of effector CD8+ T cells derived from central memory cells establishes persistent T cell memory in primates. J Clin Invest. 2008;118(1):294-305.
146. Hinrichs CS, Borman ZA, Gattinoni L, Yu Z, Burns WR, Huang J, Klebanoff CA, Johnson LA, Kerkar SP, Yang S, Muranski P, Palmer DC, Scott CD, Morgan RA, Robbins PF, Rosenberg SA, Restifo NP. Human effector CD8+ T cells derived from naive rather than memory subsets possess superior traits for adoptive immunotherapy. Blood. 2011;117(3):808-14.
147. Li J, Li W, Huang K, Zhang Y, Kupfer G, Zhao Q. Chimeric antigen receptor T cell (CAR-T) immunotherapy for solid tumors: lessons learned and strategies for moving forward. J Hematol Oncol. 2018;11(1):22.
148. Salmon H, Franciszkiewicz K, Damotte D, Dieu-Nosjean MC, Validire P, Trautmann A, Mami-Chouaib F, Donnadieu E. Matrix architecture defines the preferential localization and migration of T cells into the stroma of human lung tumors. J Clin Invest. 2012;122(3):899-910.
149. Chmielewski M, Abken H. TRUCKS, the fourth-generation CAR T cells: Current developments and clinical translation. ADVANCES IN CELL AND GENE THERAPY. 2020;3(3):e84.
150. Rafiq S, Yeku OO, Jackson HJ, Purdon TJ, van Leeuwen DG, Drakes DJ, Song M, Miele MM, Li Z, Wang P, Yan S, Xiang J, Ma X, Seshan VE, Hendrickson RC, Liu C, Brentjens RJ. Targeted delivery of a PD-1-blocking scFv by CAR-T cells enhances anti-tumor efficacy in vivo. Nat Biotechnol. 2018;36(9):847-56.
151. Neelapu SS, Locke FL, Bartlett NL, Lekakis LJ, Miklos DB, Jacobson CA, Braunschweig I, Oluwole OO, Siddiqi T, Lin Y, Timmerman JM, Stiff PJ, Friedberg JW, Flinn IW, Goy A, Hill BT, Smith MR, Deol A, Farooq U, McSweeney P, Munoz J, Avivi I, Castro JE, Westin JR, Chavez JC, Ghobadi A, Komanduri KV, Levy R, Jacobsen ED, Witzig TE, Reagan P, Bot A, Rossi J, Navale L, Jiang Y, Aycock J, Elias M, Chang D, Wiezorek J, Go WY. Axicabtagene Ciloleucel CAR T-Cell Therapy in Refractory Large B-Cell Lymphoma. New England Journal of Medicine. 2017;377(26):2531-44.
152. Schuster SJ, Bishop MR, Tam CS, Waller EK, Borchmann P, McGuirk JP, Jäger U, Jaglowski S, Andreadis C, Westin JR, Fleury I, Bachanova V, Foley SR, Ho PJ, Mielke S, Magenau JM, Holte H, Pantano S, Pacaud LB, Awasthi R, Chu J, Anak Ö, Salles G, Maziarz RT. Tisagenlecleucel in Adult Relapsed or Refractory Diffuse Large B-Cell Lymphoma. New England Journal of Medicine. 2018;380(1):45-56.
153. Wang M, Munoz J, Goy A, Locke FL, Jacobson CA, Hill BT, Timmerman JM, Holmes H, Jaglowski S, Flinn IW, McSweeney PA, Miklos DB, Pagel JM, Kersten M-J, Milpied N, Fung H, Topp MS, Houot R, Beitinjaneh A, Peng W, Zheng L, Rossi JM, Jain RK, Rao AV, Reagan PM. KTE-X19 CAR T-Cell Therapy in Relapsed or Refractory Mantle-Cell Lymphoma. New England Journal of Medicine. 2020;382(14):1331-42.
154. Abramson JS, Palomba ML, Gordon LI, Lunning MA, Wang M, Arnason J, Mehta A, Purev E, Maloney DG, Andreadis C, Sehgal A, Solomon SR, Ghosh N, Albertson TM, Garcia J, Kostic A, Mallaney M, Ogasawara K, Newhall K, Kim Y, Li D, Siddiqi T. Lisocabtagene maraleucel for patients with relapsed or refractory large B-cell lymphomas (TRANSCEND NHL 001): a multicentre seamless design study. The Lancet. 2020;396(10254):839-52.
155. Friedman KM, Garrett TE, Evans JW, Horton HM, Latimer HJ, Seidel SL, Horvath CJ, Morgan RA. Effective Targeting of Multiple B-Cell Maturation Antigen-Expressing Hematological Malignances by Anti-B-Cell Maturation Antigen Chimeric Antigen Receptor T Cells. Hum Gene Ther. 2018;29(5):585-601.
156. Munshi NC, Anderson LD, Shah N, Madduri D, Berdeja J, Lonial S, Raje N, Lin Y, Siegel D, Oriol A, Moreau P, Yakoub-Agha I, Delforge M, Cavo M, Einsele H, Goldschmidt H, Weisel K, Rambaldi A, Reece D, Petrocca F, Massaro M, Connarn JN, Kaiser S, Patel P, Huang L, Campbell TB, Hege K, San-Miguel J. Idecabtagene Vicleucel in Relapsed and Refractory Multiple Myeloma. New England Journal of Medicine. 2021;384(8):705-16.
157. Straathof K, Flutter B, Wallace R, Jain N, Loka T, Depani S, Wright G, Thomas S, Cheung GW-K, Gileadi T, Stafford S, Kokalaki E, Barton J, Marriott C, Rampling D, Ogunbiyi O, Akarca AU, Marafioti T, Inglott S, Gilmour K, Al-Hajj M, Day W, McHugh K, Biassoni L, Sizer N, Barton C,

Edwards D, Dragoni I, Silvester J, Dyer K, Traub S, Elson L, Brook S, Westwood N, Robson L, Bedi A, Howe K, Barry A, Duncan C, Barone G, Pule M, Anderson J. Antitumor activity without on-target off-tumor toxicity of GD2–chimeric antigen receptor T cells in patients with neuroblastoma. Science Translational Medicine. 2020;12(571):eabd6169.

158. Chulanetra M, Morchang A, Sayour E, Eldjerou L, Milner R, Lagmay J, Cascio M, Stover B, Slayton W, Chaicumpa W, Yenchitsomanus P-T, Chang L-J. GD2 chimeric antigen receptor modified T cells in synergy with sub-toxic level of doxorubicin targeting osteosarcomas. Am J Cancer Res. 2020;10(2):674-87.
159. Kandalaft LE, Powell DJ, Coukos G. A phase I clinical trial of adoptive transfer of folate receptor-alpha redirected autologous T cells for recurrent ovarian cancer. Journal of Translational Medicine. 2012;10(1):157.
160. Morgan RA, Dudley ME, Wunderlich JR, Hughes MS, Yang JC, Sherry RM, Royal RE, Topalian SL, Kammula US, Restifo NP, Zheng Z, Nahvi A, de Vries CR, Rogers-Freezer LJ, Mavroukakis SA, Rosenberg SA. Cancer regression in patients after transfer of genetically engineered lymphocytes. Science. 2006;314(5796):126-9.
161. Johnson LA, Morgan RA, Dudley ME, Cassard L, Yang JC, Hughes MS, Kammula US, Royal RE, Sherry RM, Wunderlich JR, Lee C-CR, Restifo NP, Schwarz SL, Cogdill AP, Bishop RJ, Kim H, Brewer CC, Rudy SF, VanWaes C, Davis JL, Mathur A, Ripley RT, Nathan DA, Laurencot CM, Rosenberg SA. Gene therapy with human and mouse T-cell receptors mediates cancer regression and targets normal tissues expressing cognate antigen. Blood. 2009;114(3):535-46.
162. Chandran SS, Paria BC, Srivastava AK, Rothermel LD, Stephens DJ, Dudley ME, Somerville R, Wunderlich JR, Sherry RM, Yang JC, Rosenberg SA, Kammula US. Persistence of CTL Clones Targeting Melanocyte Differentiation Antigens Was Insufficient to Mediate Significant Melanoma Regression in Humans. Clinical Cancer Research. 2015;21(3):534.
163. Cameron BJ, Gerry AB, Dukes J, Harper JV, Kannan V, Bianchi FC, Grand F, Brewer JE, Gupta M, Plesa G, Bossi G, Vuidepot A, Powlesland AS, Legg A, Adams KJ, Bennett AD, Pumphrey NJ, Williams DD, Binder-Scholl G, Kulikovskaya I, Levine BL, Riley JL, Varela-Rohena A, Stadtmauer EA, Rapoport AP, Linette GP, June CH, Hassan NJ, Kalos M, Jakobsen BK. Identification of a Titin-derived HLA-A1-presented peptide as a cross-reactive target for engineered MAGE A3-directed T cells. Sci Transl Med. 2013;5(197):197ra03.
164. Linette GP, Stadtmauer EA, Maus MV, Rapoport AP, Levine BL, Emery L, Litzky L, Bagg A, Carreno BM, Cimino PJ, Binder-Scholl GK, Smethurst DP, Gerry AB, Pumphrey NJ, Bennett AD, Brewer JE, Dukes J, Harper J, Tayton-Martin HK, Jakobsen BK, Hassan NJ, Kalos M, June CH. Cardiovascular toxicity and titin cross-reactivity of affinity-enhanced T cells in myeloma and melanoma. Blood. 2013;122(6):863-71.
165. Robbins PF, Li YF, El-Gamil M, Zhao Y, Wargo JA, Zheng Z, Xu H, Morgan RA, Feldman SA, Johnson LA, Bennett AD, Dunn SM, Mahon TM, Jakobsen BK, Rosenberg SA. Single and Dual Amino Acid Substitutions in TCR CDRs Can Enhance Antigen-Specific T Cell Functions. The Journal of Immunology. 2008;180(9):6116.
166. Robbins PF, Morgan RA, Feldman SA, Yang JC, Sherry RM, Dudley ME, Wunderlich JR, Nahvi AV, Helman LJ, Mackall CL, Kammula US, Hughes MS, Restifo NP, Raffeld M, Lee CC, Levy CL, Li YF, El-Gamil M, Schwarz SL, Laurencot C, Rosenberg SA. Tumor regression in patients with metastatic synovial cell sarcoma and melanoma using genetically engineered lymphocytes reactive with NY-ESO-1. J Clin Oncol. 2011;29(7):917-24.
167. Li LP, Lampert JC, Chen X, Leitao C, Popović J, Müller W, Blankenstein T. Transgenic mice with a diverse human T cell antigen receptor repertoire. Nat Med. 2010;16(9):1029-34.
168. Obenaus M, Leitão C, Leisegang M, Chen X, Gavvovidis I, van der Bruggen P, Uckert W, Schendel DJ, Blankenstein T. Identification of human T-cell receptors with optimal affinity to cancer antigens using antigen-negative humanized mice. Nature Biotechnology. 2015;33(4):402-7.
169. Hernandez I, Prasad V, Gellad WF. Total Costs of Chimeric Antigen Receptor T-Cell Immunotherapy. JAMA Oncol. 2018;4(7):994-6.

170. Roddie C, O'Reilly M, Dias Alves Pinto J, Vispute K, Lowdell M. Manufacturing chimeric antigen receptor T cells: issues and challenges. Cytotherapy. 2019;21(3):327-40.
171. Ghosh S, Brown AM, Jenkins C, Campbell K. Viral Vector Systems for Gene Therapy: A Comprehensive Literature Review of Progress and Biosafety Challenges. Applied Biosafety. 2020;25(1):7-18.
172. Raper SE, Chirmule N, Lee FS, Wivel NA, Bagg A, Gao G-p, Wilson JM, Batshaw ML. Fatal systemic inflammatory response syndrome in a ornithine transcarbamylase deficient patient following adenoviral gene transfer. Molecular Genetics and Metabolism. 2003;80(1):148-58.
173. Cavazzana-Calvo M, Hacein-Bey S, de Saint Basile G, Gross F, Yvon E, Nusbaum P, Selz F, Hue C, Certain S, Casanova JL, Bousso P, Deist FL, Fischer A. Gene therapy of human severe combined immunodeficiency (SCID)-X1 disease. Science. 2000;288(5466):669-72.
174. Hacein-Bey-Abina S, Von Kalle C, Schmidt M, McCormack MP, Wulffraat N, Leboulch P, Lim A, Osborne CS, Pawliuk R, Morillon E, Sorensen R, Forster A, Fraser P, Cohen JI, de Saint Basile G, Alexander I, Wintergerst U, Frebourg T, Aurias A, Stoppa-Lyonnet D, Romana S, Radford-Weiss I, Gross F, Valensi F, Delabesse E, Macintyre E, Sigaux F, Soulier J, Leiva LE, Wissler M, Prinz C, Rabbitts TH, Le Deist F, Fischer A, Cavazzana-Calvo M. LMO2-associated clonal T cell proliferation in two patients after gene therapy for SCID-X1. Science. 2003;302(5644):415-9.
175. Hacein-Bey-Abina S, Garrigue A, Wang GP, Soulier J, Lim A, Morillon E, Clappier E, Caccavelli L, Delabesse E, Beldjord K, Asnafi V, MacIntyre E, Dal Cortivo L, Radford I, Brousse N, Sigaux F, Moshous D, Hauer J, Borkhardt A, Belohradsky BH, Wintergerst U, Velez MC, Leiva L, Sorensen R, Wulffraat N, Blanche S, Bushman FD, Fischer A, Cavazzana-Calvo M. Insertional oncogenesis in 4 patients after retrovirus-mediated gene therapy of SCID-X1. J Clin Invest. 2008;118(9):3132-42.
176. Maguire AM, Simonelli F, Pierce EA, Pugh EN, Jr., Mingozzi F, Bennicelli J, Banfi S, Marshall KA, Testa F, Surace EM, Rossi S, Lyubarsky A, Arruda VR, Konkle B, Stone E, Sun J, Jacobs J, Dell'Osso L, Hertle R, Ma JX, Redmond TM, Zhu X, Hauck B, Zelenaia O, Shindler KS, Maguire MG, Wright JF, Volpe NJ, McDonnell JW, Auricchio A, High KA, Bennett J. Safety and efficacy of gene transfer for Leber's congenital amaurosis. N Engl J Med. 2008;358(21):2240-8.
177. Russell S, Bennett J, Wellman JA, Chung DC, Yu ZF, Tillman A, Wittes J, Pappas J, Elci O, McCague S, Cross D, Marshall KA, Walshire J, Kehoe TL, Reichert H, Davis M, Raffini L, George LA, Hudson FP, Dingfield L, Zhu X, Haller JA, Sohn EH, Mahajan VB, Pfeifer W, Weckmann M, Johnson C, Gewaily D, Drack A, Stone E, Wachtel K, Simonelli F, Leroy BP, Wright JF, High KA, Maguire AM. Efficacy and safety of voretigene neparvovec (AAV2-hRPE65v2) in patients with RPE65-mediated inherited retinal dystrophy: a randomised, controlled, open-label, phase 3 trial. Lancet. 2017;390(10097):849-60.
178. Lowes L, Al-Zaidy S, Shell R, Arnold W, Rodino-Klapac L, Prior T, Alfano L, Berry K, Church K, Kissel J, Nagendran S, L'Italien J, Sproule D, Wells C, Burghes A, Foust K, Meyer K, Likhite S, Kaspar B, Mendell J. AVXS-101 phase 1 gene therapy clinical trial in SMA Type 1: patients treated early with the proposed therapeutic dose were able to sit unassisted at a younger age. Neuromuscular Disorders. 2017;27:S208-S9.
179. Mendell JR, Al-Zaidy S, Shell R, Arnold WD, Rodino-Klapac LR, Prior TW, Lowes L, Alfano L, Berry K, Church K, Kissel JT, Nagendran S, L'Italien J, Sproule DM, Wells C, Cardenas JA, Heitzer MD, Kaspar A, Corcoran S, Braun L, Likhite S, Miranda C, Meyer K, Foust KD, Burghes AHM, Kaspar BK. Single-Dose Gene-Replacement Therapy for Spinal Muscular Atrophy. New England Journal of Medicine. 2017;377(18):1713-22.
180. Day JW, Finkel RS, Chiriboga CA, Connolly AM, Crawford TO, Darras BT, Iannaccone ST, Kuntz NL, Peña LDM, Shieh PB, Smith EC, Kwon JM, Zaidman CM, Schultz M, Feltner DE, Tauscher-Wisniewski S, Ouyang H, Chand DH, Sproule DM, Macek TA, Mendell JR. Onasemnogene abeparvovec gene therapy for symptomatic infantile-onset spinal muscular atrophy in patients with two copies of SMN2 (STR1VE): an open-label, single-arm, multicentre, phase 3 trial. Lancet Neurol. 2021;20(4):284-93.

181. Levine BL, Miskin J, Wonnacott K, Keir C. Global Manufacturing of CAR T Cell Therapy. Molecular Therapy - Methods & Clinical Development. 2017;4:92-101.
182. Kurian KM, Watson CJ, Wyllie AH. Retroviral vectors. Mol Pathol. 2000;53(4):173-6.
183. Chen YH, Keiser MS, Davidson BL. Viral Vectors for Gene Transfer. Curr Protoc Mouse Biol. 2018;8(4):e58.
184. Kootstra NA, Verma IM. Gene therapy with viral vectors. Annu Rev Pharmacol Toxicol. 2003;43:413-39.
185. Engels B, Cam H, Schüler T, Indraccolo S, Gladow M, Baum C, Blankenstein T, Uckert W. Retroviral vectors for high-level transgene expression in T lymphocytes. Hum Gene Ther. 2003;14(12):1155-68.
186. Uckert W, Pedersen L, Gunzburg W. Green fluorescent protein retroviral vector : generation of high-titer producer cells and virus supernatant. Methods Mol Med. 2000;35:275-85.
187. Gunzburg WH, Fleuchaus A, Saller R, Salmons B. Retroviral vector targeting for gene therapy. Cytokines Mol Ther. 1996;2(3):177-84.
188. Landau NR, Page KA, Littman DR. Pseudotyping with human T-cell leukemia virus type I broadens the human immunodeficiency virus host range. J Virol. 1991;65(1):162-9.
189. de Andrade Pereira B, Fraefel C. Novel immunotherapeutic approaches in targeting dendritic cells with virus vectors. Discov Med. 2015;20(109):111-9.
190. Russell SJ, Hawkins RE, Winter G. Retroviral vectors displaying functional antibody fragments. Nucleic Acids Res. 1993;21(5):1081-5.
191. Buchholz CJ, Muhlebach MD, Cichutek K. Lentiviral vectors with measles virus glycoproteins - dream team for gene transfer? Trends Biotechnol. 2009;27(5):259-65.
192. Martin F, Neil S, Kupsch J, Maurice M, Cosset F, Collins M. Retrovirus targeting by tropism restriction to melanoma cells. J Virol. 1999;73(8):6923-9.
193. Marin M, Noël D, Valsesia-Wittman S, Brockly F, Etienne-Julan M, Russell S, Cosset FL, Piechaczyk M. Targeted infection of human cells via major histocompatibility complex class I molecules by Moloney murine leukemia virus-derived viruses displaying single-chain antibody fragment-envelope fusion proteins. J Virol. 1996;70(5):2957-62.
194. Han X, Kasahara N, Kan YW. Ligand-directed retroviral targeting of human breast cancer cells. Proc Natl Acad Sci U S A. 1995;92(21):9747-51.
195. Ager S, Nilson BH, Morling FJ, Peng KW, Cosset FL, Russell SJ. Retroviral display of antibody fragments; interdomain spacing strongly influences vector infectivity. Hum Gene Ther. 1996;7(17):2157-64.
196. Morizono K, Bristol G, Xie YM, Kung SK, Chen IS. Antibody-directed targeting of retroviral vectors via cell surface antigens. Journal of virology. 2001;75(17):8016-20.
197. Morizono K, Xie Y, Ringpis G-E, Johnson M, Nassanian H, Lee B, Wu L, Chen ISY. Lentiviral vector retargeting to P-glycoprotein on metastatic melanoma through intravenous injection. Nature Medicine. 2005;11(3):346-52.
198. Smit JM, Bittman R, Wilschut J. Low-pH-dependent fusion of Sindbis virus with receptor-free cholesterol- and sphingolipid-containing liposomes. J Virol. 1999;73(10):8476-84.
199. Buchholz CJ, Mühlebach MD, Cichutek K. Lentiviral vectors with measles virus glycoproteins – dream team for gene transfer? Trends in Biotechnology. 2009;27(5):259-65.
200. Plattet P, Alves L, Herren M, Aguilar HC. Measles Virus Fusion Protein: Structure, Function and Inhibition. Viruses. 2016;8(4):112-.
201. Jardetzky TS, Lamb RA. Activation of paramyxovirus membrane fusion and virus entry. Curr Opin Virol. 2014;5:24-33.
202. Moll M, Klenk H-D, Maisner A. Importance of the cytoplasmic tails of the measles virus glycoproteins for fusogenic activity and the generation of recombinant measles viruses. Journal of virology. 2002;76(14):7174-86.
203. Vongpunsawad S, Oezgun N, Braun W, Cattaneo R. Selectively receptor-blind measles viruses: Identification of residues necessary for SLAM- or CD46-induced fusion and their localization on a new hemagglutinin structural model. J Virol. 2004;78(1):302-13.

204. Funke S, Schneider IC, Glaser S, Mühlebach MD, Moritz T, Cattaneo R, Cichutek K, Buchholz CJ. Pseudotyping lentiviral vectors with the wild-type measles virus glycoproteins improves titer and selectivity. Gene Therapy. 2009;16(5):700-5.
205. Zhou Q, Schneider IC, Edes I, Honegger A, Bach P, Schönfeld K, Schambach A, Wels WS, Kneissl S, Uckert W, Buchholz CJ. T-cell receptor gene transfer exclusively to human CD8(+) cells enhances tumor cell killing. Blood. 2012;120(22):4334-42.
206. Zhou Q, Uhlig KM, Muth A, Kimpel J, Lévy C, Münch RC, Seifried J, Pfeiffer A, Trkola A, Coulibaly C, von Laer D, Wels WS, Hartwig UF, Verhoeyen E, Buchholz CJ. Exclusive Transduction of Human CD4+ T Cells upon Systemic Delivery of CD4-Targeted Lentiviral Vectors. J Immunol. 2015;195(5):2493-501.
207. Buchholz CJ, Friedel T, Büning H. Surface-Engineered Viral Vectors for Selective and Cell Type-Specific Gene Delivery. Trends Biotechnol. 2015;33(12):777-90.
208. Edes I. Targeted transduction of T cell subsets for immunotherapy of cancer and infectious disease: Humboldt-Universität zu Berlin, Lebenswissenschaftliche Fakultät; 2016.
209. Lyman MA, Nugent CT, Marquardt KL, Biggs JA, Pamer EG, Sherman LA. The fate of low affinity tumor-specific CD8+ T cells in tumor-bearing mice. The Journal of Immunology. 2005;174(5):2563-72.
210. Lo D, Freedman J, Hesse S, Palmiter RD, Brinster RL, Sherman LA. Peripheral tolerance to an islet cell-specific hemagglutinin transgene affects both CD4+ and CD8+ T cells. European Journal of Immunology. 1992;22(4):1013-22.
211. Nugent CT, Morgan DJ, Biggs JA, Ko A, Pilip IM, Pamer EG, Sherman LA. Characterization of CD8+ T lymphocytes that persist after peripheral tolerance to a self antigen expressed in the pancreas. J Immunol. 2000;164(1):191-200.
212. Patten PA, Rock EP, Sonoda T, Fazekas de St Groth B, Jorgensen JL, Davis MM. Transfer of putative complementarity-determining region loops of T cell receptor V domains confers toxin reactivity but not peptide/MHC specificity. The Journal of Immunology. 1993;150(6):2281.
213. Morgan DJ, Liblau R, Scott B, Fleck S, McDevitt HO, Sarvetnick N, Lo D, Sherman LA. CD8(+) T cell-mediated spontaneous diabetes in neonatal mice. The Journal of Immunology. 1996;157(3):978.
214. Kirberg J, Baron A, Jakob S, Rolink A, Karjalainen K, von Boehmer H. Thymic selection of CD8+ single positive cells with a class II major histocompatibility complex-restricted receptor. J Exp Med. 1994;180(1):25-34.
215. Taylor AH, Haberman AM, Gerhard W, Caton AJ. Structure-function relationships among highly diverse T cells that recognize a determinant from influenza virus hemagglutinin. J Exp Med. 1990;172(6):1643-51.
216. Hackett CJ, Dietzschold B, Gerhard W, Ghrist B, Knorr R, Gillessen D, Melchers F. Influenza virus site recognized by a murine helper T cell specific for H1 strains. Localization to a nine amino acid sequence in the hemagglutinin molecule. J Exp Med. 1983;158(2):294-302.
217. Weber S, Traunecker A, Oliveri F, Gerhard W, Karjalainen K. Specific low-affinity recognition of major histocompatibility complex plus peptide by soluble T-cell receptor. Nature. 1992;356(6372):793-6.
218. Wong SBJ, Bos R, Sherman LA. Tumor-Specific CD4+ T Cells Render the Tumor Environment Permissive for Infiltration by Low-Avidity CD8+; T Cells. The Journal of Immunology. 2008;180(5):3122.
219. Apostolou I, von Boehmer H. The TCR-HA, INS-HA transgenic model of autoimmune diabetes: limitations and expectations. Journal of Autoimmunity. 2004;22(2):111-4.
220. Haberman AM, Moller C, McCreedy D, Gerhard WU. A large degree of functional diversity exists among helper T cells specific for the same antigenic site of influenza hemagglutinin. J Immunol. 1990;145(9):3087-94.
221. Brochet X, Lefranc MP, Giudicelli V. IMGT/V-QUEST: the highly customized and integrated system for IG and TR standardized V-J and V-D-J sequence analysis. Nucleic Acids Res. 2008;36(Web Server issue):W503-8.

222. Winter G, Fields S, Brownlee GG. Nucleotide sequence of the haemagglutinin gene of a human influenza virus H1 subtype. Nature. 1981;292(5818):72-5.
223. Zhang Y, Aevermann BD, Anderson TK, Burke DF, Dauphin G, Gu Z, He S, Kumar S, Larsen CN, Lee AJ, Li X, Macken C, Mahaffey C, Pickett BE, Reardon B, Smith T, Stewart L, Suloway C, Sun G, Tong L, Vincent AL, Walters B, Zaremba S, Zhao H, Zhou L, Zmasek C, Klem EB, Scheuermann RH. Influenza Research Database: An integrated bioinformatics resource for influenza virus research. Nucleic Acids Res. 2017;45(D1):D466-D74.
224. Cui Z, Geurts AM, Liu G, Kaufman CD, Hackett PB. Structure–Function Analysis of the Inverted Terminal Repeats of the Sleeping Beauty Transposon. Journal of Molecular Biology. 2002;318(5):1221-35.
225. Davis MR, Manning LS, Whitaker D, Garlepp MJ, Robinson BW. Establishment of a murine model of malignant mesothelioma. Int J Cancer. 1992;52(6):881-6.
226. Blazar BA, Laing CA, Miller FR, Heppner GH. Activity of lymphoid cells separated from mammary tumors in blastogenesis and Winn assays. J Natl Cancer Inst. 1980;65(2):405-10.
227. Miller BE, Miller FR, Wilburn DJ, Heppner GH. Analysis of tumour cell composition in tumours composed of paired mixtures of mammary tumour cell lines. Br J Cancer. 1987;56(5):561-9.
228. Letourneur F, Malissen B. Derivation of a T cell hybridoma variant deprived of functional T cell receptor alpha and beta chain transcripts reveals a nonfunctional alpha-mRNA of BW5147 origin. Eur J Immunol. 1989;19(12):2269-74.
229. Ralph P. Retention of lymphocyte characteristics by myelomas and theta + -lymphomas: sensitivity to cortisol and phytohemagglutinin. J Immunol. 1973;110(6):1470-5.
230. Giudicelli V, Brochet X, Lefranc MP. IMGT/V-QUEST: IMGT standardized analysis of the immunoglobulin (IG) and T cell receptor (TR) nucleotide sequences. Cold Spring Harb Protoc. 2011;2011(6):695-715.
231. Engels B, Cam H, Schüler T, Indraccolo S, Gladow M, Baum C, Blankenstein T, Uckert W. Retroviral Vectors for High-Level Transgene Expression in T Lymphocytes. Human Gene Therapy. 2003;14(12):1155-68.
232. Miller FR, Miller BE, Heppner GH. Characterization of metastatic heterogeneity among subpopulations of a single mouse mammary tumor: heterogeneity in phenotypic stability. Invasion Metastasis. 1983;3(1):22-31.
233. Aslakson CJ, Miller FR. Selective Events in the Metastatic Process Defined by Analysis of the Sequential Dissemination of Subpopulations of a Mouse Mammary Tumor. Cancer Research. 1992;52(6):1399.
234. Pulaski BA, Terman DS, Khan S, Muller E, Ostrand-Rosenberg S. Cooperativity of Staphylococcal aureus enterotoxin B superantigen, major histocompatibility complex class II, and CD80 for immunotherapy of advanced spontaneous metastases in a clinically relevant postoperative mouse breast cancer model. Cancer Res. 2000;60(10):2710-5.
235. Baram T, Erlichman N, Dadiani M, Balint-Lahat N, Pavlovski A, Meshel T, Morzaev-Sulzbach D, Gal-Yam EN, Barshack I, Ben-Baruch A. Chemotherapy Shifts the Balance in Favor of CD8+ TNFR2+ TILs in Triple-Negative Breast Tumors. Cells. 2021;10(6):1429.
236. Schoch CL, Ciufo S, Domrachev M, Hotton CL, Kannan S, Khovanskaya R, Leipe D, McVeigh R, O'Neill K, Robbertse B, Sharma S, Soussov V, Sullivan JP, Sun L, Turner S, Karsch-Mizrachi I. NCBI Taxonomy: a comprehensive update on curation, resources and tools. Database (Oxford). 2020;2020.
237. Conzelmann A, Pink R, Acuto O, Mach JP, Dolivo S, Nabholz M. Presence of T 145 on cytolytic T cell lines and their lectin-resistant mutants. Eur J Immunol. 1980;10(11):860-8.
238. Ostergaard HL, Shackelford DA, Hurley TR, Johnson P, Hyman R, Sefton BM, Trowbridge IS. Expression of CD45 alters phosphorylation of the lck-encoded tyrosine protein kinase in murine lymphoma T-cell lines. Proc Natl Acad Sci U S A. 1989;86(22):8959-63.
239. Gattinoni L, Klebanoff CA, Restifo NP. Paths to stemness: building the ultimate antitumour T cell. Nat Rev Cancer. 2012;12(10):671-84.

240. Busch DH, Fräßle SP, Sommermeyer D, Buchholz VR, Riddell SR. Role of memory T cell subsets for adoptive immunotherapy. Semin Immunol. 2016;28(1):28-34.
241. Sommermeyer D, Hudecek M, Kosasih PL, Gogishvili T, Maloney DG, Turtle CJ, Riddell SR. Chimeric antigen receptor-modified T cells derived from defined CD8+ and CD4+ subsets confer superior antitumor reactivity in vivo. Leukemia. 2016;30(2):492-500.
242. Yang Y, Kohler ME, Chien CD, Sauter CT, Jacoby E, Yan C, Hu Y, Wanhainen K, Qin H, Fry TJ. TCR engagement negatively affects CD8 but not CD4 CAR T cell expansion and leukemic clearance. Sci Transl Med. 2017;9(417).
243. Agarwal S, Hanauer JD, Frank AM, Riechert V, Thalheimer FB, Buchholz CJ. In vivo generation of CAR T cells selectively in human CD4+ lymphocytes. Molecular Therapy. 2020;28(8):1783-94.
244. Liadi I, Singh H, Romain G, Roysam B, Cooper LJ, Varadarajan N. Defining potency of CAR(+) T cells: Fast and furious or slow and steady. Oncoimmunology. 2019;8(10):e1051298.
245. Christian M, Cermak T, Doyle EL, Schmidt C, Zhang F, Hummel A, Bogdanove AJ, Voytas DF. Targeting DNA Double-Strand Breaks with TAL Effector Nucleases. Genetics. 2010;186(2):757-61.
246. Carroll D. Progress and prospects: zinc-finger nucleases as gene therapy agents. Gene Ther. 2008;15(22):1463-8.
247. LaFountaine JS, Fathe K, Smyth HDC. Delivery and therapeutic applications of gene editing technologies ZFNs, TALENs, and CRISPR/Cas9. International Journal of Pharmaceutics. 2015;494(1):180-94.
248. Jinek M, Chylinski K, Fonfara I, Hauer M, Doudna JA, Charpentier E. A programmable dual-RNA-guided DNA endonuclease in adaptive bacterial immunity. Science. 2012;337(6096):816-21.
249. Jin M-Z, Jin W-L. The updated landscape of tumor microenvironment and drug repurposing. Signal Transduction and Targeted Therapy. 2020;5(1):166.
250. Joyce JA, Fearon DT. T cell exclusion, immune privilege, and the tumor microenvironment. Science. 2015;348(6230):74-80.
251. Parks SK, Mueller-Klieser W, Pouysségur J. Lactate and Acidity in the Cancer Microenvironment. Annual Review of Cancer Biology. 2020;4(1):141-58.
252. Bonaventura P, Shekarian T, Alcazer V, Valladeau-Guilemond J, Valsesia-Wittmann S, Amigorena S, Caux C, Depil S. Cold Tumors: A Therapeutic Challenge for Immunotherapy. Front Immunol. 2019;10:168.
253. Garfall AL, Dancy EK, Cohen AD, Hwang WT, Fraietta JA, Davis MM, Levine BL, Siegel DL, Stadtmauer EA, Vogl DT, Waxman A, Rapoport AP, Milone MC, June CH, Melenhorst JJ. T-cell phenotypes associated with effective CAR T-cell therapy in postinduction vs relapsed multiple myeloma. Blood Adv. 2019;3(19):2812-5.
254. Wang D, Aguilar B, Starr R, Alizadeh D, Brito A, Sarkissian A, Ostberg JR, Forman SJ, Brown CE. Glioblastoma-targeted CD4+ CAR T cells mediate superior antitumor activity. JCI Insight. 2018;3(10).
255. Yang Y, Kohler ME, Chien Christopher D, Sauter Christopher T, Jacoby E, Yan C, Hu Y, Wanhainen K, Qin H, Fry Terry J. TCR engagement negatively affects CD8 but not CD4 CAR T cell expansion and leukemic clearance. Science Translational Medicine. 2017;9(417):eaag1209.
256. Tay RE, Richardson EK, Toh HC. Revisiting the role of CD4+ T cells in cancer immunotherapy—new insights into old paradigms. Cancer Gene Therapy. 2021;28(1):5-17.
257. Hor Jyh L, Whitney Paul G, Zaid A, Brooks Andrew G, Heath William R, Mueller Scott N. Spatiotemporally Distinct Interactions with Dendritic Cell Subsets Facilitates CD4+ and CD8+ T Cell Activation to Localized Viral Infection. Immunity. 2015;43(3):554-65.
258. Schietinger A, Philip M, Liu RB, Schreiber K, Schreiber H. Bystander killing of cancer requires the cooperation of CD4(+) and CD8(+) T cells during the effector phase. The Journal of experimental medicine. 2010;207(11):2469-77.
259. Spiotto MT, Rowley DA, Schreiber H. Bystander elimination of antigen loss variants in established tumors. Nat Med. 2004;10(3):294-8.

260. Dieu-Nosjean MC, Giraldo NA, Kaplon H, Germain C, Fridman WH, Sautès-Fridman C. Tertiary lymphoid structures, drivers of the anti-tumor responses in human cancers. Immunol Rev. 2016;271(1):260-75.
261. Bos R, Sherman LA. CD4+ T-cell help in the tumor milieu is required for recruitment and cytolytic function of CD8+ T lymphocytes. Cancer Res. 2010;70(21):8368-77.
262. Arina A, Karrison T, Galka E, Schreiber K, Weichselbaum RR, Schreiber H. Transfer of Allogeneic CD4+ T Cells Rescues CD8+ T Cells in Anti-PD-L1-Resistant Tumors Leading to Tumor Eradication. Cancer Immunol Res. 2017;5(2):127-36.
263. Li K, Donaldson B, Young V, Ward V, Jackson C, Baird M, Young S. Adoptive cell therapy with CD4(+) T helper 1 cells and CD8(+) cytotoxic T cells enhances complete rejection of an established tumour, leading to generation of endogenous memory responses to non-targeted tumour epitopes. Clin Transl Immunology. 2017;6(10):e160-e.
264. Li CW, Lim SO, Chung EM, Kim YS, Park AH, Yao J, Cha JH, Xia W, Chan LC, Kim T, Chang SS, Lee HH, Chou CK, Liu YL, Yeh HC, Perillo EP, Dunn AK, Kuo CW, Khoo KH, Hsu JL, Wu Y, Hsu JM, Yamaguchi H, Huang TH, Sahin AA, Hortobagyi GN, Yoo SS, Hung MC. Eradication of Triple-Negative Breast Cancer Cells by Targeting Glycosylated PD-L1. Cancer Cell. 2018;33(2):187-201.e10.
265. Lian S, Xie R, Ye Y, Lu Y, Cheng Y, Xie X, Li S, Jia L. Dual blockage of both PD-L1 and CD47 enhances immunotherapy against circulating tumor cells. Scientific Reports. 2019;9(1):4532.
266. Sun T, Zhang W, Li Y, Jin Z, Du Y, Tian J, Xue H. Combination Immunotherapy with Cytotoxic T-Lymphocyte–Associated Antigen-4 and Programmed Death Protein-1 Inhibitors Prevents Postoperative Breast Tumor Recurrence and Metastasis. Molecular Cancer Therapeutics. 2020;19(3):802.
267. Fear VS, Tilsed C, Chee J, Forbes CA, Casey T, Solin JN, Lansley SM, Lesterhuis WJ, Dick IM, Nowak AK, Robinson BW, Lake RA, Fisher SA. Combination immune checkpoint blockade as an effective therapy for mesothelioma. Oncoimmunology. 2018;7(10):e1494111-e.
268. Demaria S, Kawashima N, Yang AM, Devitt ML, Babb JS, Allison JP, Formenti SC. Immune-mediated inhibition of metastases after treatment with local radiation and CTLA-4 blockade in a mouse model of breast cancer. Clin Cancer Res. 2005;11(2 Pt 1):728-34.
269. Li J, Duran MA, Dhanota N, Chatila WK, Bettigole SE, Kwon J, Sriram RK, Humphries MP, Salto-Tellez M, James JA, Hanna MG, Melms JC, Vallabhaneni S, Litchfield K, Usaite I, Biswas D, Bareja R, Li HW, Martin ML, Dorsaint P, Cavallo J-A, Li P, Pauli C, Gottesdiener L, DiPardo BJ, Hollmann TJ, Merghoub T, Wen HY, Reis-Filho JS, Riaz N, Su S-SM, Kalbasi A, Vasan N, Powell SN, Wolchok JD, Elemento O, Swanton C, Shoushtari AN, Parkes EE, Izar B, Bakhoum SF. Metastasis and Immune Evasion from Extracellular cGAMP Hydrolysis. Cancer Discovery. 2021;11(5):1212.
270. Garrido F, Aptsiauri N, Doorduijn EM, Garcia Lora AM, van Hall T. The urgent need to recover MHC class I in cancers for effective immunotherapy. Current opinion in immunology. 2016;39:44-51.
271. Zinn KR, Chaudhuri TR, Szafran AA, O'Quinn D, Weaver C, Dugger K, Lamar D, Kesterson RA, Wang X, Frank SJ. Noninvasive bioluminescence imaging in small animals. ILAR J. 2008;49(1):103-15.
272. Liu TW, Gammon ST, Piwnica-Worms D. Multi-Modal Multi-Spectral Intravital Microscopic Imaging of Signaling Dynamics in Real-Time during Tumor-ImmuneInteractions. Cells. 2021;10(3):499.
273. Funke S, Maisner A, Mühlebach MD, Koehl U, Grez M, Cattaneo R, Cichutek K, Buchholz CJ. Targeted Cell Entry of Lentiviral Vectors. Molecular Therapy. 2008;16(8):1427-36.
274. Bender RR, Muth A, Schneider IC, Friedel T, Hartmann J, Plückthun A, Maisner A, Buchholz CJ. Receptor-Targeted Nipah Virus Glycoproteins Improve Cell-Type Selective Gene Delivery and Reveal a Preference for Membrane-Proximal Cell Attachment. PLOS Pathogens. 2016;12(6):e1005641.

275. Witting SR, Vallanda P, Gamble AL. Characterization of a third generation lentiviral vector pseudotyped with Nipah virus envelope proteins for endothelial cell transduction. Gene Therapy. 2013;20(10):997-1005.
276. Wang Z, Cao YJ. Adoptive Cell Therapy Targeting Neoantigens: A Frontier for Cancer Research. Frontiers in Immunology. 2020;11.
277. Leisegang M, Kammertoens T, Uckert W, Blankenstein T. Targeting human melanoma neoantigens by T cell receptor gene therapy. J Clin Invest. 2016;126(3):854-8.
278. Blankenstein T, Leisegang M, Uckert W, Schreiber H. Targeting cancer-specific mutations by T cell receptor gene therapy. Curr Opin Immunol. 2015;33:112-9.
279. Kato T, Matsuda T, Ikeda Y, Park JH, Leisegang M, Yoshimura S, Hikichi T, Harada M, Zewde M, Sato S, Hasegawa K, Kiyotani K, Nakamura Y. Effective screening of T cells recognizing neoantigens and construction of T-cell receptor-engineered T cells. Oncotarget. 2018;9(13):11009-19.
280. Ren L, Leisegang M, Deng B, Matsuda T, Kiyotani K, Kato T, Harada M, Park JH, Saloura V, Seiwert T, Vokes E, Agrawal N, Nakamura Y. Identification of neoantigen-specific T cells and their targets: implications for immunotherapy of head and neck squamous cell carcinoma. Oncoimmunology. 2019;8(4):e1568813.
281. Wei T, Leisegang M, Xia M, Kiyotani K, Li N, Zeng C, Deng C, Jiang J, Harada M, Agrawal N, Li L, Qi H, Nakamura Y, Ren L. Generation of neoantigen-specific T cells for adoptive cell transfer for treating head and neck squamous cell carcinoma. Oncoimmunology. 2021;10(1):1929726.
282. Li L-P, Lampert JC, Chen X, Leitao C, Popović J, Müller W, Blankenstein T. Transgenic mice with a diverse human T cell antigen receptor repertoire. Nature Medicine. 2010;16(9):1029-34.
283. Rockinger GA, Guillaume P, Cachot A, Saillard M, Speiser DE, Coukos G, Harari A, Romero PJ, Schmidt J, Jandus C. Optimized combinatorial pMHC class II multimer labeling for precision immune monitoring of tumor-specific CD4 T cells in patients. J Immunother Cancer. 2020;8(1).

Eidesstattliche Versicherung

„Ich, Christoph Philipp Kemna, versichere an Eides statt durch meine eigenhändige Unterschrift, dass ich die vorgelegte Dissertation mit dem Thema: „Subset-specific transduction of $CD4^+$ and $CD8^+$ T cells in vivo; Subgruppen-spezifische in vivo Transduktion von $CD4^+$ und $CD8^+$ T-Zellen“ selbstständig und ohne nicht offengelegte Hilfe Dritter verfasst und keine anderen als die angegebenen Quellen und Hilfsmittel genutzt habe.

Alle Stellen, die wörtlich oder dem Sinne nach auf Publikationen oder Vorträgen anderer Autoren/innen beruhen, sind als solche in korrekter Zitierung kenntlich gemacht. Die Abschnitte zu Methodik (insbesondere praktische Arbeiten, Laborbestimmungen, statistische Aufarbeitung) und Resultaten (insbesondere Abbildungen, Graphiken und Tabellen) werden von mir verantwortet.

Ich versichere ferner, dass ich die in Zusammenarbeit mit anderen Personen generierten Daten, Datenauswertungen und Schlussfolgerungen korrekt gekennzeichnet und meinen eigenen Beitrag sowie die Beiträge anderer Personen korrekt kenntlich gemacht habe (siehe Anteilserklärung). Texte oder Textteile, die gemeinsam mit anderen erstellt oder verwendet wurden, habe ich korrekt kenntlich gemacht.

Meine Anteile an etwaigen Publikationen zu dieser Dissertation entsprechen denen, die in der untenstehenden gemeinsamen Erklärung mit dem/der Erstbetreuer/in, angegeben sind. Für sämtliche im Rahmen der Dissertation entstandenen Publikationen wurden die Richtlinien des ICMJE (International Committee of Medical Journal Editors; www.icmje.og) zur Autorenschaft eingehalten. Ich erkläre ferner, dass ich mich zur Einhaltung der Satzung der Charité – Universitätsmedizin Berlin zur Sicherung Guter Wissenschaftlicher Praxis verpflichte.

Weiterhin versichere ich, dass ich diese Dissertation weder in gleicher noch in ähnlicher Form bereits an einer anderen Fakultät eingereicht habe.

Die Bedeutung dieser eidesstattlichen Versicherung und die strafrechtlichen Folgen einer unwahren eidesstattlichen Versicherung (§§156, 161 des Strafgesetzbuches) sind mir bekannt und bewusst.“

Datum	Unterschrift

13. Curriculum Vitae

Mein Lebenslauf wird aus datenschutzrechtlichen Gründen in der elektronischen Version meiner Arbeit nicht veröffentlicht.

14. Publications

S. Jeuthe, J. Kemna, C.P. Kemna, D. Zocholl, R. Klopfleisch, R. Palme, C. Kirschbaum, C. Thoene-Reineke, T. Kammertoens, Stress hormones or general well-being are not altered in immune-deficient mice lacking either T- and B- lymphocytes or Interferon gamma signaling if kept under specific pathogen free housing conditions, PLOS ONE, 2020

15. Acknowledgements

I would like to thank my supervisor Wolfgang Uckert for the opportunity to work in his group and his continued support, striking a perfect balance between guidance, developmental freedom, and scientific leadership. I want to thank Inan Edes dearly, for trusting me to work on a project he so expertly developed, for teaching me all necessary laboratory skills, for his advice and hands-on expertise without which this dissertation would not have been feasible, all the while inviting me into his circle of friends at the MDC. I want to thank Matthias Leisegang for his mentorship, his willingness to share scientific and cooking insight and for becoming a dear friend.

Special thanks go out to the entire Team of the AG Uckert I had a great time with you all, I especially want to thank Michaela Naschke and Kordelia Hummel for showing me around the technical side of laboratory work, for sharing their protocols and troubleshooting with me.

I would like to thank my parents and my sisters for unconditional support. In particular my mother, who never lost faith in the completion of this thesis.

My deepest thanks go to Josephine Kemna, the love of my life, who I first met in the laboratory, I am honoured to call you my wife, you have always supported and encouraged me and without you much, this thesis included, would not have been possible. Last but not least, I would like to thank our son Vincent, who joined us on the last stretch of this scientific endeavour, for his valued contributions.

16. Statistics certificate

CHARITÉ

CharitéCentrum für Human- und Gesundheitswissenschaften

Charité | Campus Charité Mitte | 10117 Berlin

Institut für Biometrie und Klinische Epidemiologie (iBikE)

Direktor: Prof. Dr. Geraldine Rauch

Postanschrift:
Charitéplatz 1 | 10117 Berlin
Besucheranschrift:
Reinhardtstr. 58 | 10117 Berlin

Tel. +49 (0)30 450 562171
geraldine.rauch@charite.de
https://biometrie.charite.de/

Name, Vorname: Christoph Philipp Kemna

Emailadresse: christoph.kemna@charite.de

Matrikelnummer: 216062

Promotionsbetreuer: Prof. Wolfgang Uckert

Promotionsinstitution/Klinik: Max-Delbrück-Centrum

Bescheinigung

Hiermit bescheinige ich, dass Herr Christoph Philipp Kemna innerhalb der Service Unit Biometrie des Instituts für Biometrie und Klinische Epidemiologie (iBikE) bei mir eine statistische Beratung zu einem Promotionsvorhaben wahrgenommen hat. Folgende Beratungstermine wurden wahrgenommen:

- Termin 1: 27.05.2021
- Termin 2: 26.10.2021

Folgende wesentliche Ratschläge hinsichtlich einer sinnvollen Auswertung und Interpretation der Daten wurden während der Beratung erteilt:

- Fokussierung auf deskriptive Auswertungen bei sehr kleinen Stichproben.
- Wenn möglich, graphische Darstellung der tatsächlichen Messwerte anstelle von zusammenfassenden statistischen Maßen wie Mittelwert und Standardabweichung.

Diese Bescheinigung garantiert nicht die richtige Umsetzung der in der Beratung gemachten Vorschläge, die korrekte Durchführung der empfohlenen statistischen Verfahren und die richtige Darstellung und Interpretation der Ergebnisse. Die Verantwortung hierfür obliegt allein dem Promovierenden. Das Institut für Biometrie und Klinische Epidemiologie übernimmt hierfür keine Haftung.

Datum: 26.11.2021 [redacted]

Unterschrift BeraterIn, Institutsstempel